LHC detectors

P. Ferreira da Silva (CERN)
Course on Physics at the LHC
LIP, 11th-13th March 2019

Outline

- From collision remnants to physics
- Connecting the dots with tracking
- Si-based detectors
- Calorimetry for pedestrians
- Getting data on tape: trigger systems

From collision remnants to physics

We hunt for new physics with exciting signatures

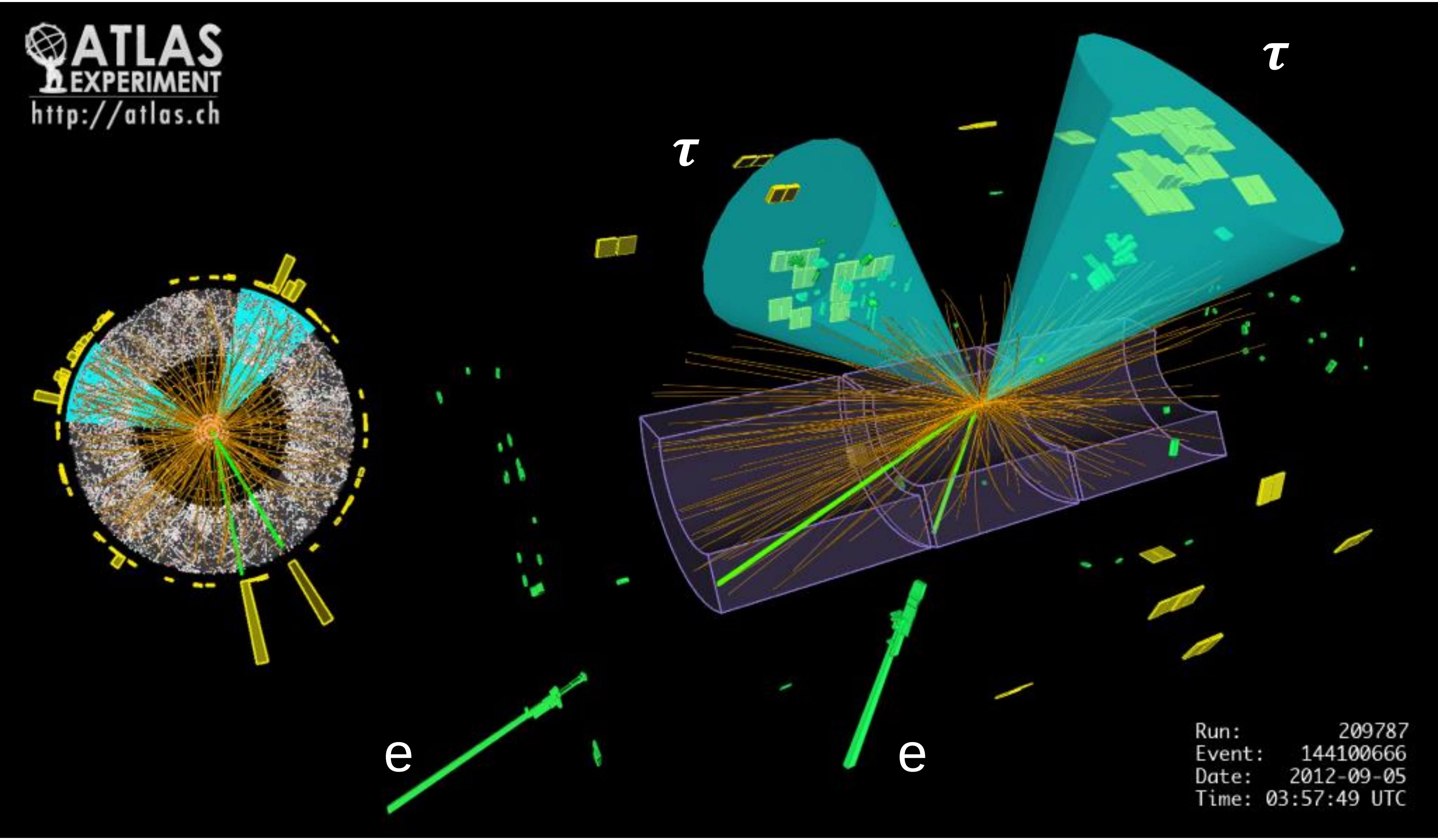

Discovery drives the LHC detectors concept

- Before discovery different signatures to be expected depending on the Higgs mass
- 4π-hermetic general purpose detectors are needed covering: leptons, photons, jets, …

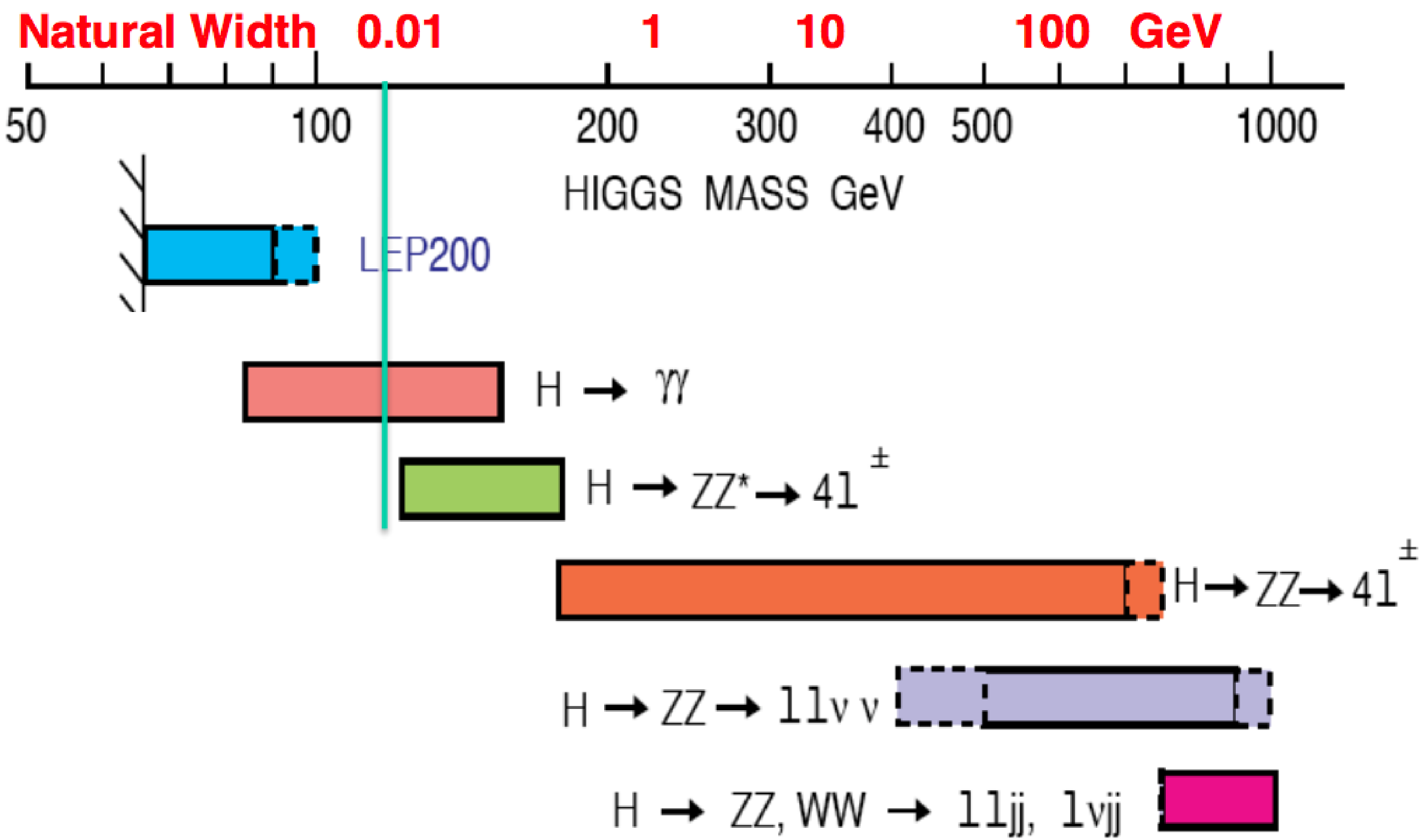

Proton-remnants underly the hard processes

- Single proton collisions produce high multiplicity events

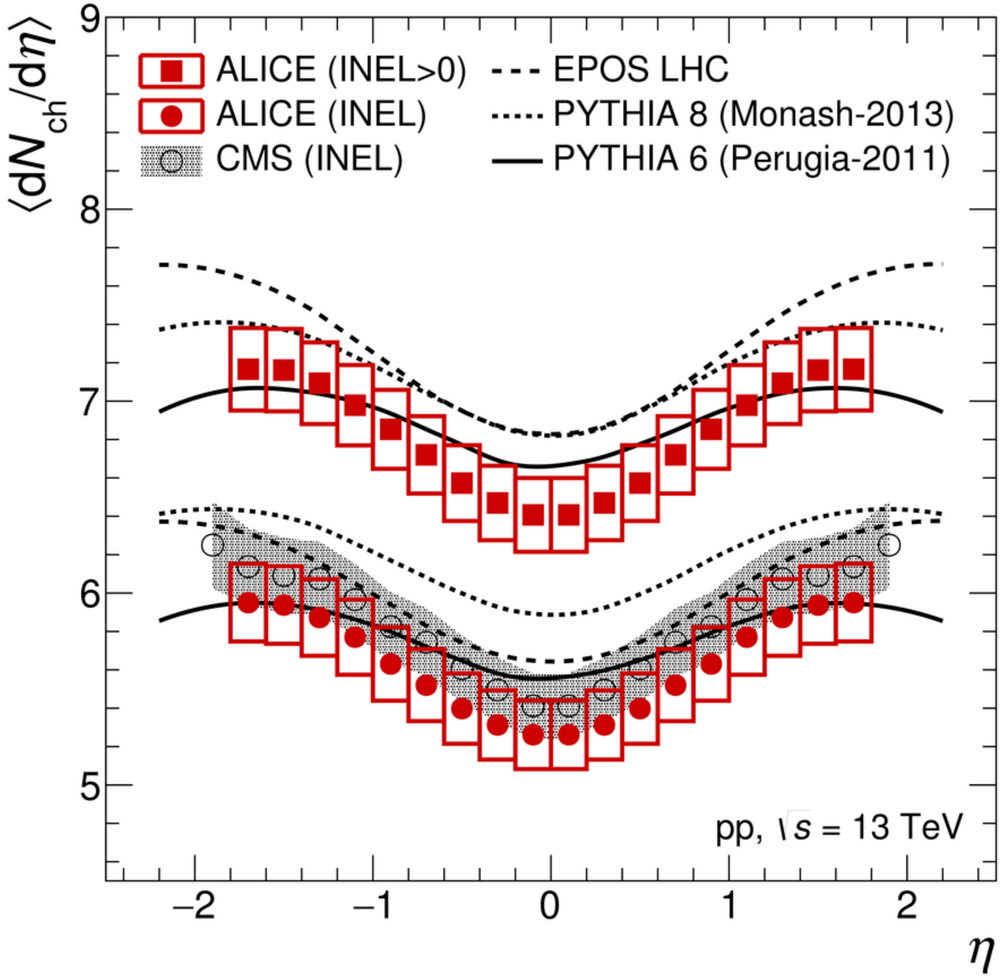

Proton-remnants underly the hard processes

- Single proton collisions produce high multiplicity events
- Distributions are approximately uniform in pseudo-rapidity

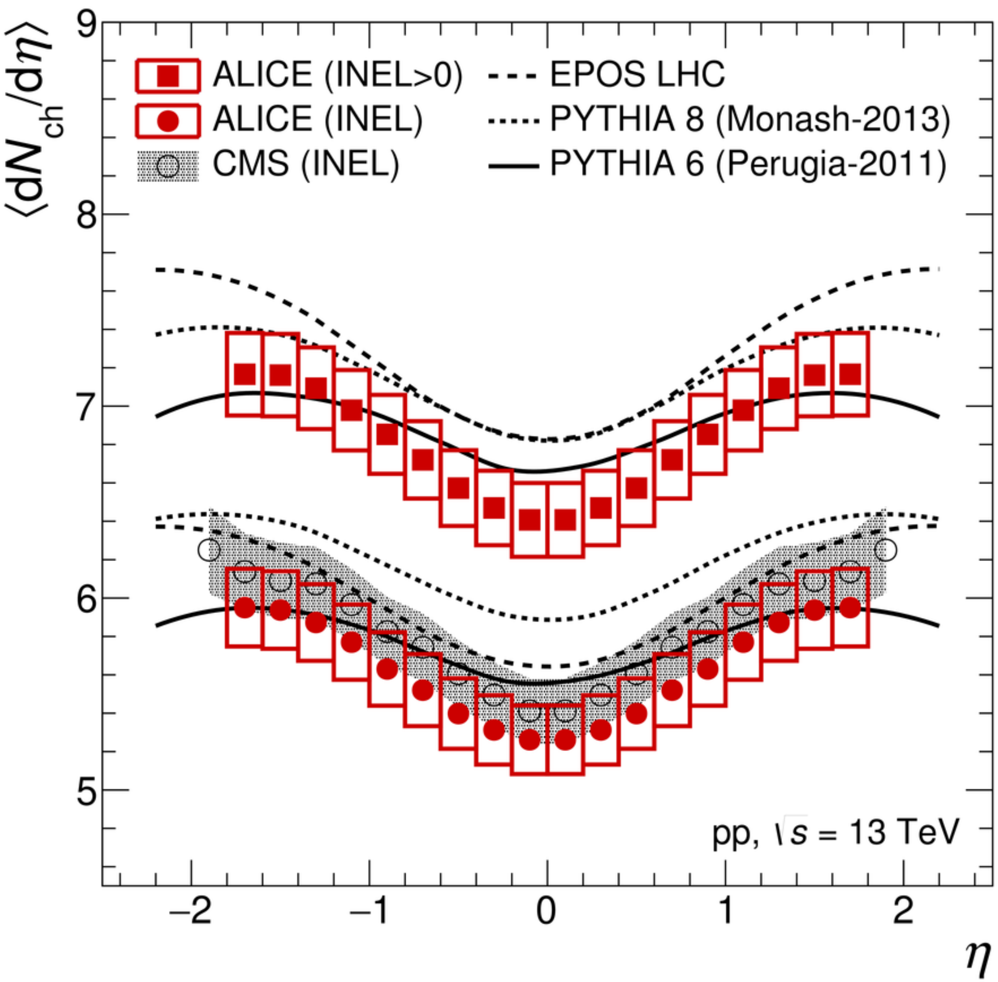

Average 15-20 charged particles per inelastic collision

Proton-remnants underly the hard processes

- Single proton collisions produce high multiplicity events
- Distributions are approximately uniform in pseudo-rapidity
- Most particles are pions with $N(\pi^0) \approx \frac{1}{2} N(\pi^\pm)$

$$\pi^+ = |u\bar{d}>$$

$$\pi^- = |\bar{u}d>$$

$$\pi^0 = \frac{1}{\sqrt{2}}\left(|u\bar{u}> - |d\bar{d}>\right)$$

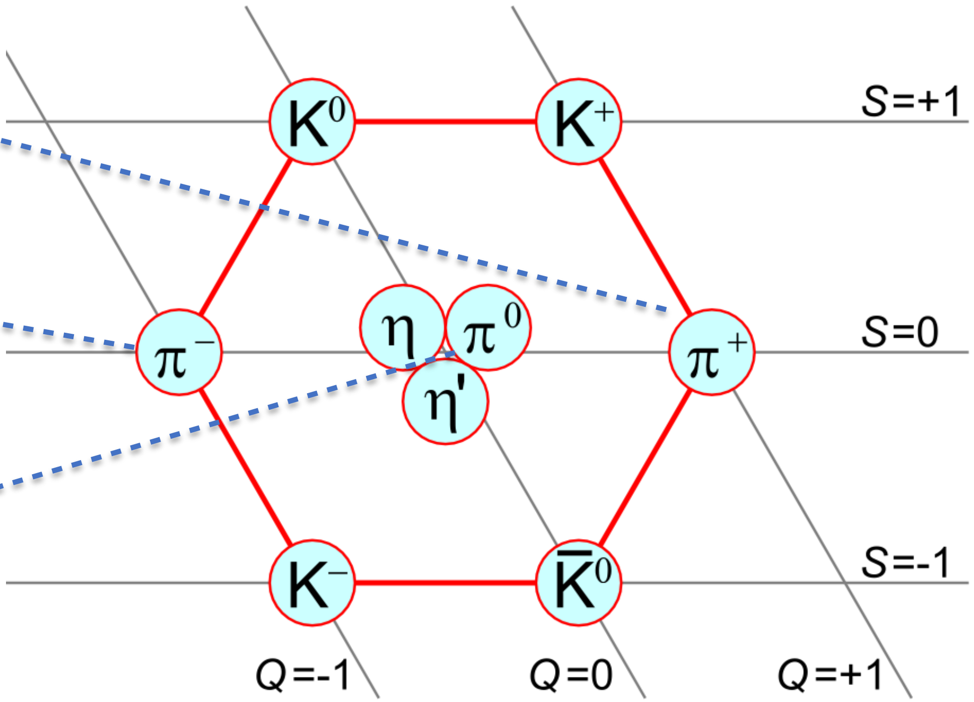

strong interactions preserve isospin

Proton-remnants underly the hard processes

- Single proton collisions produce high multiplicity events
- Distributions are approximately uniform in pseudo-rapidity
- Most particles are pions with $N(\pi^0) \approx \frac{1}{2} N(\pi^\pm)$
- As $\pi^0 \to \gamma\gamma$ dominates $N(\gamma) \approx N(\pi^\pm)$ in the detector

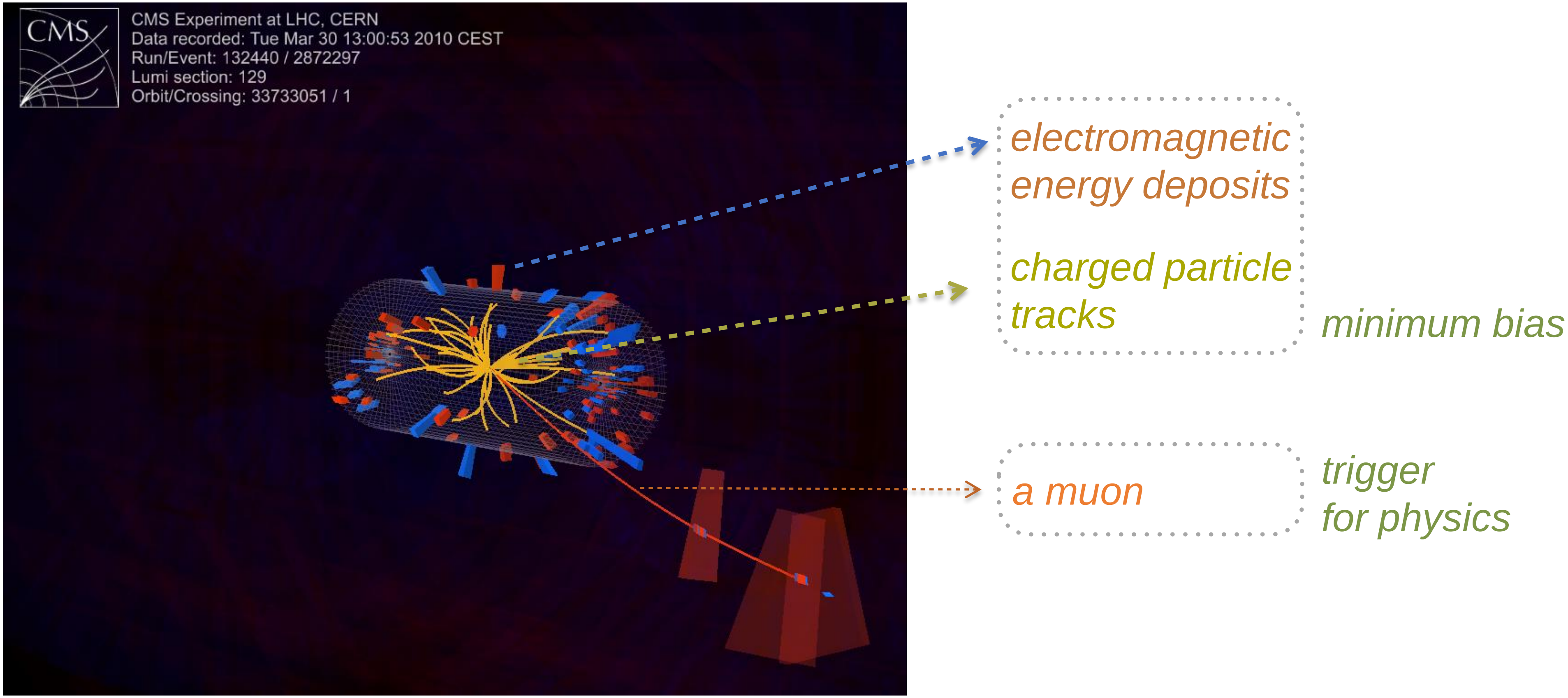

Beyond pions and photons

- Production of other particles suppressed by
  - content of the proton (PDFs)
  - mass (m_s~$19m_d$)
  - interactions

strange particles account for O(10%) of the multiplicities

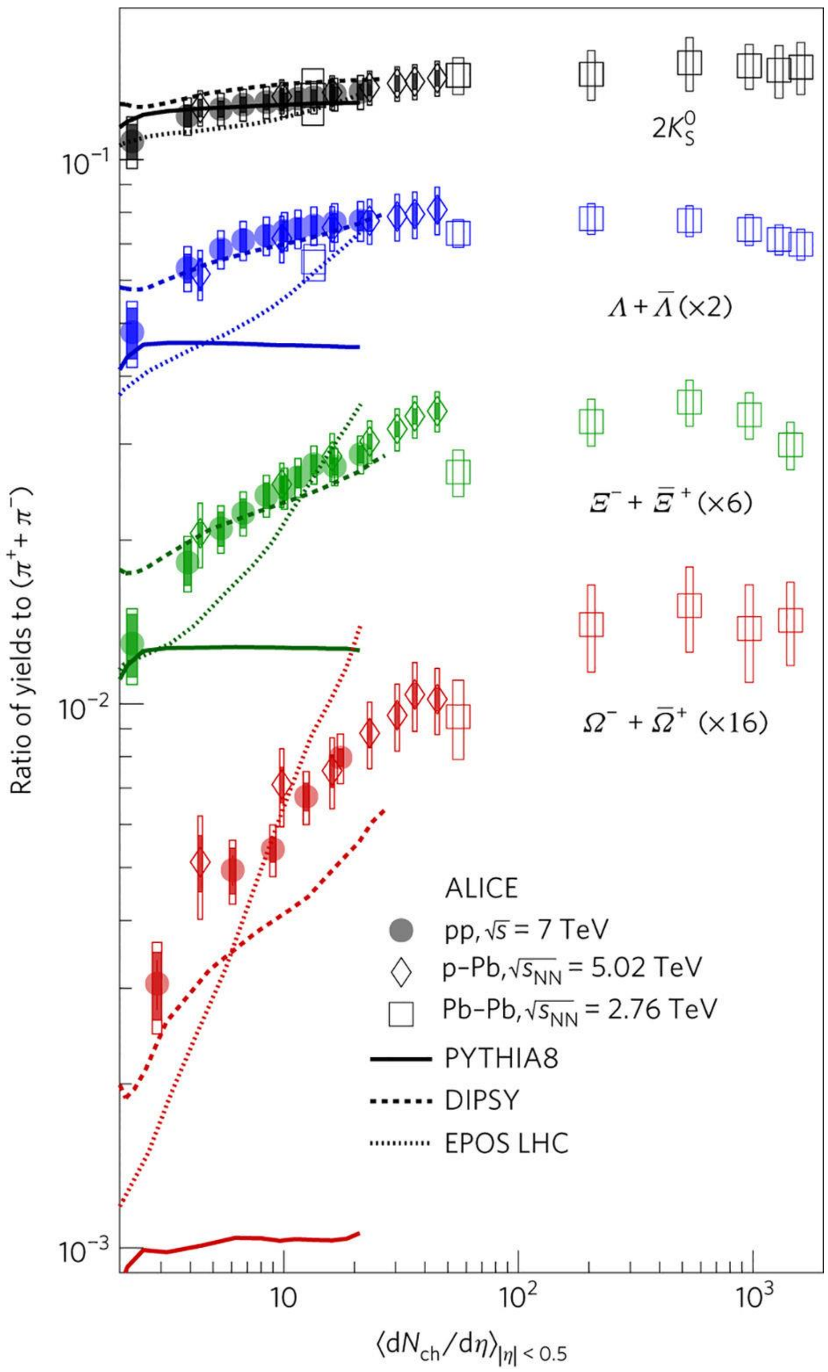

What can we detect?

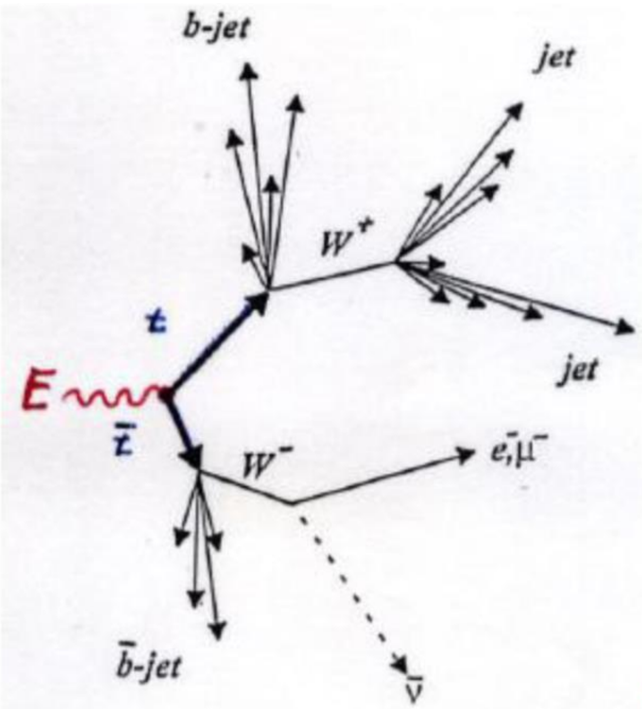

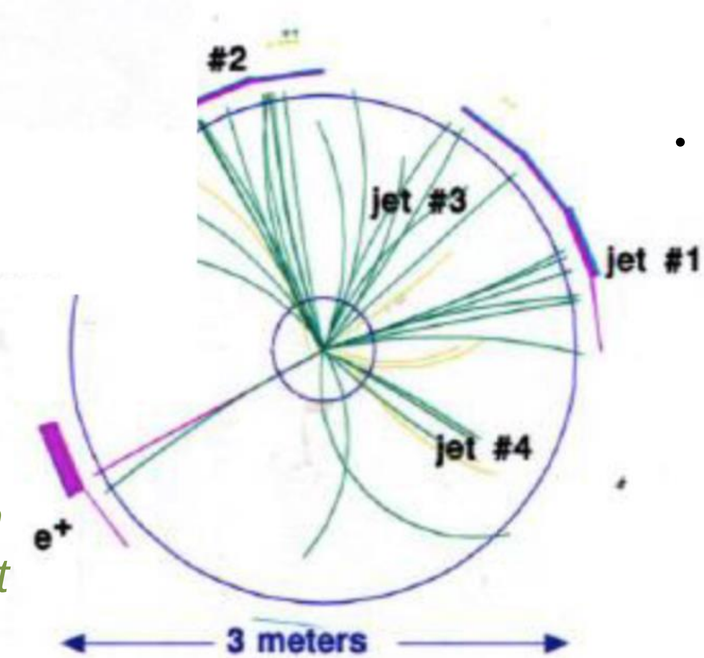

maximum information needed to reconstruct the hard process

- Final states
  - secondary vertices from long-lived decays only in rare cases
- Must interact within detector volume
  - electromagnetic or strong interactions
  - electrons, muons, photons
  - neutral or charged hadrons
- Long-lived weakly interacting particles
  - indirectly detected
  - missing transverse energy
  - good resolution when balancing energy

Particles and their interactions

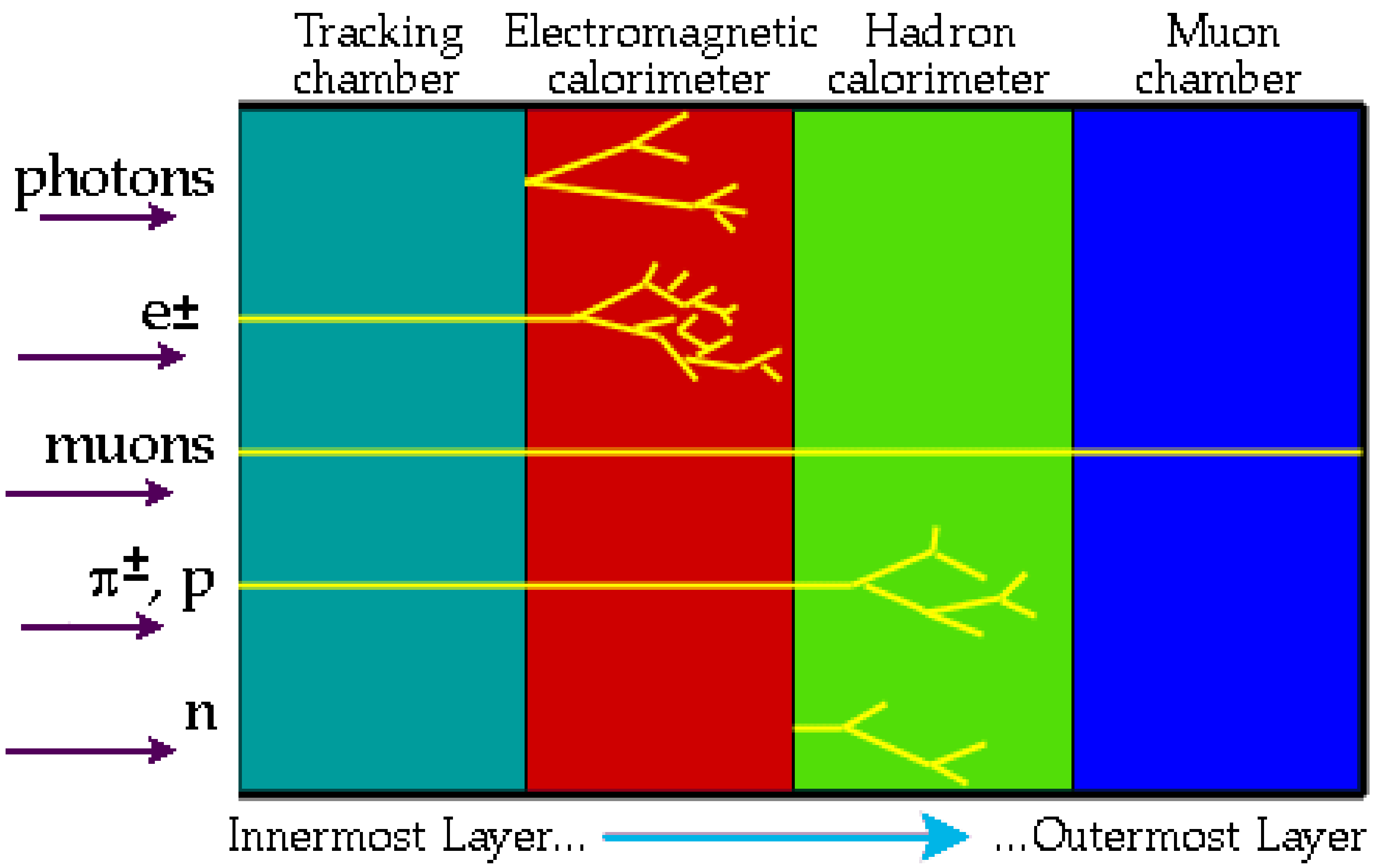

- Detectors register the passage of particle through matter
- Combine absorbers (start interactions) with sensitive materials (convert to optical/voltage)

Main concepts behind general purpose detectors

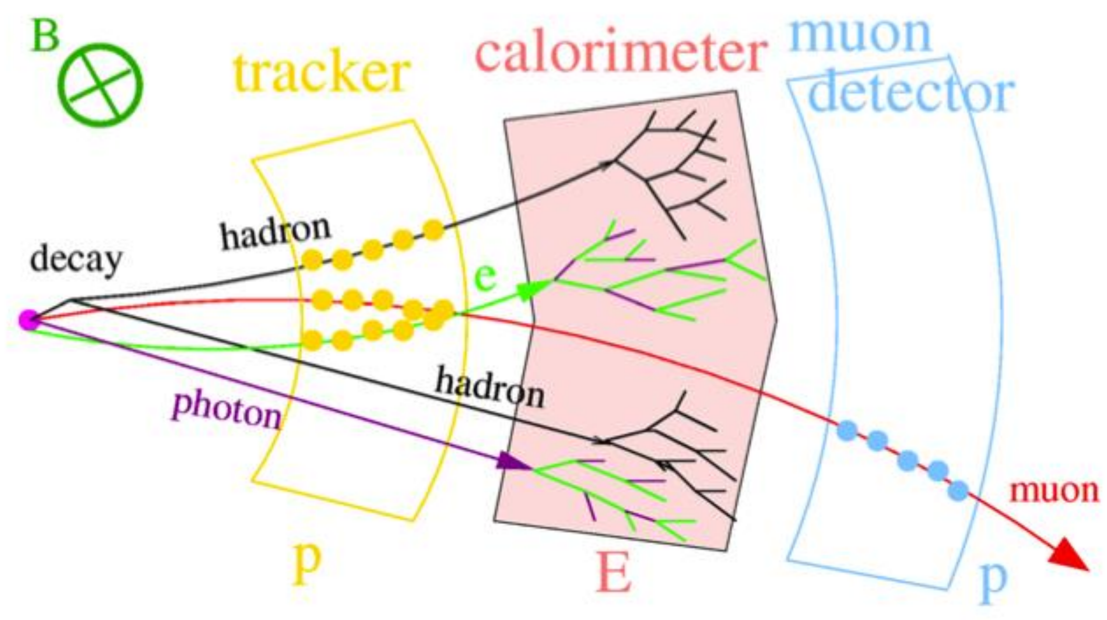

Magnetic field "$F_c = qvB$"

- separate by charge
- measure p by curvature

Calorimetry

- measure E from deposits
- electromagnetic and hadronic

Inner tracking

- minimal interference with event
- points to measure curved tracks
- particle identification

Outer tracking

- muons (weakly interacting)

The two general purpose detectors

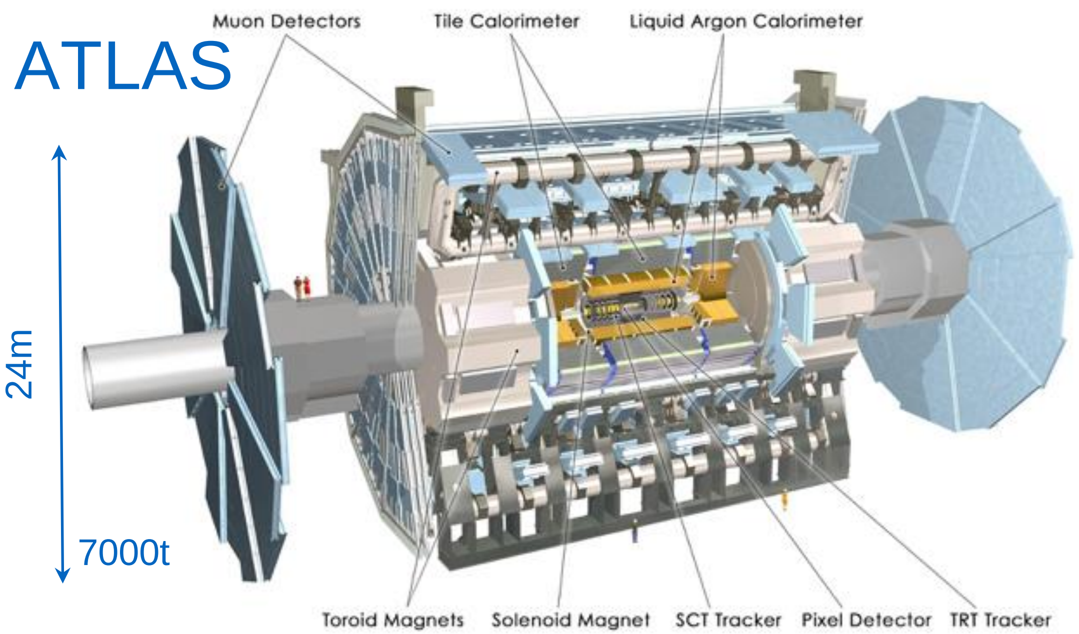

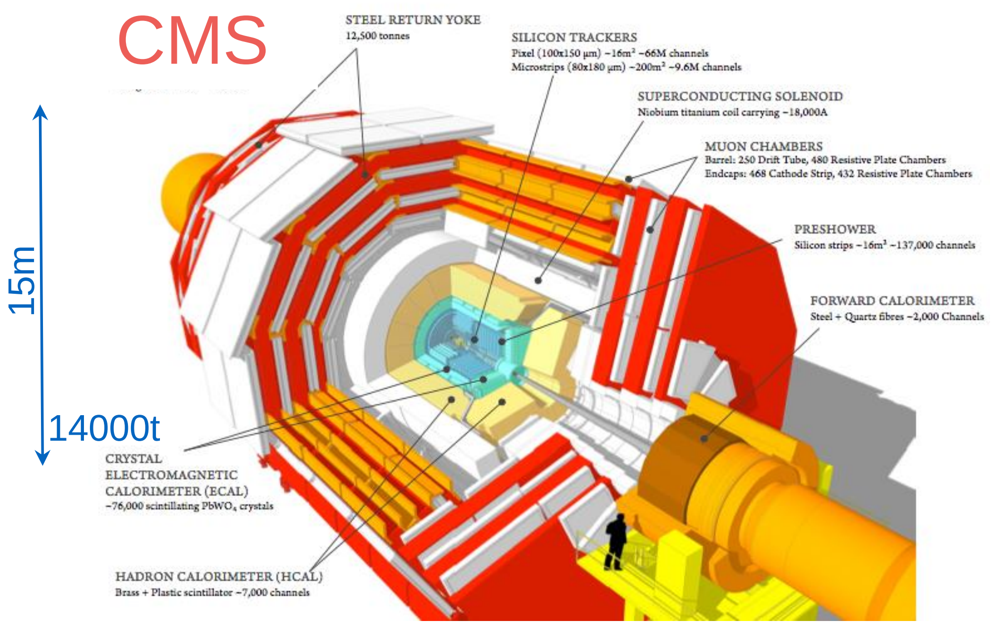

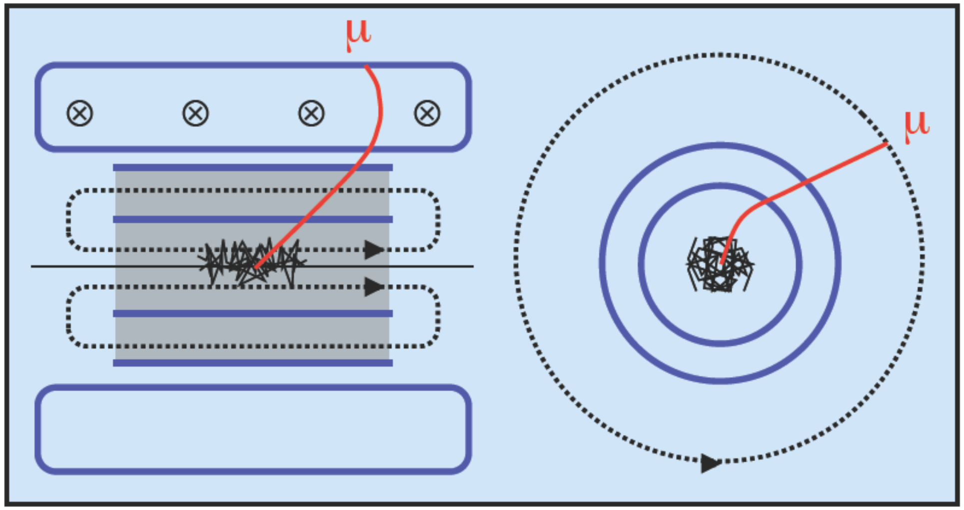

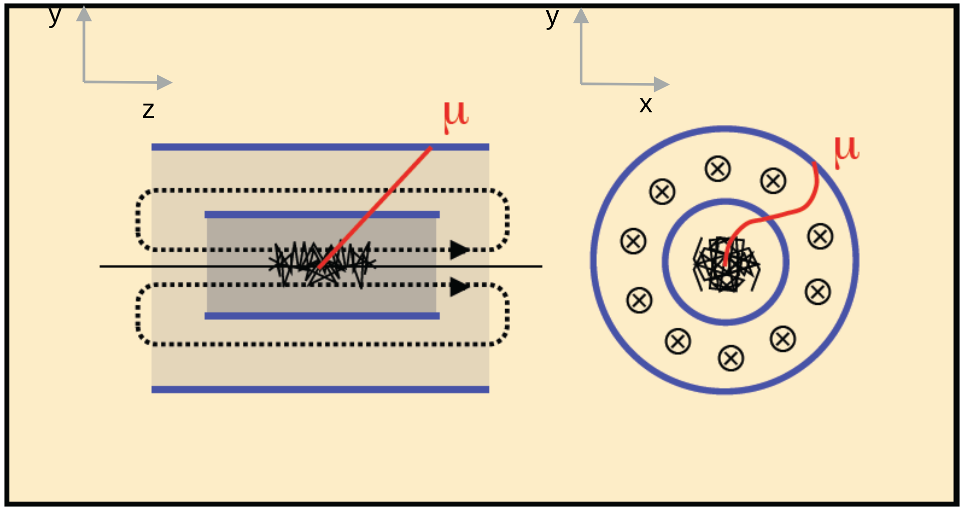

- Standalone measurement of p(μ)
- Resolution is flat in η and independent of pileup

- Two complementary p(μ) measurements
- Tracks point to primary vertex

Particles and their interactions

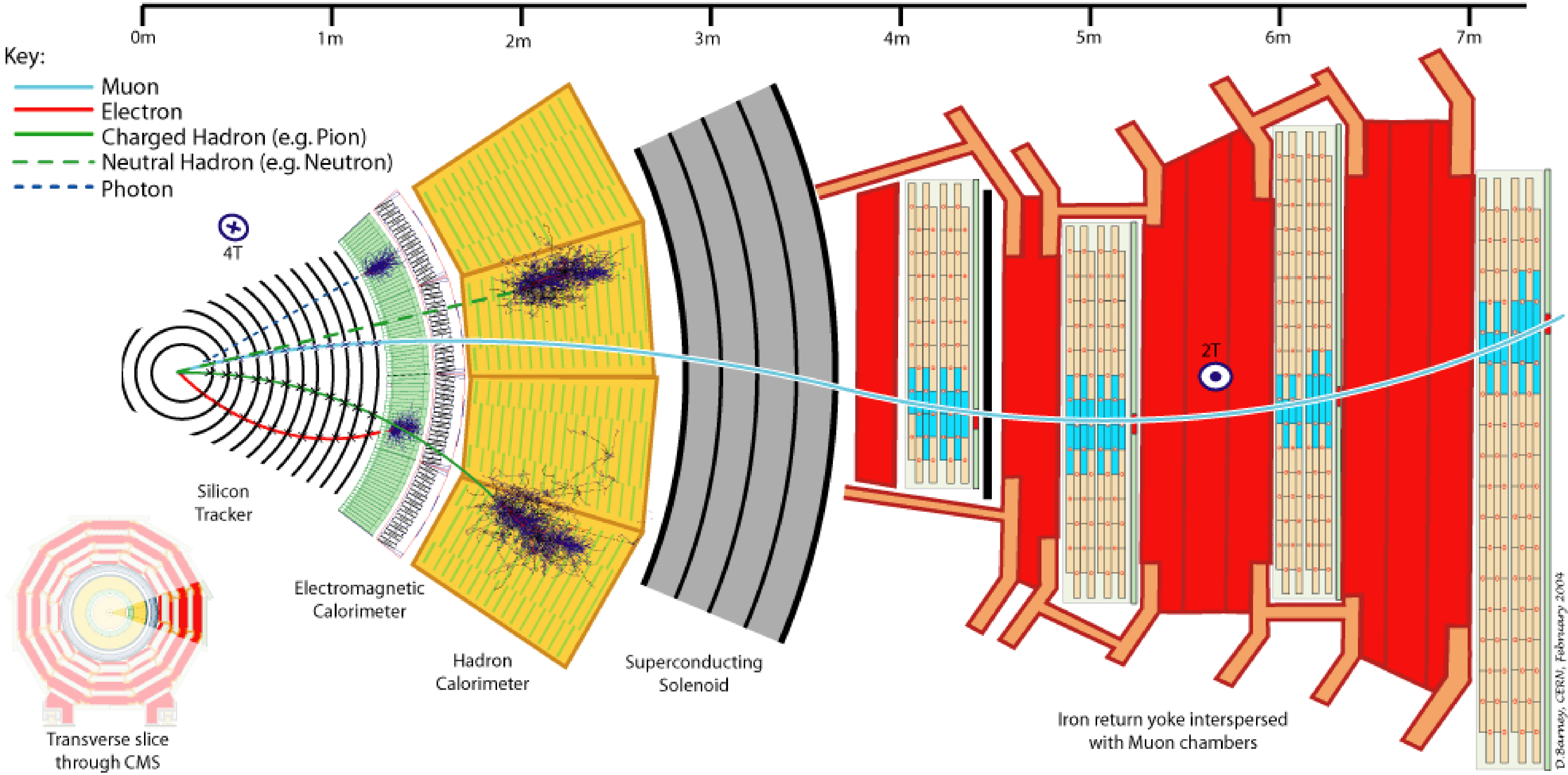

Material distribution in general purpose detectors

B field source

High-Z materials

Dense materials (e.g. Iron, Copper, Brass, Stainless Steel, Uranium)

Lightweight materials (Si, gaseous)

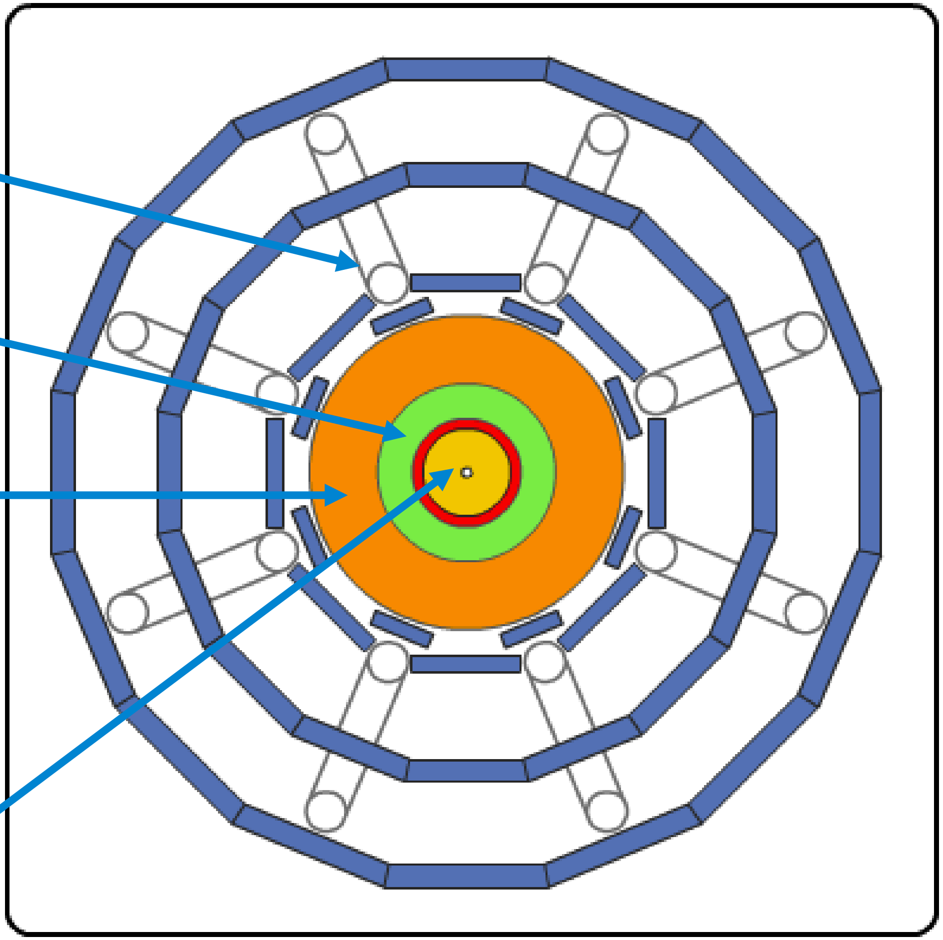

it’s a challenge to fit it all within volume
trade-off between best energy resolution and particle identification

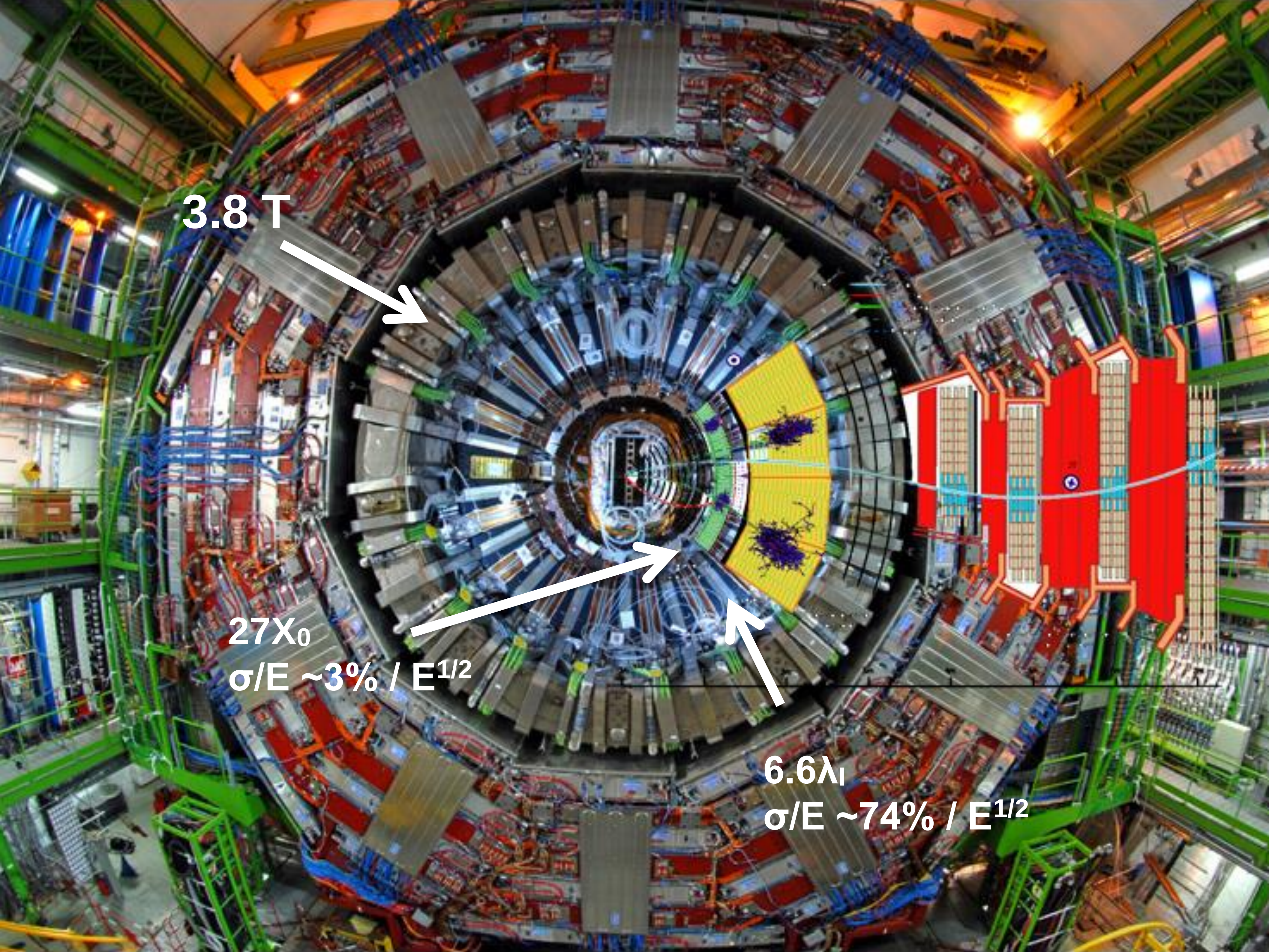
3.8 T
27X0
σ/E ~3% / E1/2
6.6λI
σ/E ~74% / E1/2

Particle flow

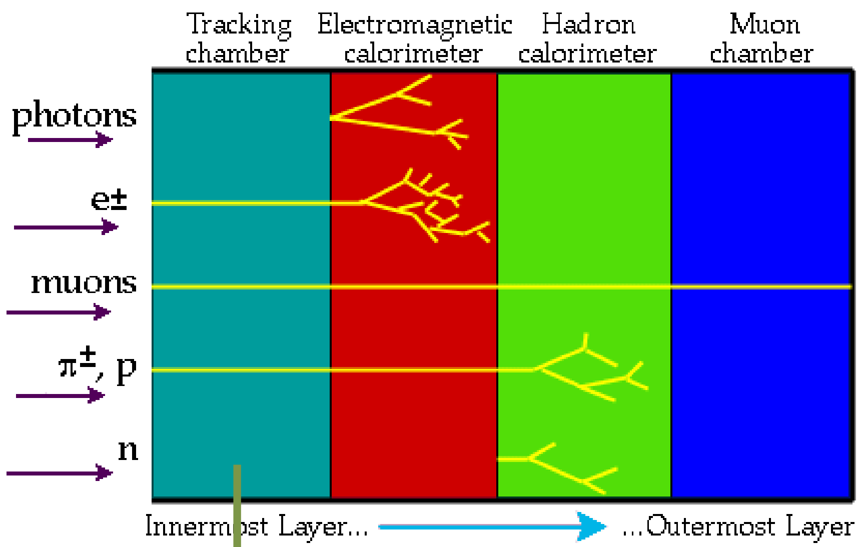

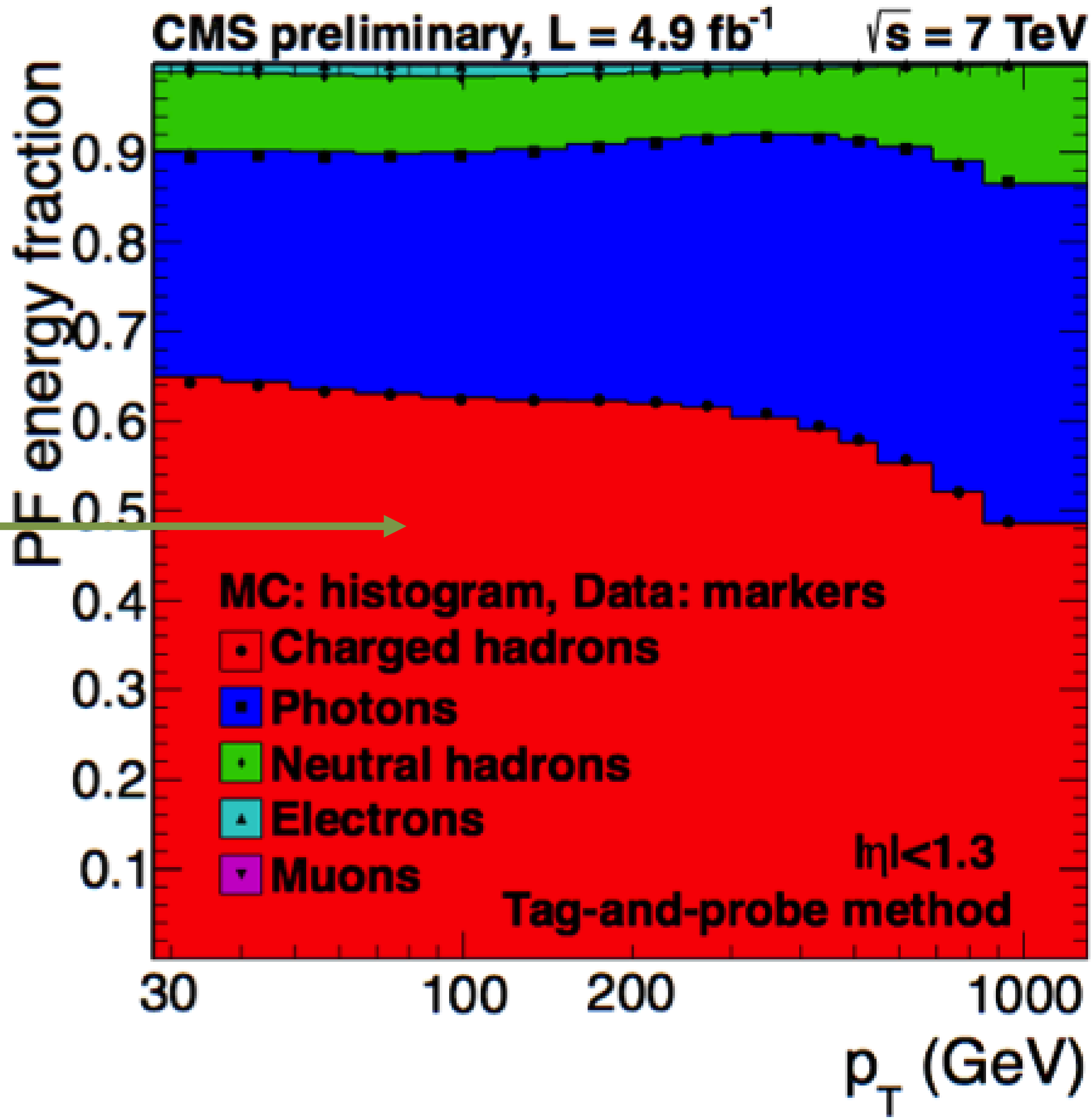

>60% of the energy of a jet may be reconstructed at the level of the tracker

Example: a jet of 5 particles

- Reconstruction starts in the tracker (start from easy tracks, use remaining hits for others)
  - but that does 2/3 particles in this jet

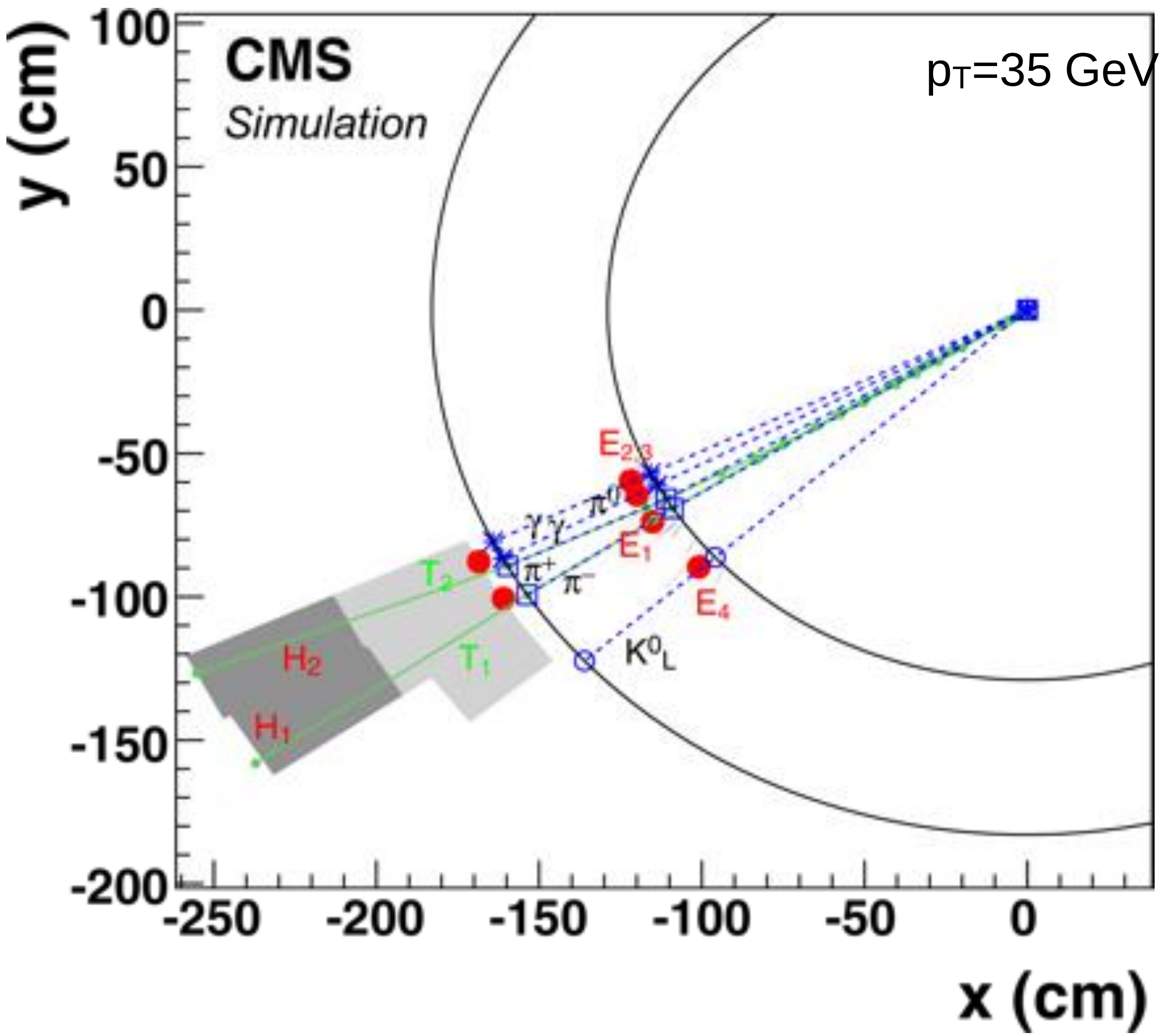

Example: a jet of 5 particles

- Coarse granularity in the hadronic calorimeter
- See local energy maxima, connect neighbours
- Determine energy sharing iteratively

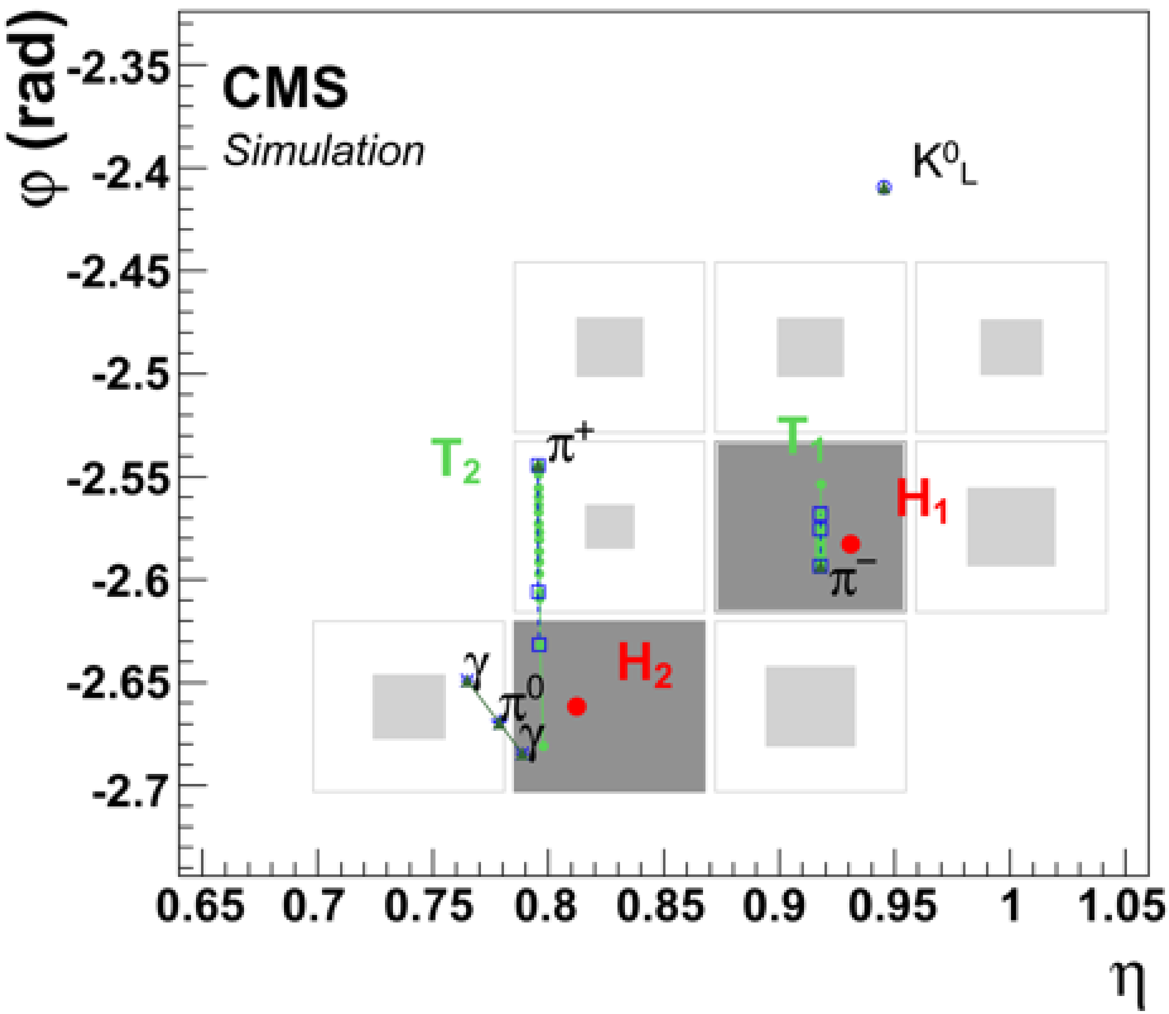

Example: a jet of 5 particles

- The electromagnetic calorimeter sees things in coarser detail ($\Delta\phi,\Delta\eta$~0.02)
- Use to refine entry point in calorimeter, link to tracks and balance energy
- Cluster energy unassociated to tracks: photons and neutral hadrons

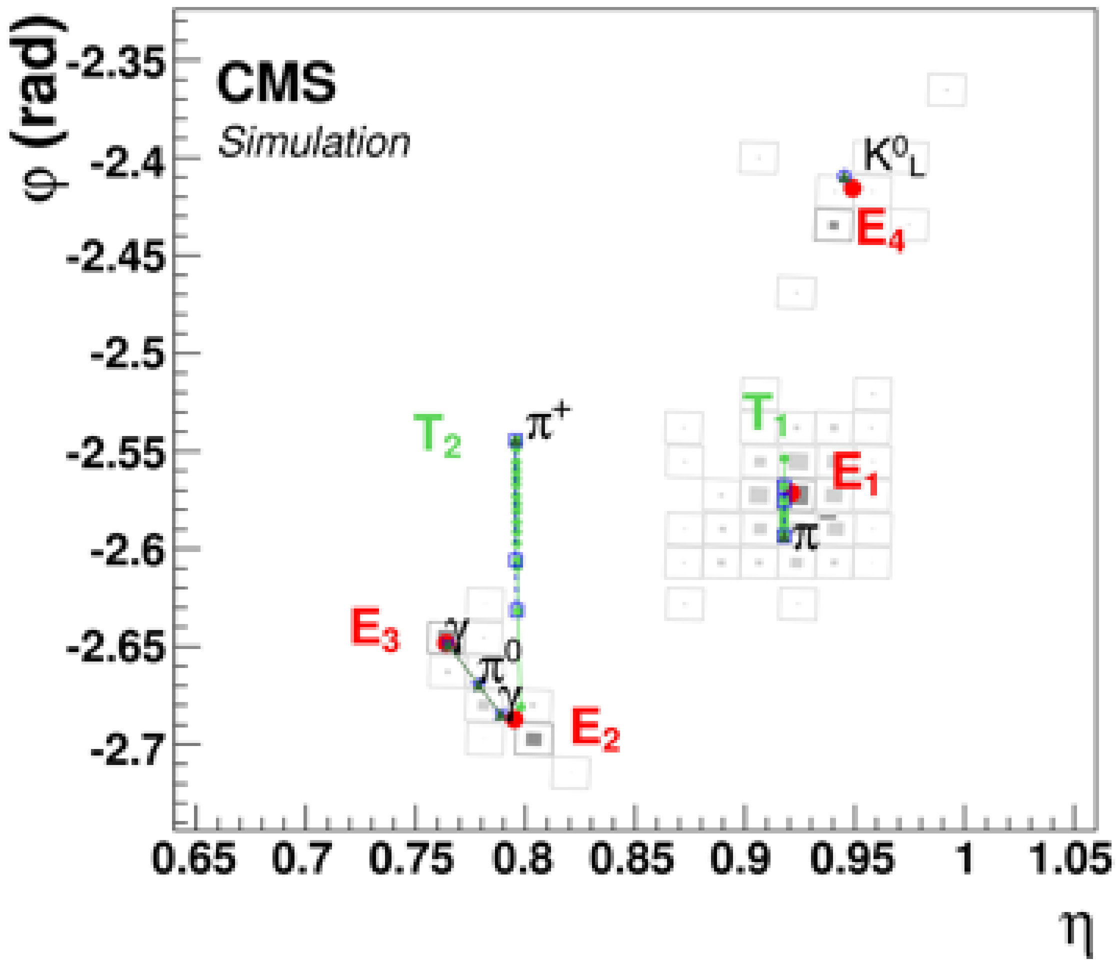

Particle flow algorithm is a reconstruction paradigm

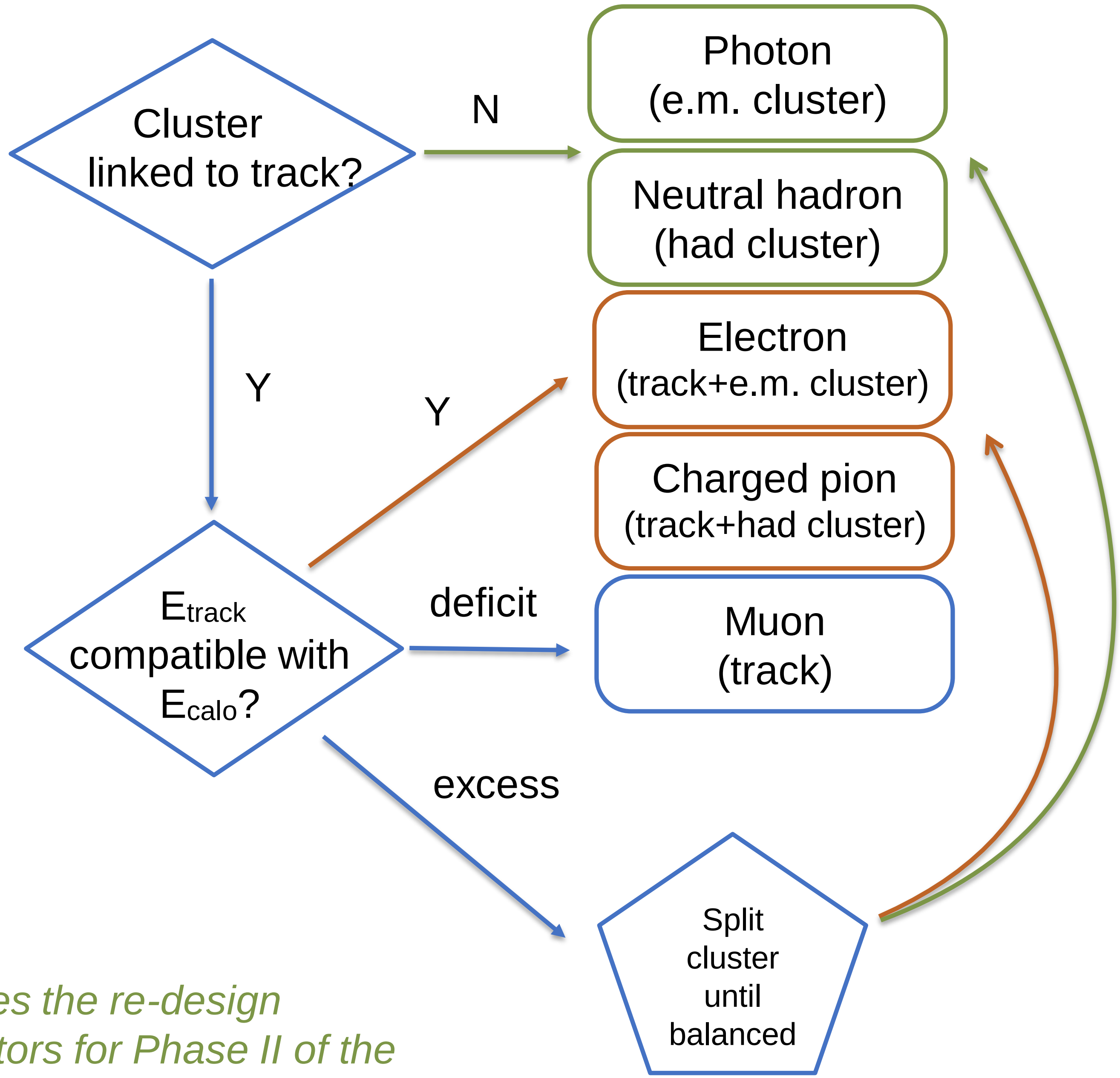

it also shapes the re-design of the detectors for Phase II of the LHC

Particle flow algorithm is a reconstruction paradigm

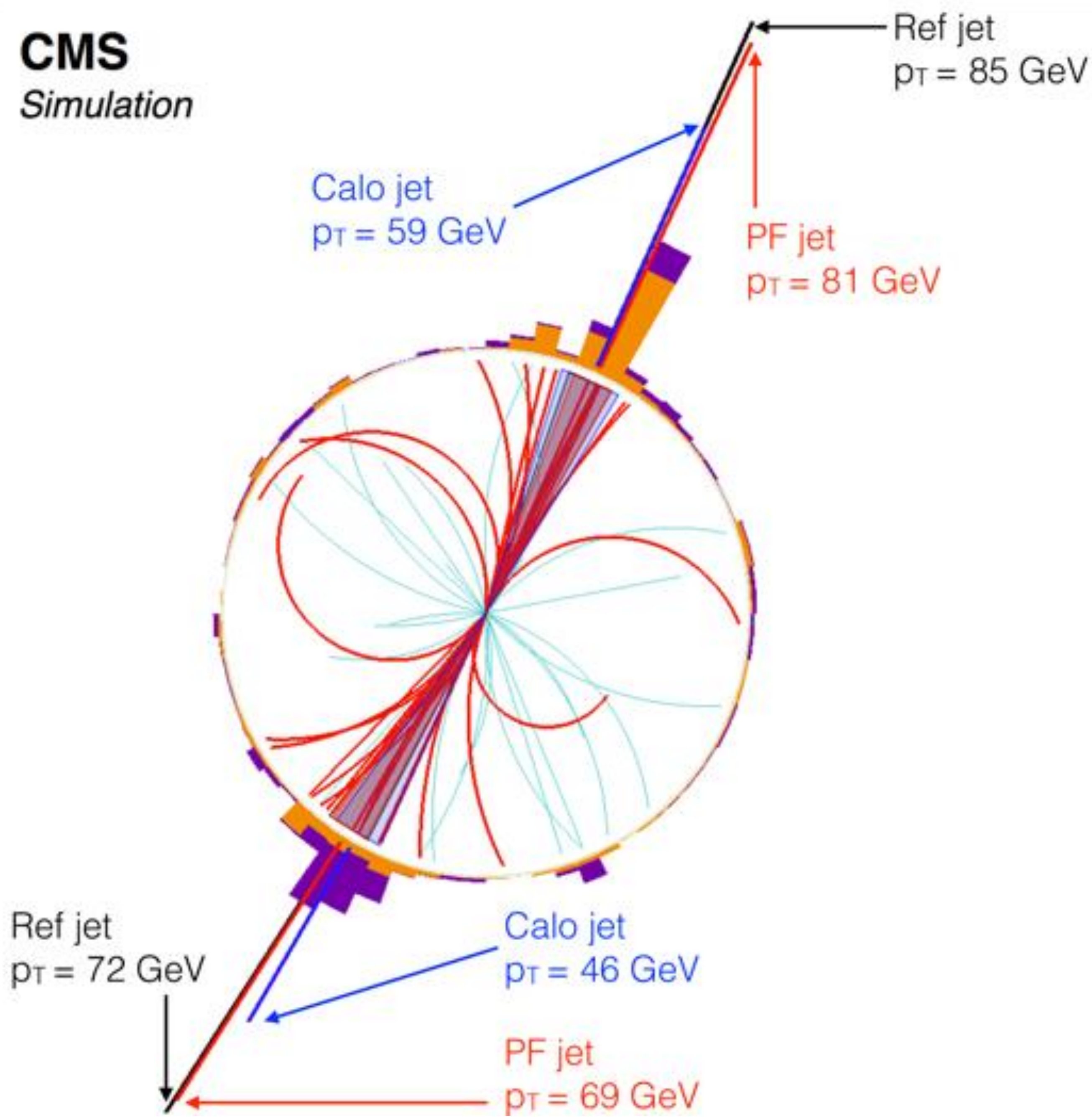

Connecting the dots with tracking

Why?

- Identify the vertex from the hard interaction

…but also secondary vertices from long lived particles

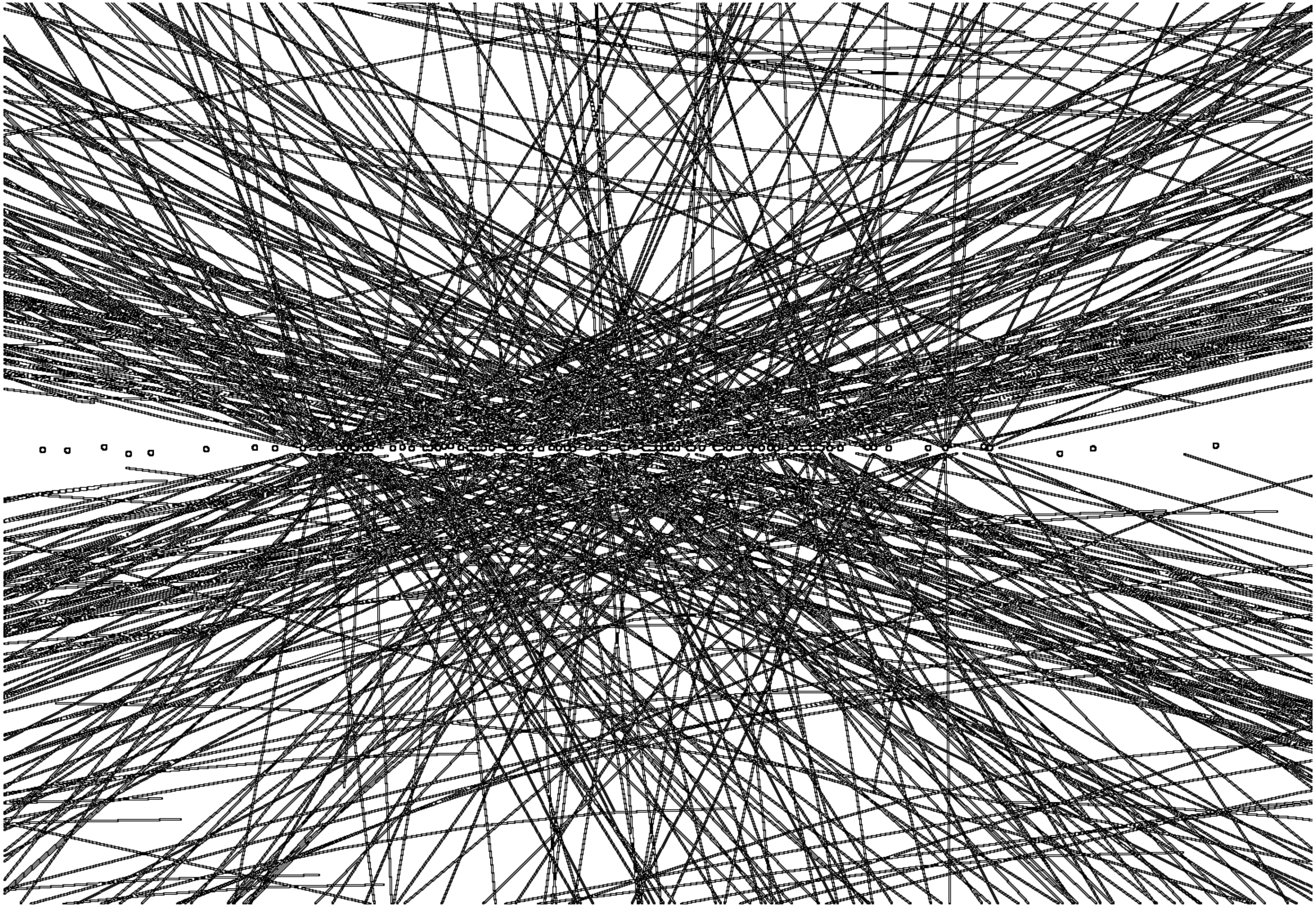

Why?

- Identify the vertex from the hard interaction

  …but also secondary vertices from long lived particles

- Measure particle trajectories
  - momentum (p), energy loss (dE/dx), link to coarser calorimeters and muon chambers

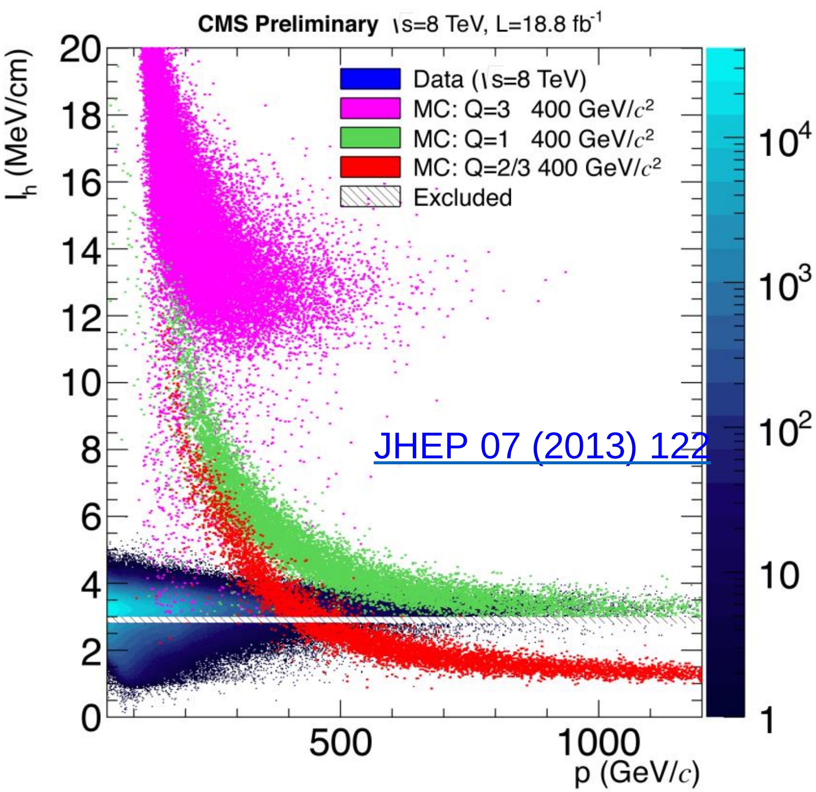

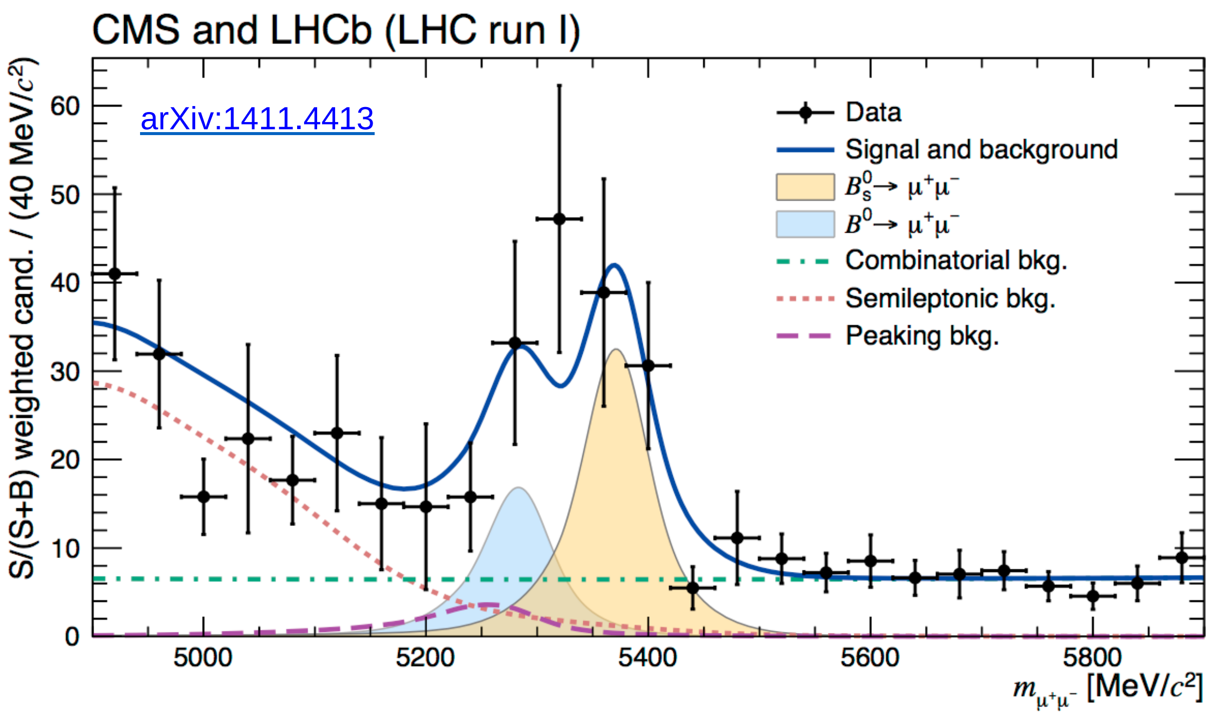

With what?

- Solid state detectors
  - Ge, Si, Diamond,...
  - pixels and strips

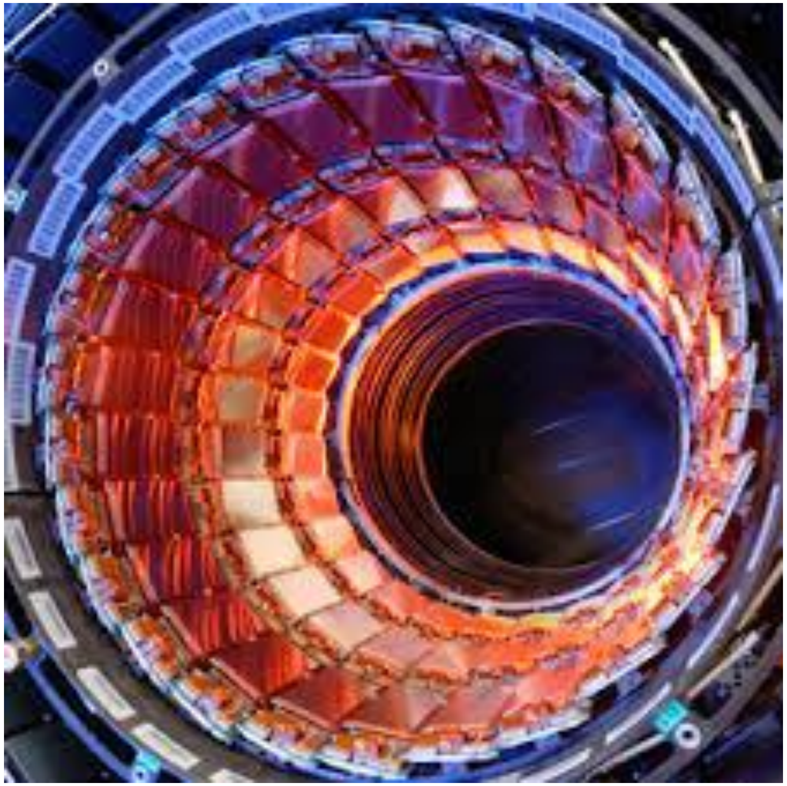

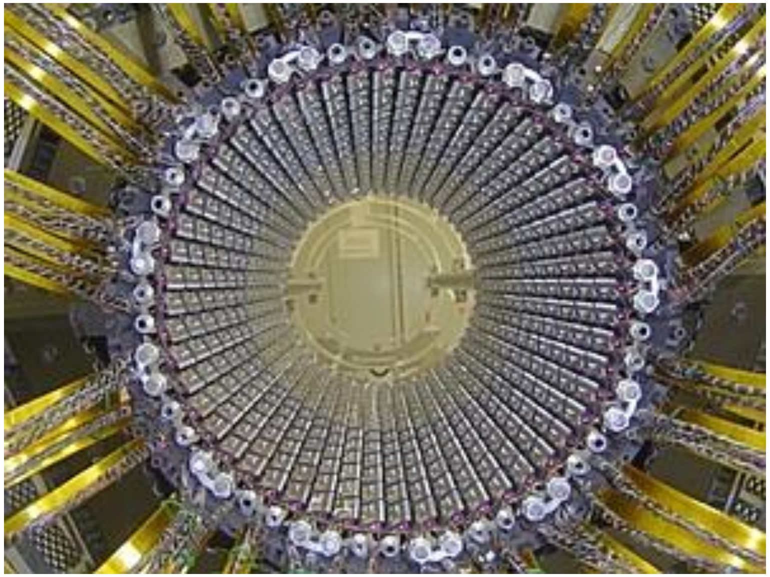

With what?

- Gaseous detectors
  - drift tubes, resistive plate chambers, cathod strip chambers, gas electron multipliers, ...
  - usually for outer tracking

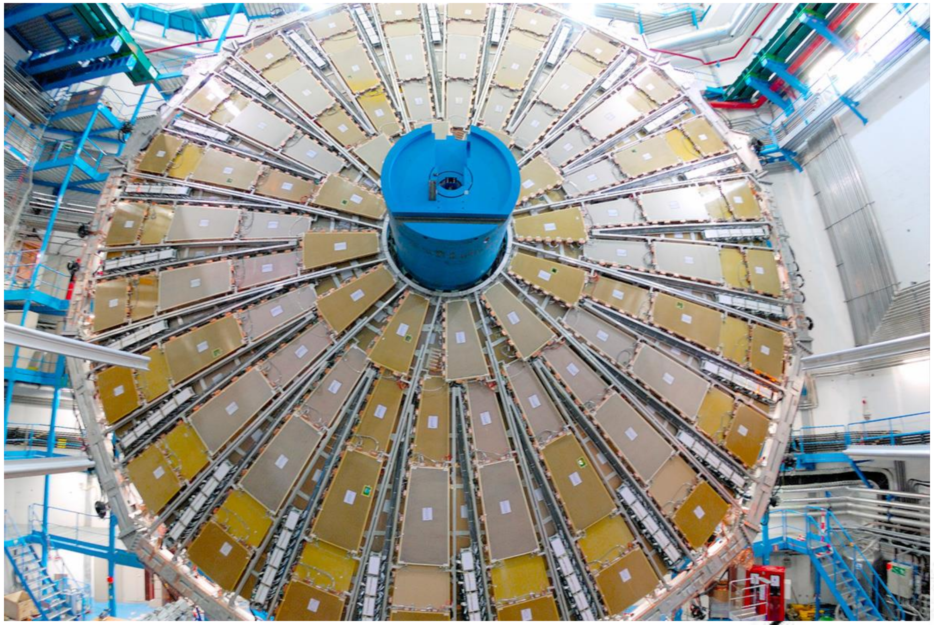

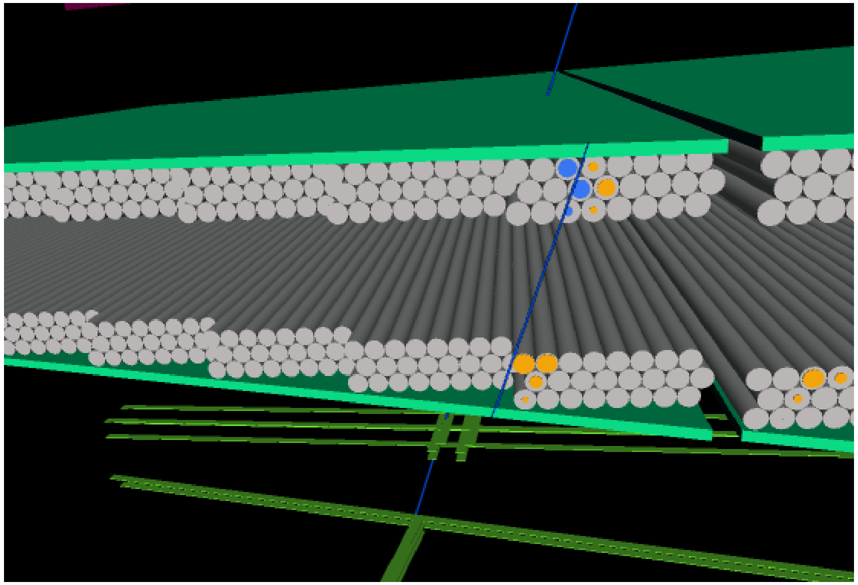

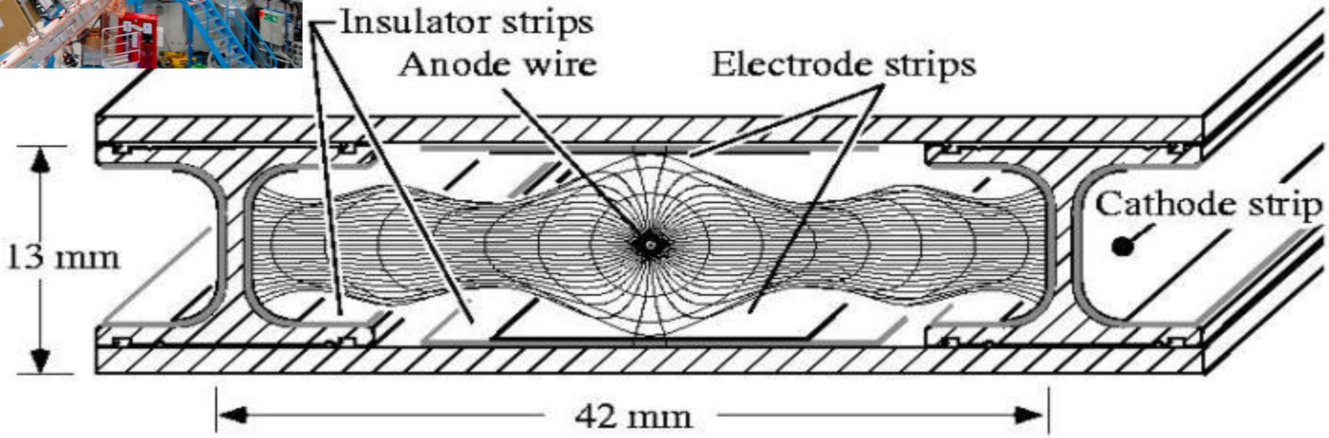

How?

- While transversing a medium a charged particle leaves an ionization trace
  - create a depletion zone in between electrodes: gaseous, liquid or solid-state (semi-conductor)
  - ionization charges drift towards electrodes
  - amplify electric charge signal and deduce position from signals collected in individual strips

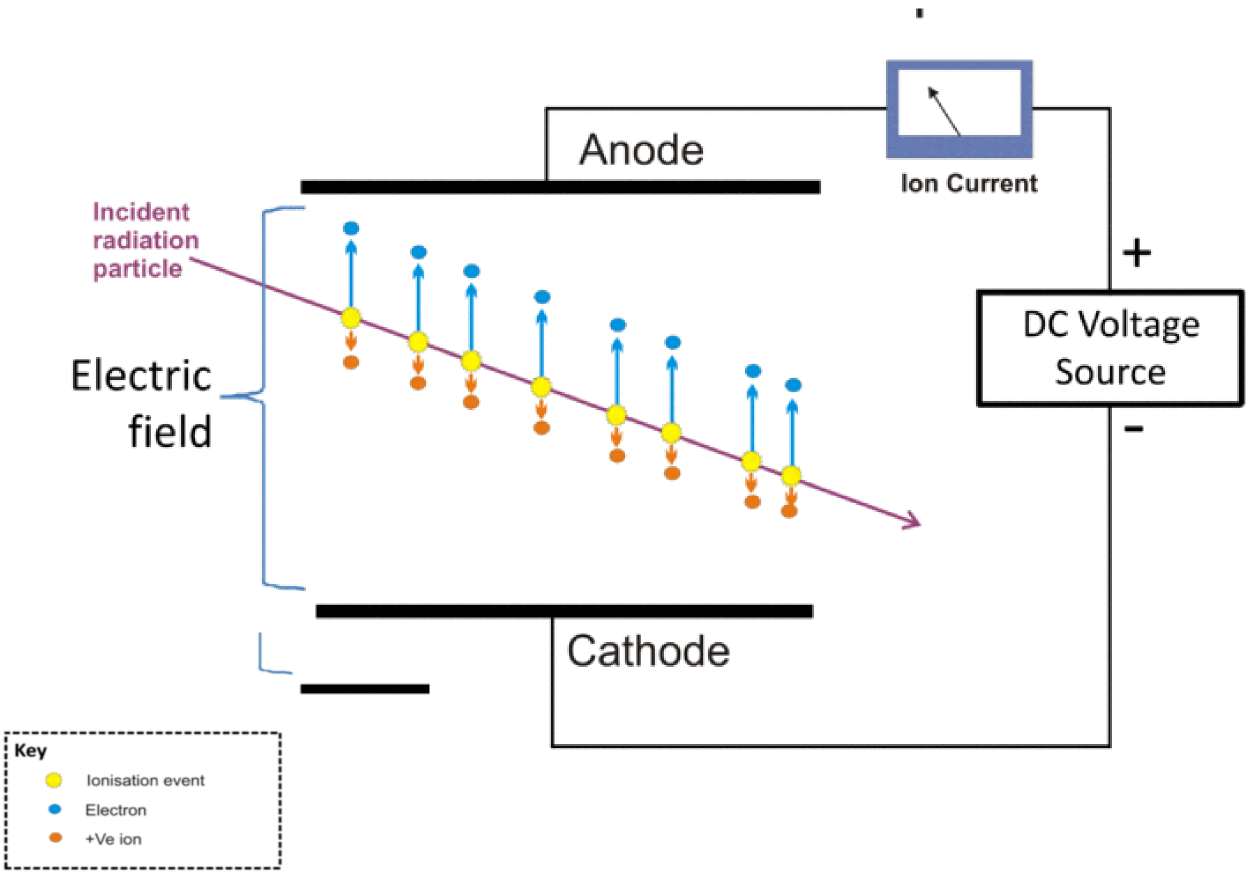

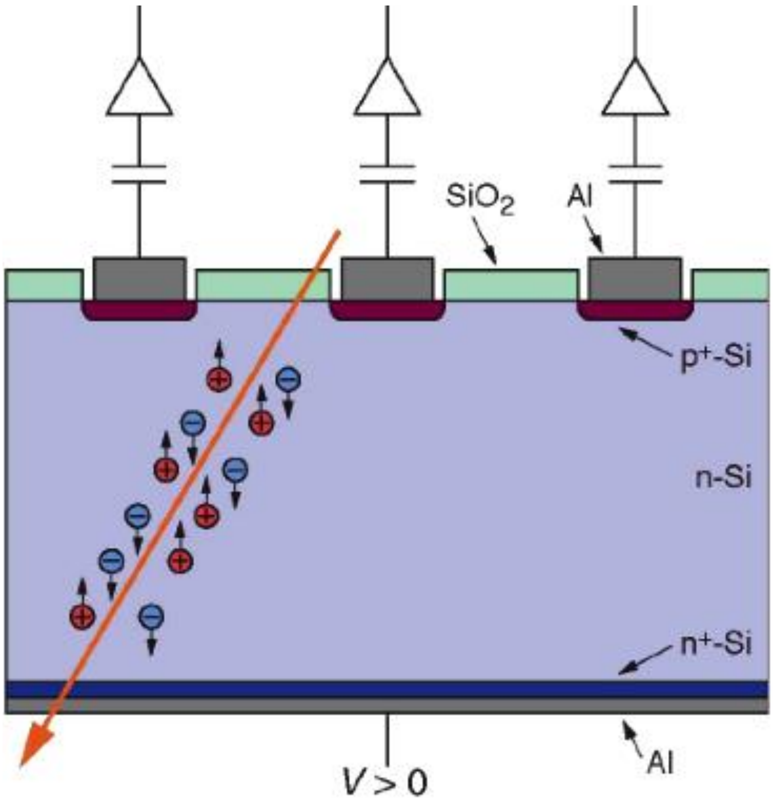

ionization chamber ≈ ***Si strip detector***

Gaseous versus solid state

- In solid state detectors ionization energy converts in e-h pairs
  - 10 times smaller with respect to gaseous-based ionization
  - charge is increased → improved E resolution

	Gas		Solid state	
Density (g/cm^3)	Low	$C_2H_2F_4$	High	Si
Atomic number (Z)	Low	(~95% for CMS RPC)	Moderate	
Ionization energy (ε_I)	Moderate	30eV	Low	3.6eV
Signal speed	Moderate	10ns-10μs	Fast	<20ns

$$n = \frac{E_{loss}}{E_{eh}} \rightarrow \frac{\sigma_E}{E} \propto \frac{1}{\sqrt{n}} \propto \sqrt{\frac{E_{eh}}{E_{loss}}}$$

Gaseous versus solid state

- Higher density materials are used in solid state detectors
  - charge collected is proportional to the thickness
  - most probable value for Silicon

$$\frac{\Delta_p}{x} \sim 0.74 \cdot 3.876\ \mathrm{MeV/cm} \rightarrow N_{eh} \sim \frac{23 \cdot 10^3}{300\ \mu m}$$

  - excellent spatial resolution: short range for secondary electrons

Inner tracking at the LHC

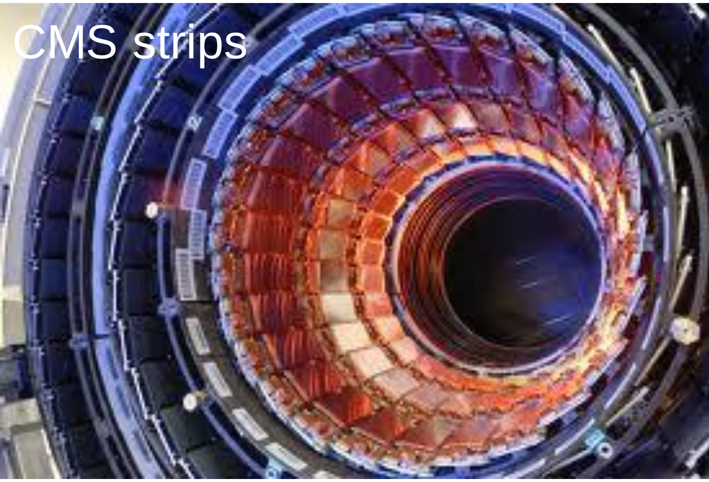

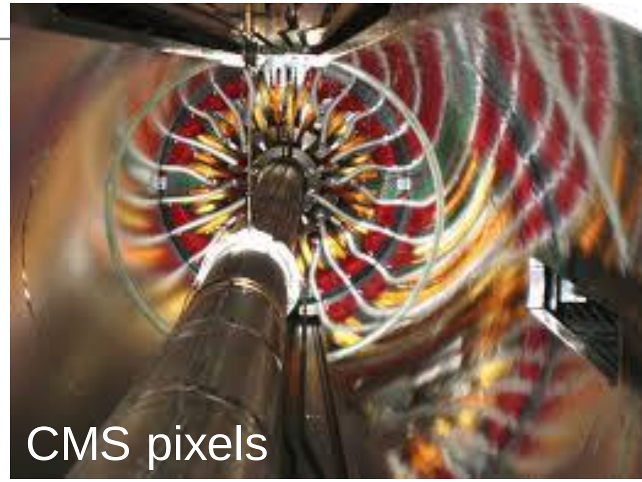

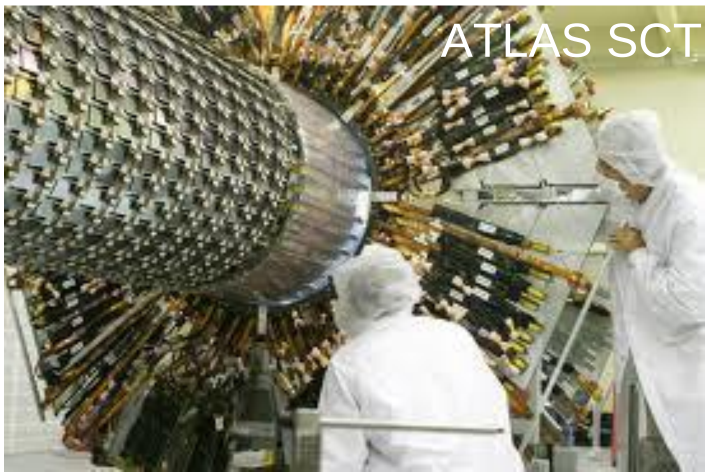

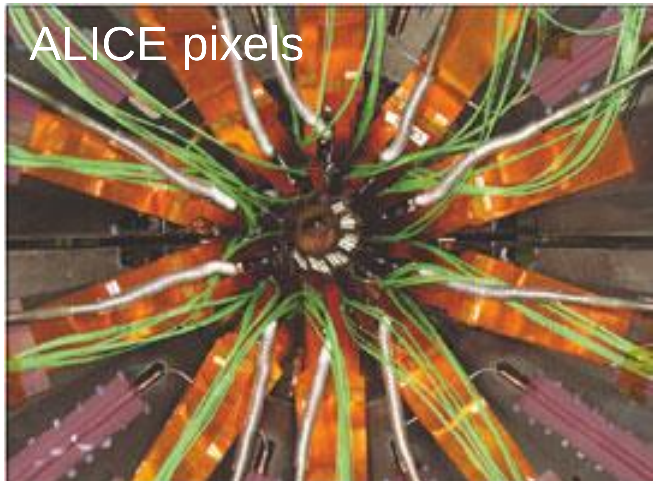

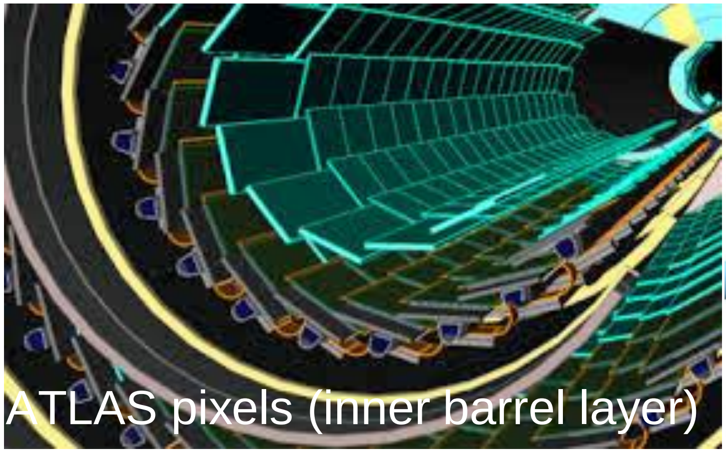

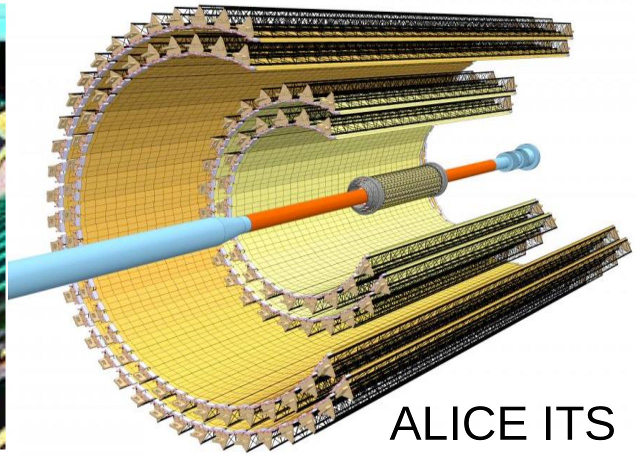

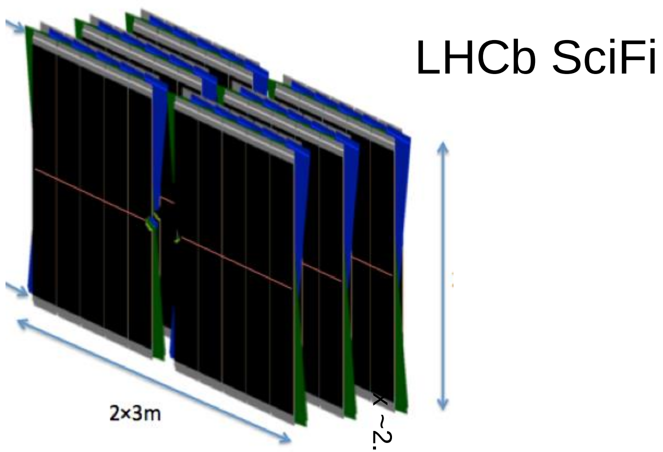

Outer ⟷ inner tracking

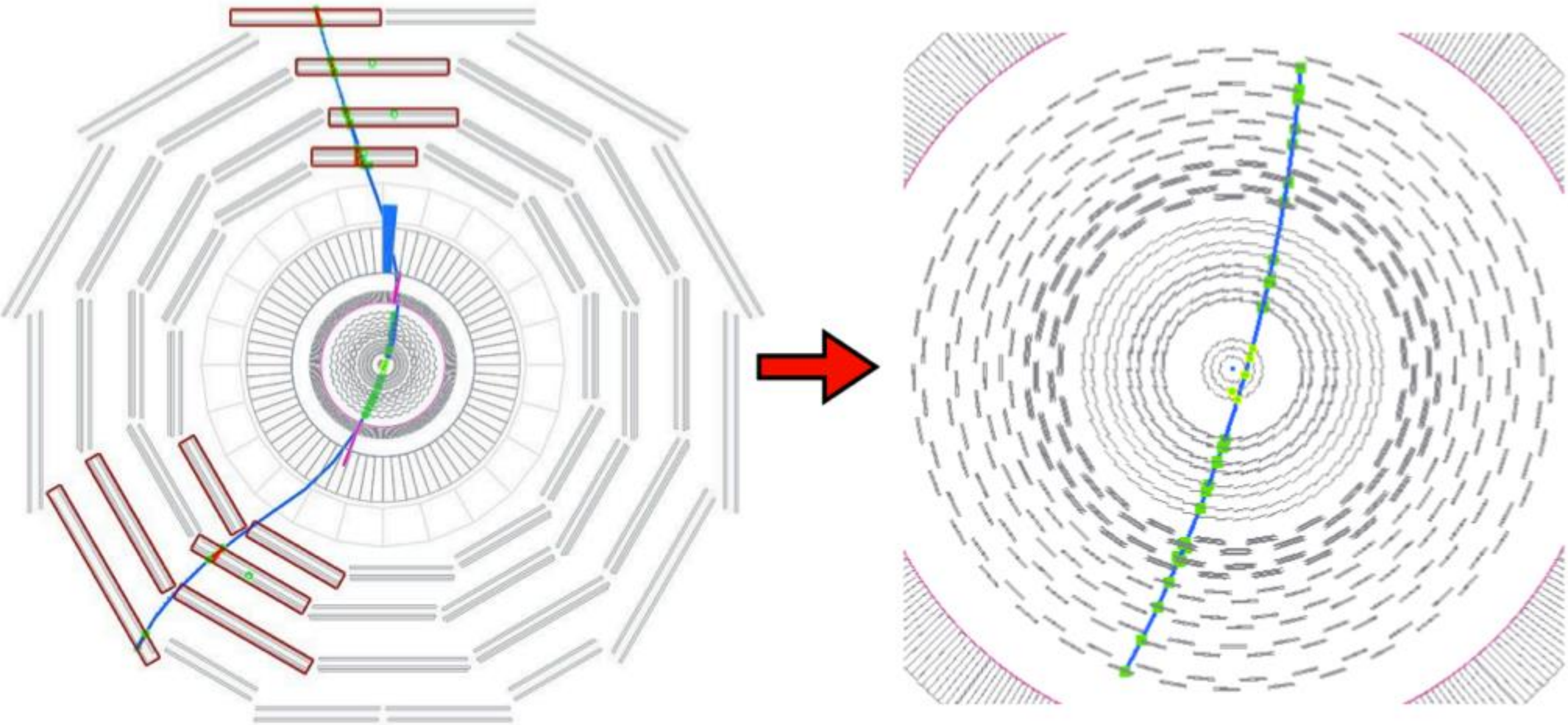

Coordinates for tracking

- The LHC experiments use a uniform B field along the beam line (z-axis)
  - trajectory of charged particles is an helix – radius R
  - use transverse (xy) and longitudinal (rz) projections
  - pseudo-rapidity: $\eta = -\ln \tan\frac{\theta}{2}$ transverse momentum: $p_{\mathrm{T}} = p \sin\theta = p/\cosh\eta$
- Impact parameter is defined from distance of closest approach to primary vertex

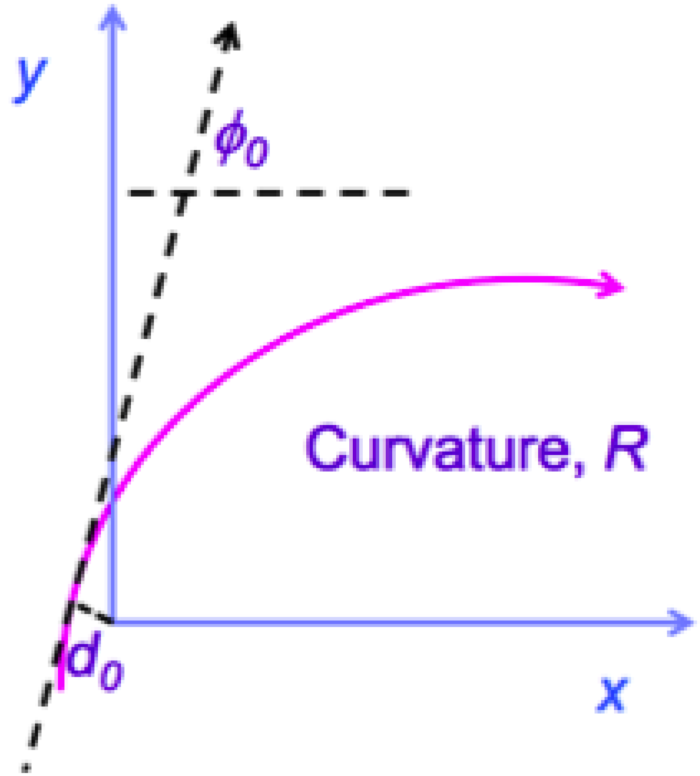

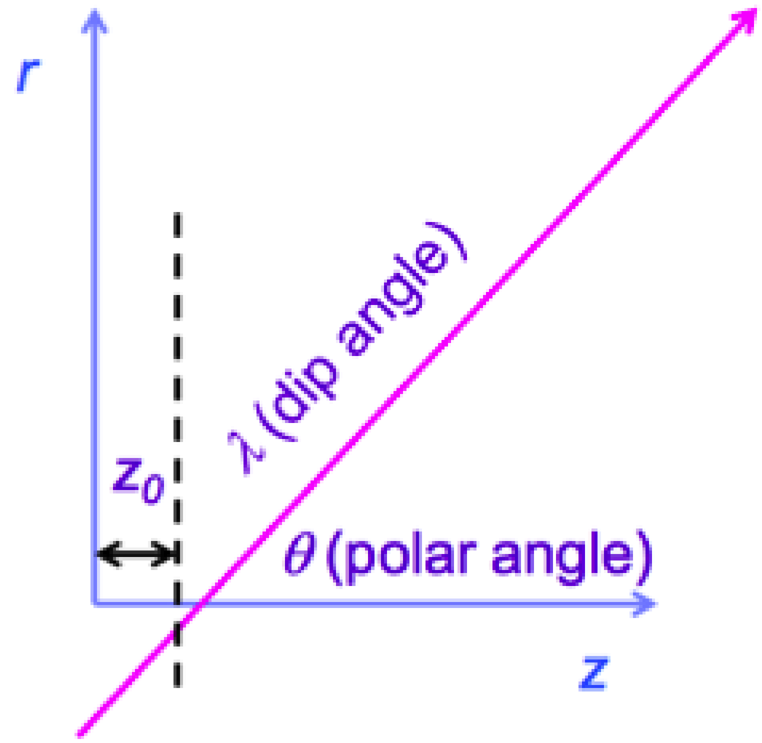

Resolution for the impact parameter

- Depends on radii+space point precisions

- For two layers we expect

$$\sigma_{d0}^2 = \frac{r_2^2\sigma_1^2 + r_1^2\sigma_2^2}{(r_2 - r_1)^2}$$

  - Improve with small r_1, large r_2
  - Improves with better σ_i

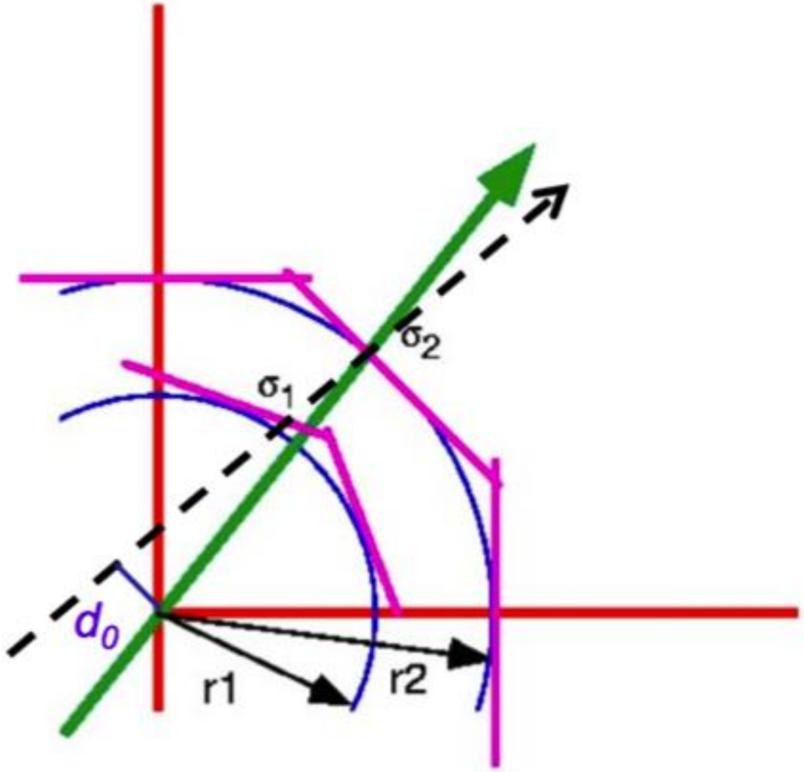

Resolution for the impact parameter

- Depends on radii+space point precisions

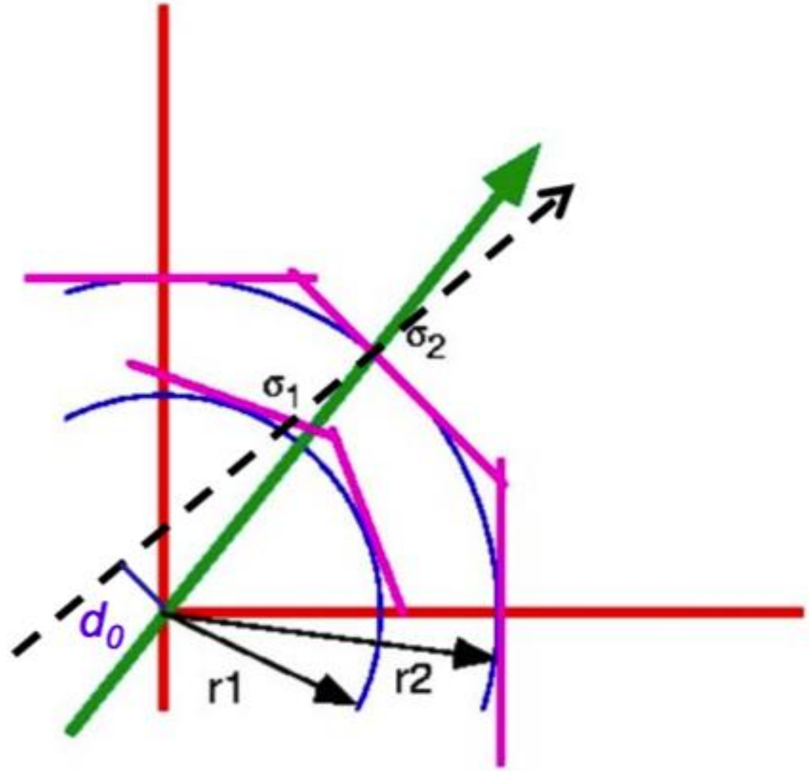

- For two layers we expect

$$\sigma_{d0}^2 = \frac{r_2^2\sigma_1^2 + r_1^2\sigma_2^2}{(r_2 - r_1)^2}$$

  - Improve with small r_1, large r_2
  - Improves with better σ_i

- Precision is degraded by multiple scattering
  - Gaussian approximation is valid
  - Width given by

$$\theta_0 = \frac{13.6\text{MeV}}{\beta c p} z \sqrt{x / X_0}\left[1 + 0.038 \ln(x / X_0)\right]$$

  - extra degradation term for d_0 $\quad \sigma_{d_0} \sim \theta_0$

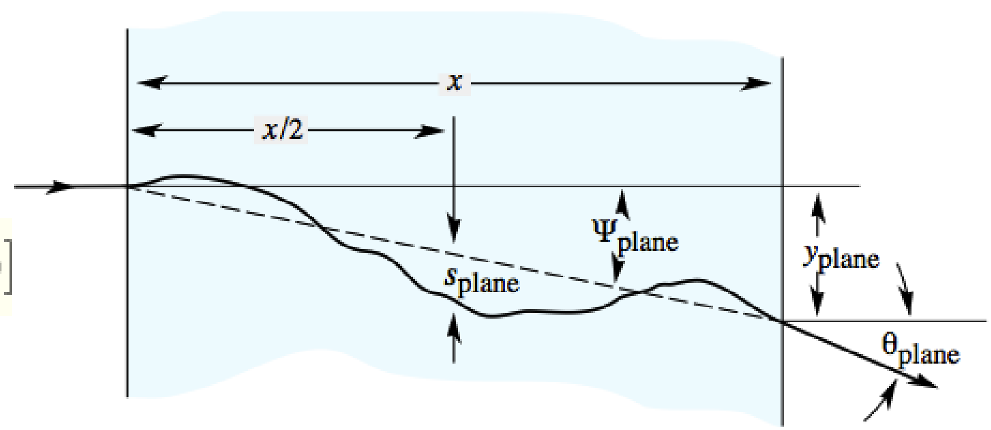

Resolution for the impact parameter

- For a track with $\theta \neq 90^0$ we can write $r \to r/\sin\theta$ and $x \to x/\sin\theta$

- By substitution in the formulas of the previous slide we have:

$$\sigma_{d_0} \sim \sqrt{\frac{r_2^2\sigma_1^2 + r_1^2\sigma_2^2}{(r_2 - r_1)^2}} \oplus \frac{r}{p\sin^{3/2}\theta} \to a \oplus \frac{b}{p_T \sin^{1/2}\theta}$$

geometry-dependent Material- and p_T-dependent

- Typical resolution expected/measured
  - 100 μm @ 1 GeV 20 μm @ 20 GeV

- Typical lifetimes (rest frame)
  - B ~ 500μm D^0 ~120μm τ ~ 87 μm

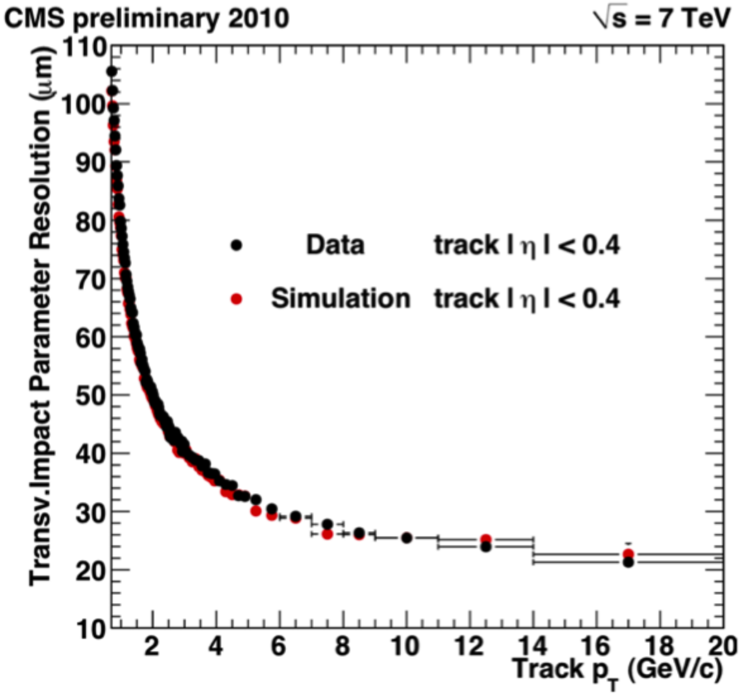

Momentum measurement

- Circular motion under uniform B-field

$$p_T[\mathrm{GeV}] = 0.3 \times q \times B[\mathrm{T}] \times R[\mathrm{m}]$$

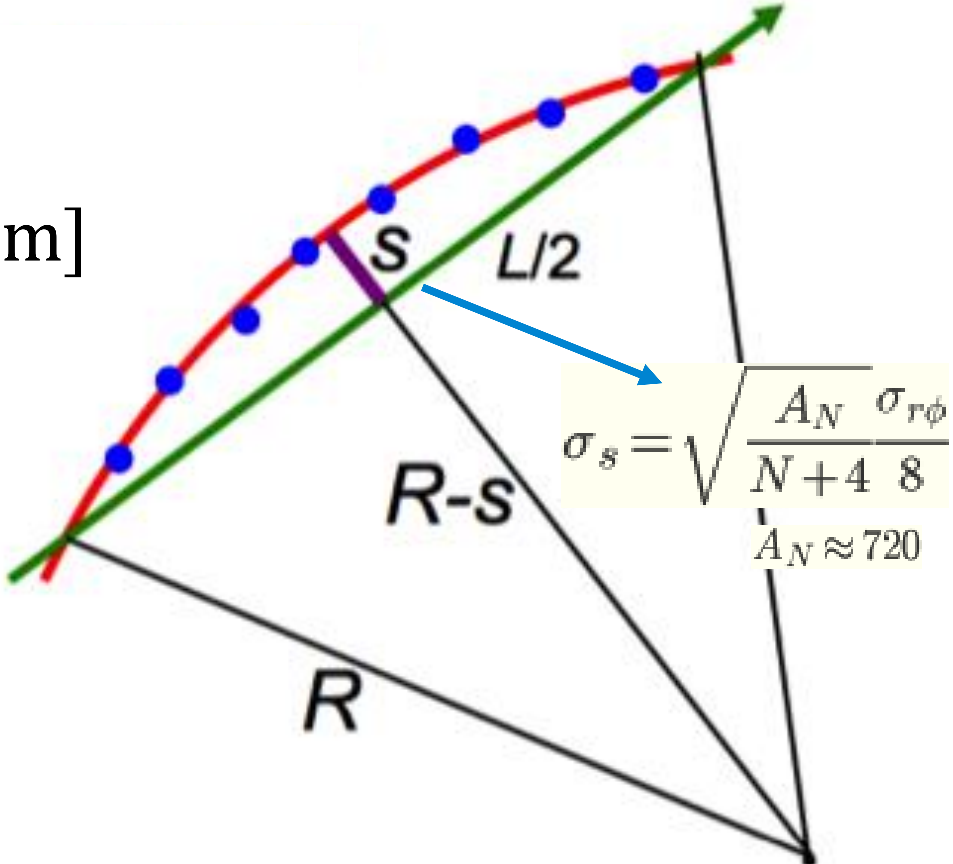

- Typically measure the sagitta
  - deviation to straight line relates to R by

$$R = \frac{L^2}{2s} + \frac{s}{2} \approx \frac{L^2}{2s}$$

- Uncertainty in pT measurement improves with B, number of hits and path

$$\frac{\sigma_{p_\mathrm{T}}}{p_\mathrm{T}} = \frac{8 p_\mathrm{T}}{0.3 B L^2}\sigma_s$$

- Multiple scattering introduces, again extra degradation

$$\frac{\sigma_{p_\mathrm{T}}}{p_\mathrm{T}} \sim a p_\mathrm{T} \oplus \frac{b}{\sin^{1/2}\theta}$$

Momentum resolution

$$\frac{\sigma_{p_T}}{p_T} \sim a\,p_T \oplus \frac{b}{\sin^{1/2}\theta}$$

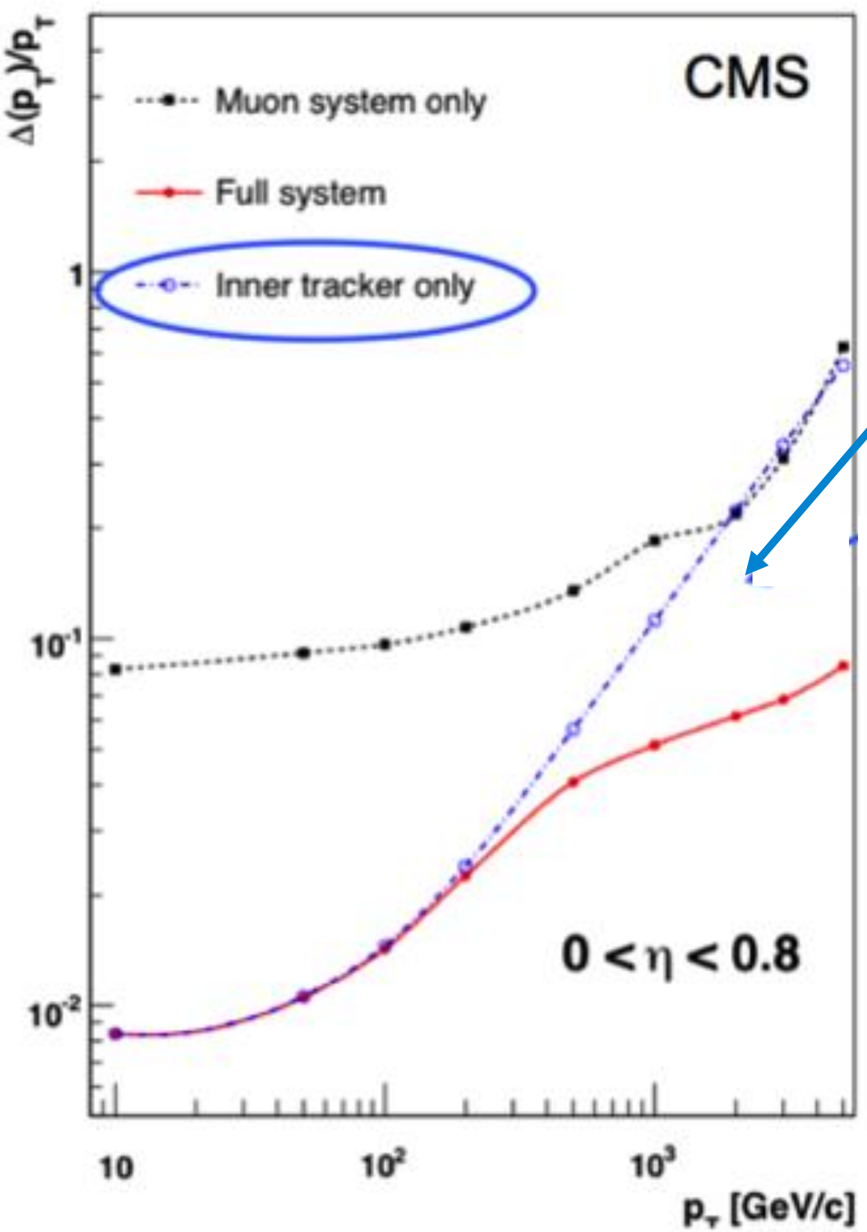

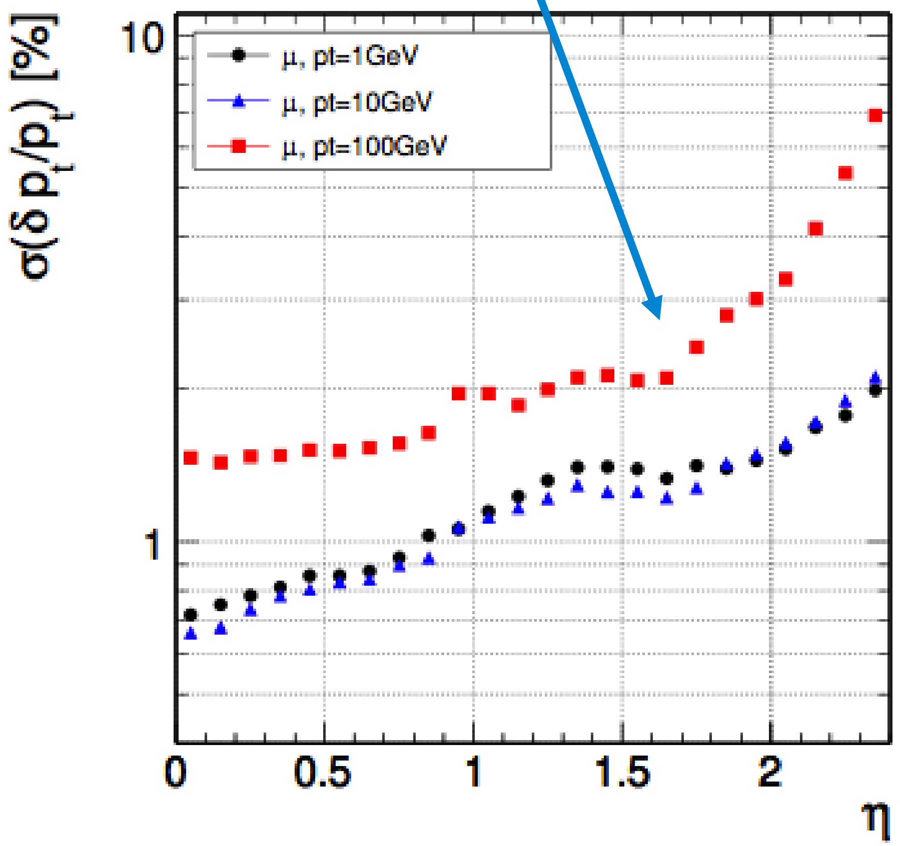

Si-based detectors

Usage of Si-based trackers for HEP

- Kemmer, 1979 transferred Si-technology for electrons to detector - NIM 169(1980)499
- NA11/32 spectrometer at CERN →
  - 6 planes Si-Strip, <2k channels
  - Resolution ~4.5μm
- SLD vertex detector at SLAC →
  - 120-307 M pixels: 0.4%X0
  - Resolution <4μm, d_0~11-9μm
- ALEPH detector at LEP →
  - Enable precise measurements for B-physics (lifetime, b-tagging)

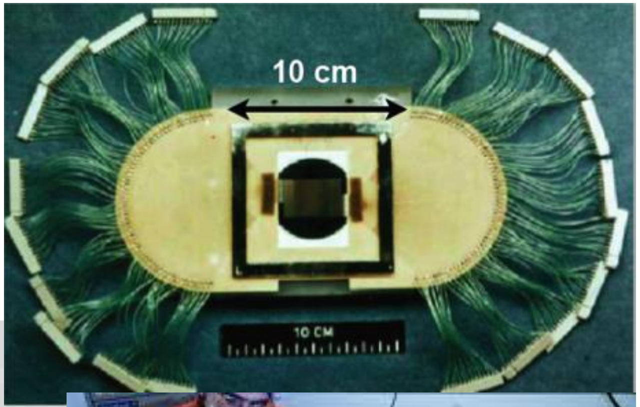

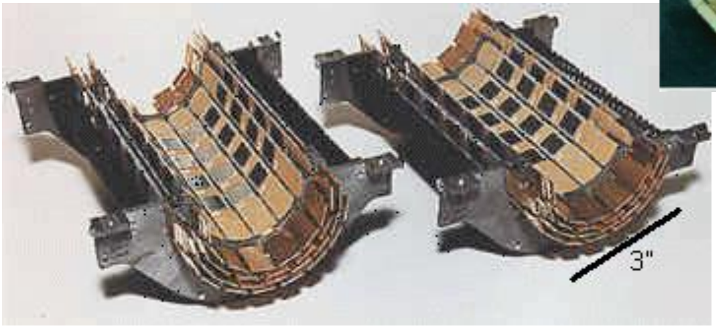

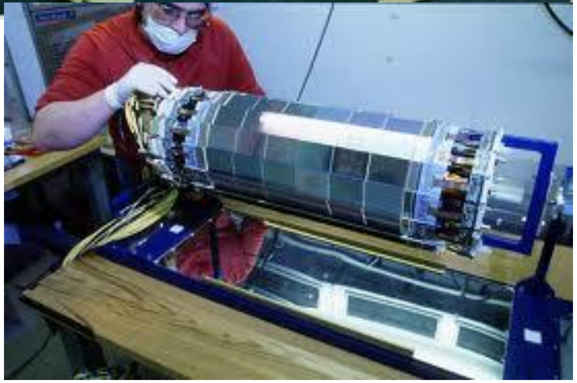

Experiment	Detectors	Channels (10^3)	Si area [m^2]
Aleph (LEP)	144	95	0.49
CDF II (TEV)	720	405	1.9
D0 II (TEV)	768	793	4.7
AMS II	2300	196	6.5
ATLAS (LHC)	4088	6300	61
CMS (LHC)	15148	10000	200

Ionization energy loss in the Si

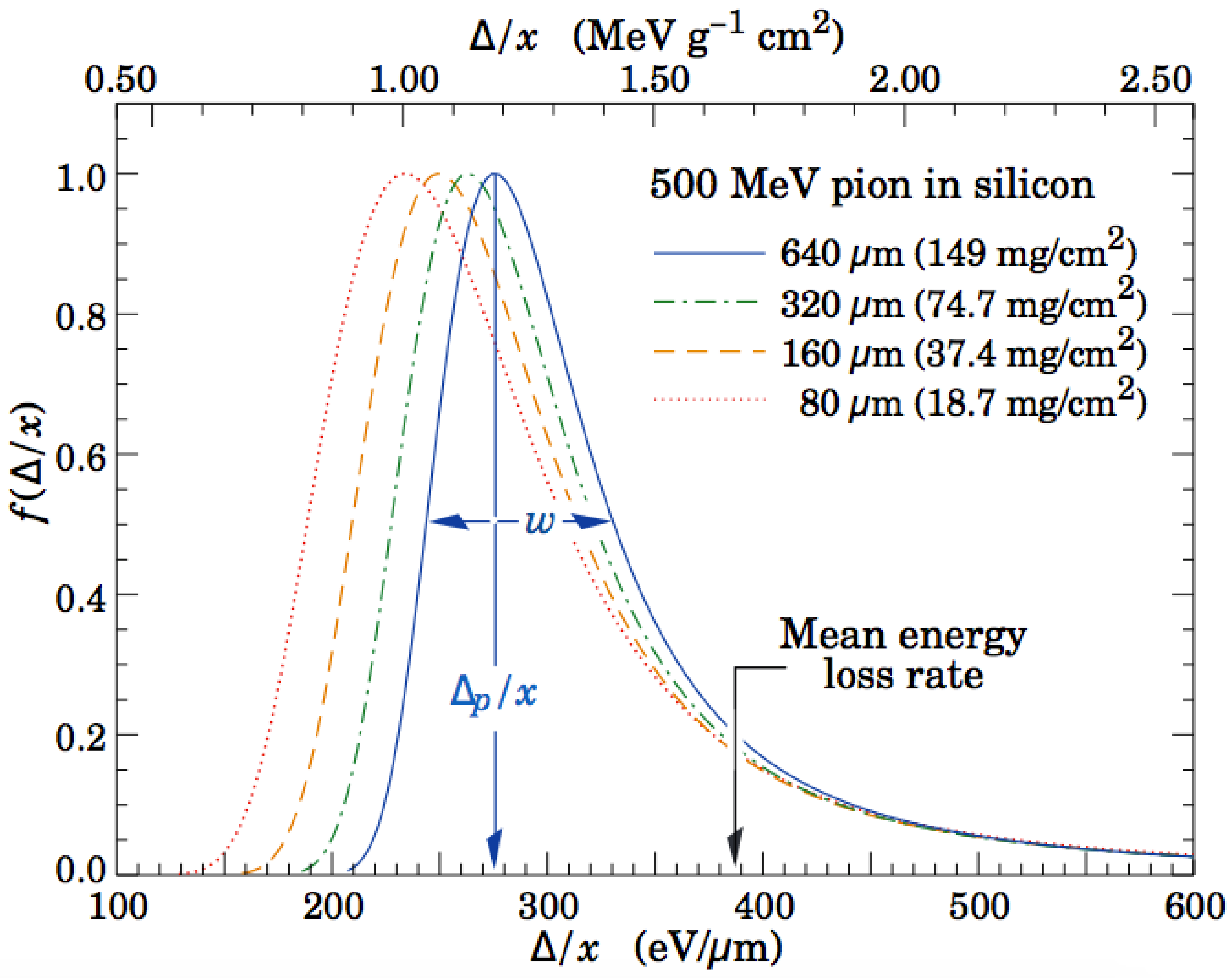

Most probable value of the Landau distribution for energy loss defines the minimum ionizing particle

Si properties

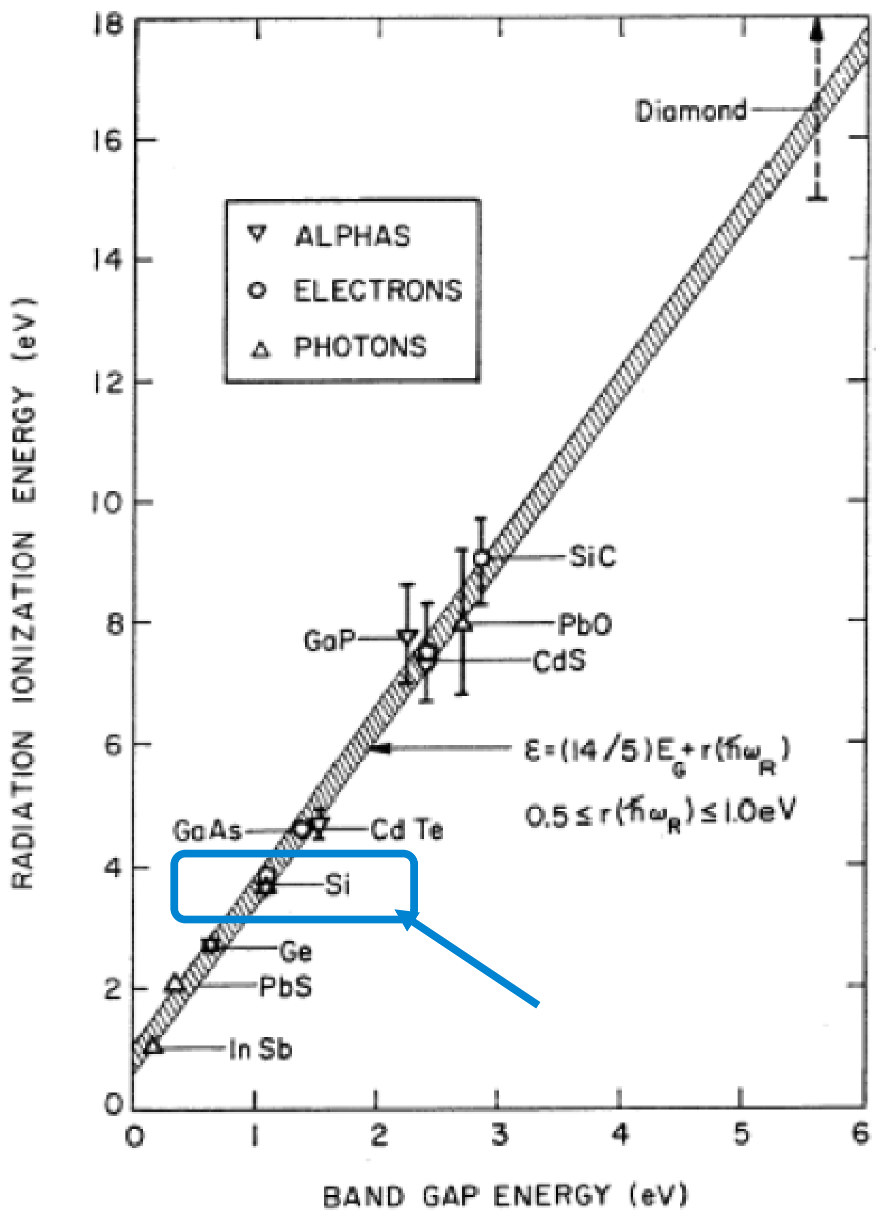

- Widely used in high energy physics and industry
- Low ionization energy
  - Band gap is 1.12 eV
  - Takes 3.6 eV to ionize atom → remaining yields phonon excitations
  - Long free mean path → good charge collection efficiency
  - High mobility → fast charge collection
  - Low Z → reduced multiple scattering
- Good electrical properties (SiO_2)
- Good mechanical properties
  - Easily patterned to small dimensions
  - Can be operated at room temperature
  - Crystalline → resilient against radiation

Bond model of semi-conductors

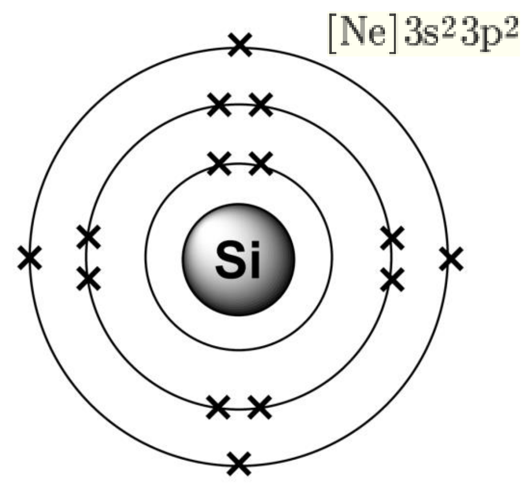

- Covalent bonds formed after sharing electrons in the outermost she
- Thermal vibrations
  - break bonds and yield electron conduction (free e$^-$)
  - remaining open bonds attract free e- → holes change position → hole conduction

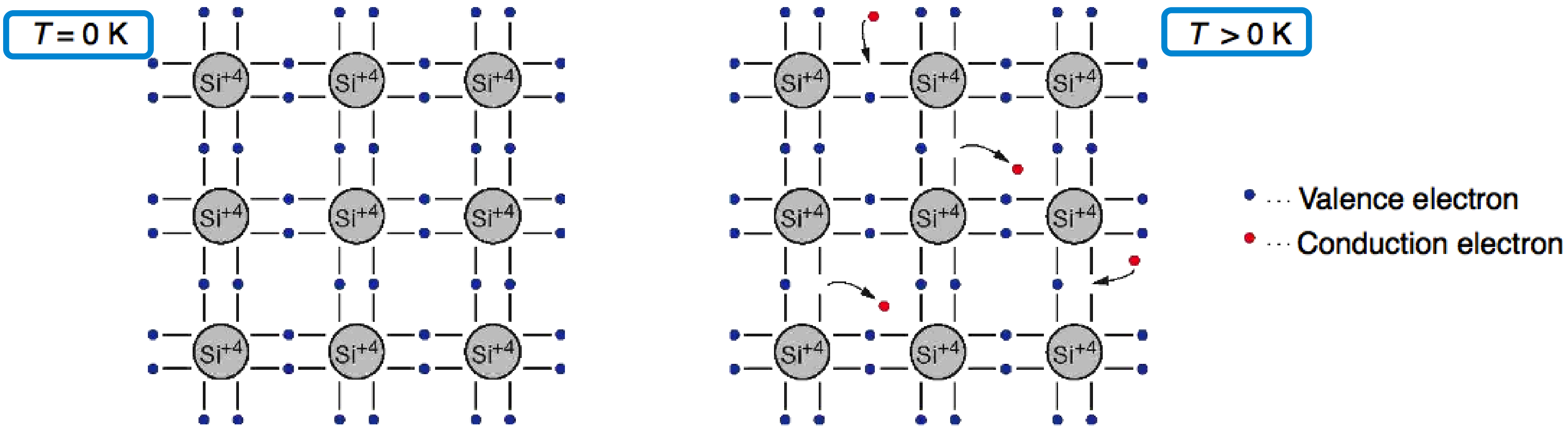

Energy bands structure compared

- In solids, the quantized energy levels merge
  - <u>Metals</u>: conduction and valence band overlap
  - <u>Insulators and semi-conductors</u>: conduction and valence band separated by energy (band) gap
  - If μ (band gap) sufficiently low : electrons fill conduction band according to Fermi-Dirac statistics

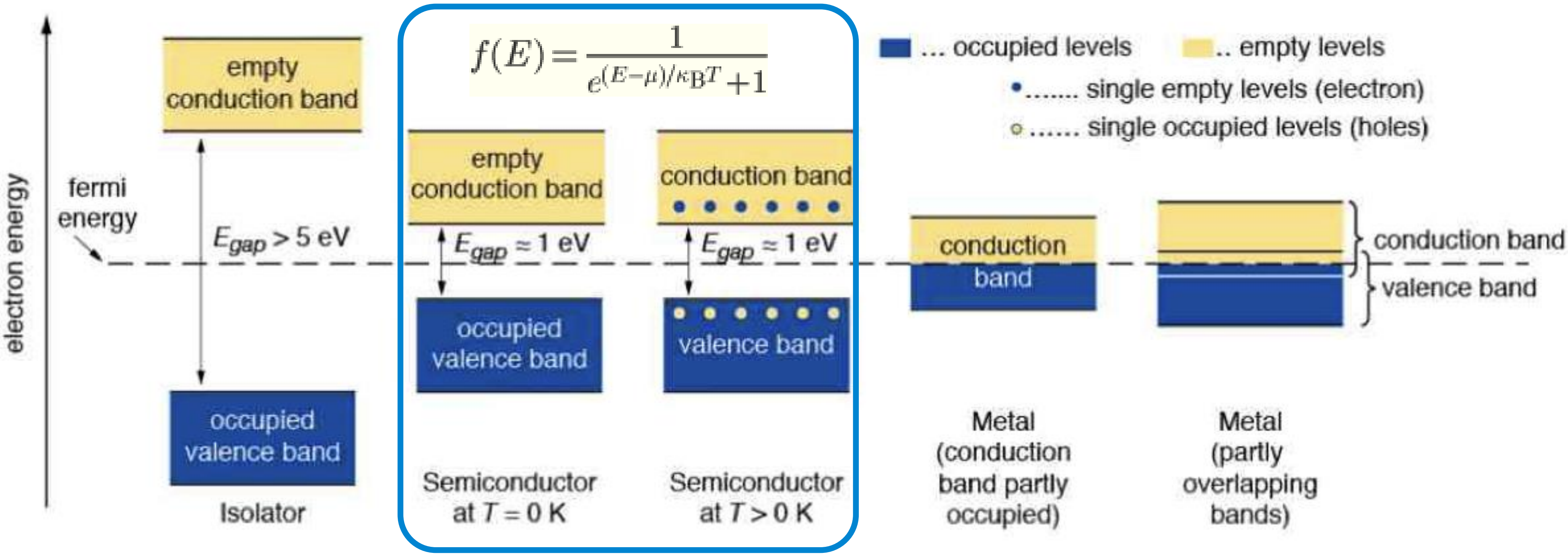

Intrinsic carrier concentration

- Energy state occupation probability follows Fermi statistics distribution

$$f(E) = \frac{1}{e^{(E-\mu)/\kappa_B T} + 1}$$

- Typical behaviour @ room temperature
  - excited electrons move to conduction band
  - electrons recombine with holes

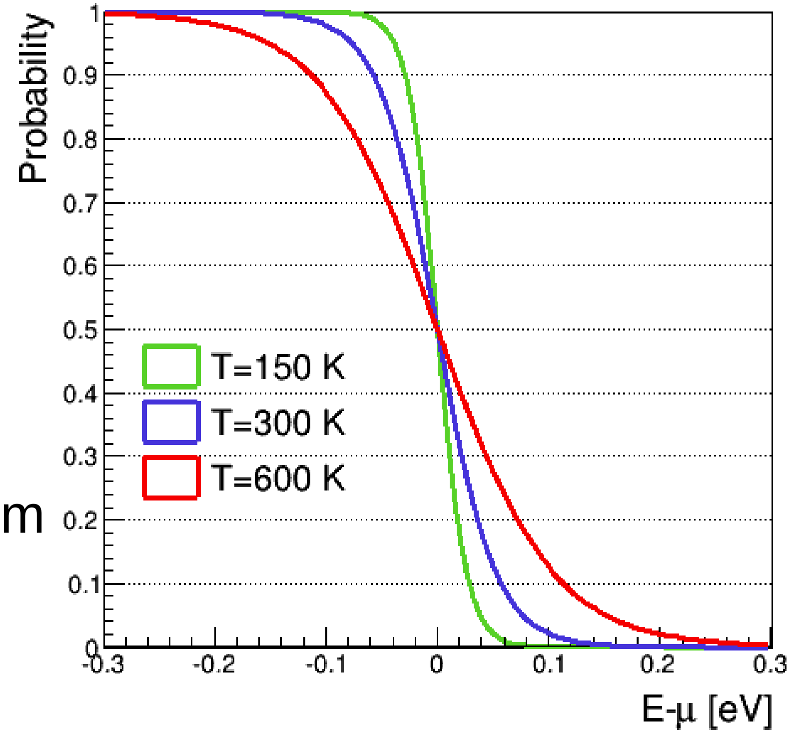

- Excitation and recombination in thermal equilibrium

- Intrinsic carrier concentration given by

$$n_e = n_h = n_i = A \cdot T^{3/2} \cdot e^{-E_g/k_B T}$$

with $A=3.1\times10^{16}\ K^{-3/2}cm^{-3}$ *and* $E_g/2k_B=7\times10^3 K$

$n_i \sim 1.45\times10^{10}\ cm^{-3}$

$\Rightarrow 1/10^{12}$ Si atoms is ionized

Energy loss in the Si: the Landau PDF

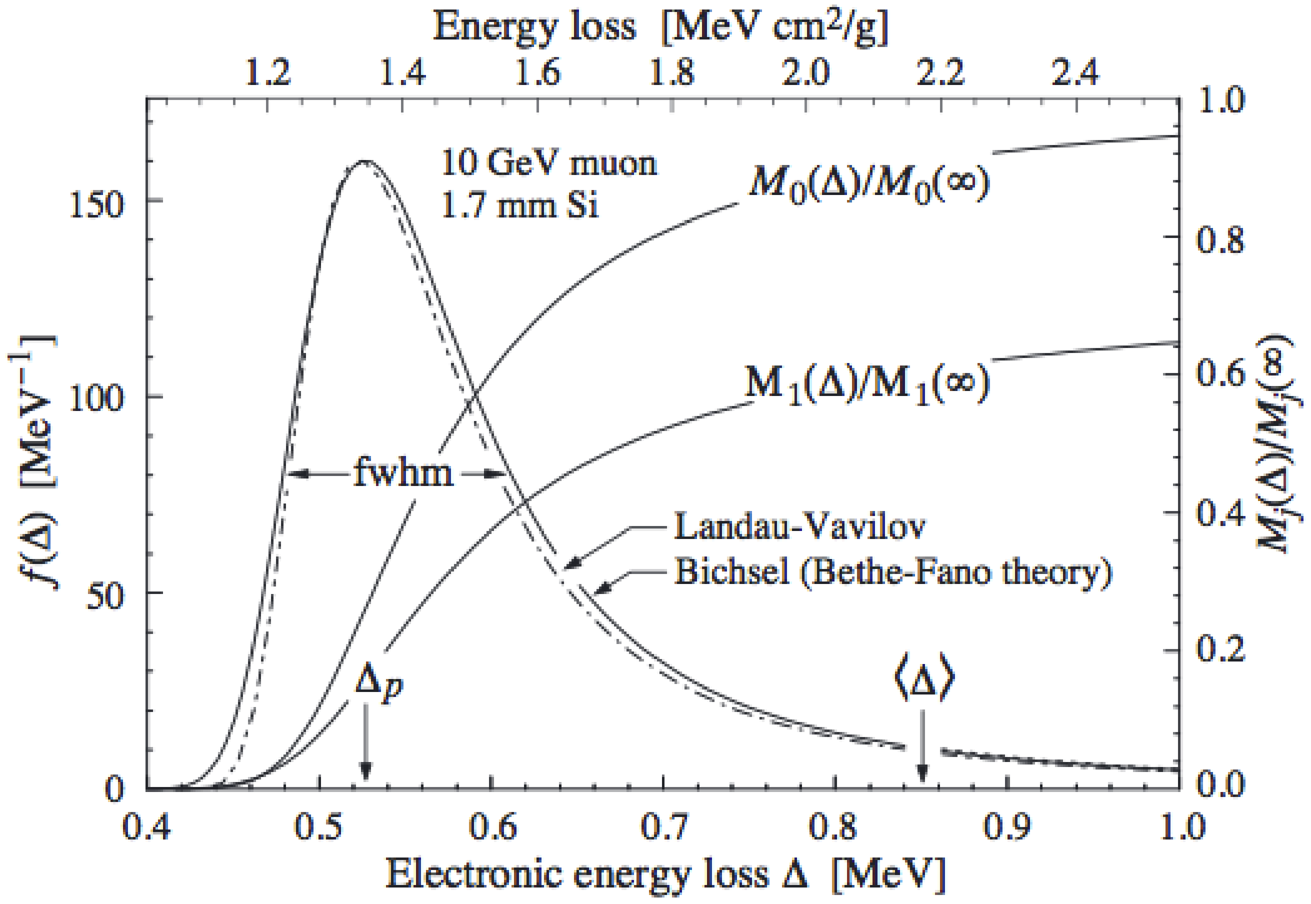

MIP as function of the energy: Bethe-Bloch curve

Example: Si detector with thickness d=300μm

$$\left\langle -\frac{dE}{dx}\right\rangle = K z^2 \frac{Z}{A}\frac{1}{\beta^2}\left[\frac{1}{2}\ln\frac{2m_e c^2\beta^2\gamma^2 W_{\max}}{I^2} - \beta^2 - \frac{\delta(\beta\gamma)}{2}\right]$$

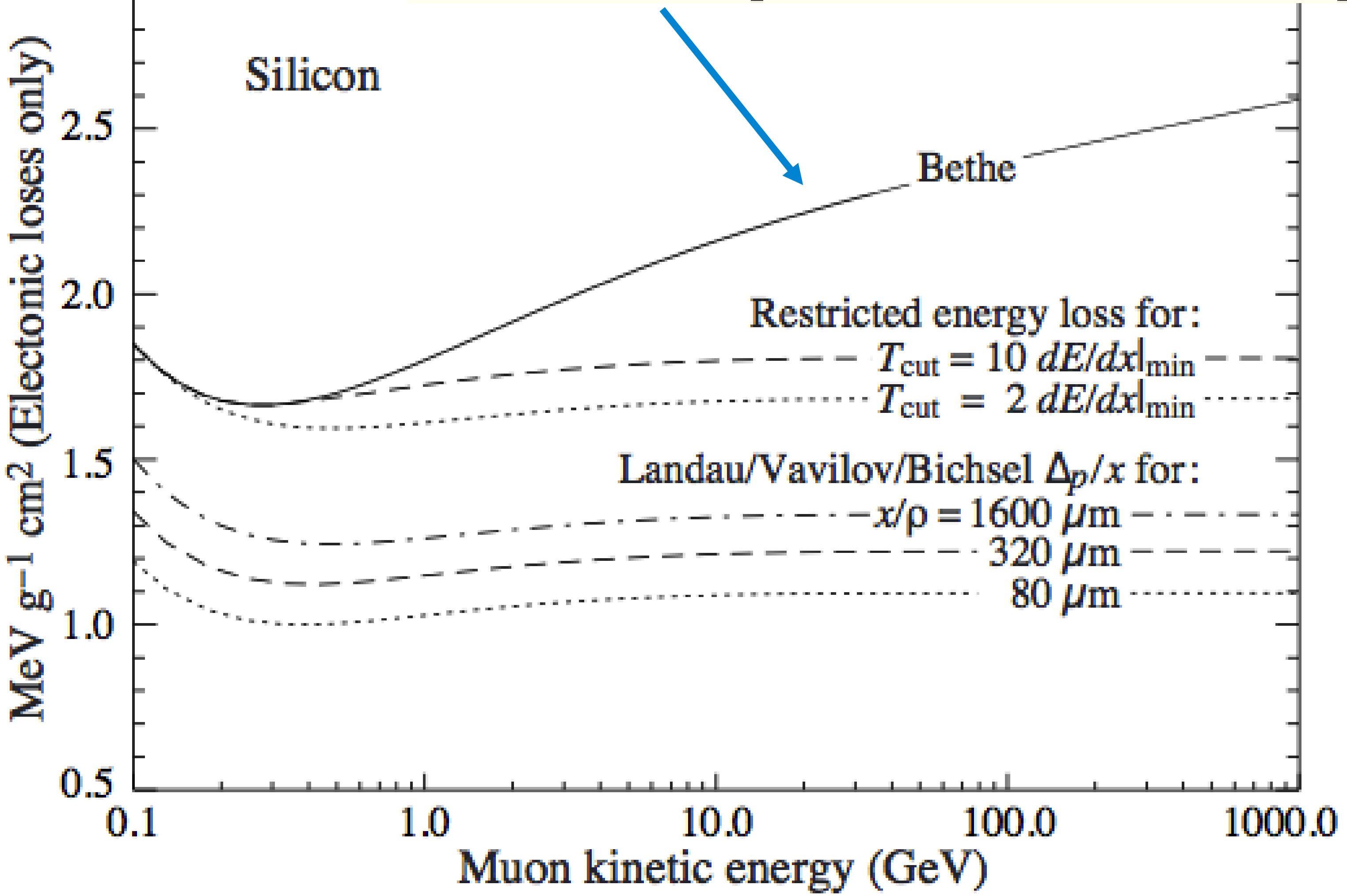

Intrinsic S/N in a Si detector

For a 300μm thickness sensor

- Minimum ionizing particle (MIP) creates:

$$\frac{1}{E_{\mathrm{eh}}}\frac{dE}{dx}\cdot d = \frac{3.87\cdot 10^6 \mathrm{eV/cm}}{3.63\mathrm{eV}}\cdot 0.03\mathrm{cm} = 3.2\cdot 10^4 \mathrm{eh\ pairs}$$

- Intrinsic charge carriers (recall slide 43):

$$n_i \cdot d = 1.45\cdot 10^{10} cm^{-3}\cdot 0.03 cm = 4.35\cdot 10^8 \mathrm{eh\ pairs}$$

Number of thermally-created e-h pairs exceeds mip signal by factor 10!

Si doping: n-dope bond model

- Doping with a group 5 atom (e.g. P, As, Sb)
  - atom is an electron donor/donator
  - Weakly bound 5^{th} valence electron
  - Positive ion is left after conduction electron is released

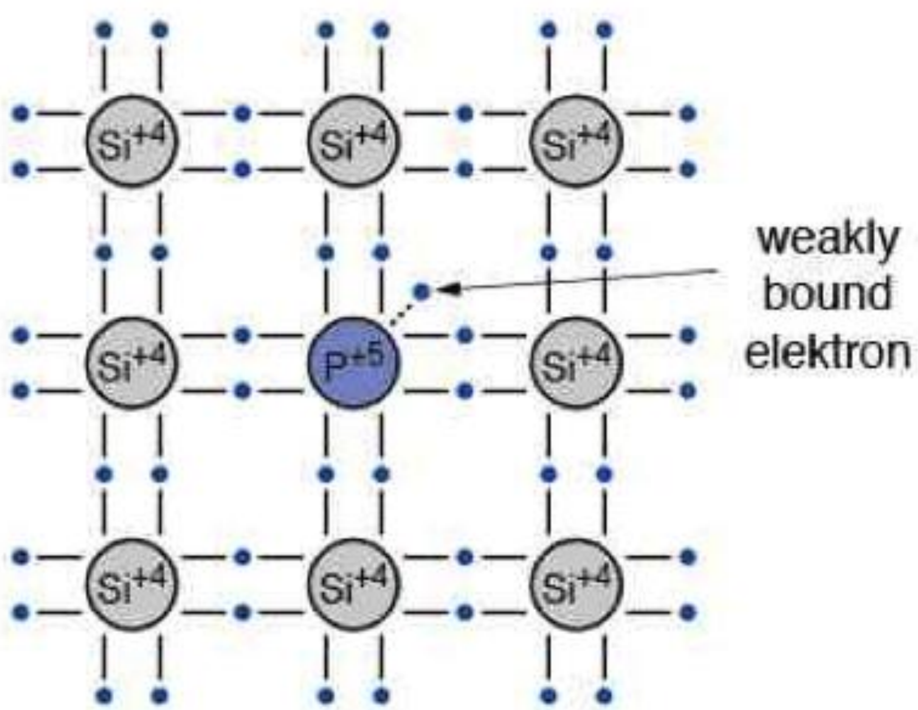

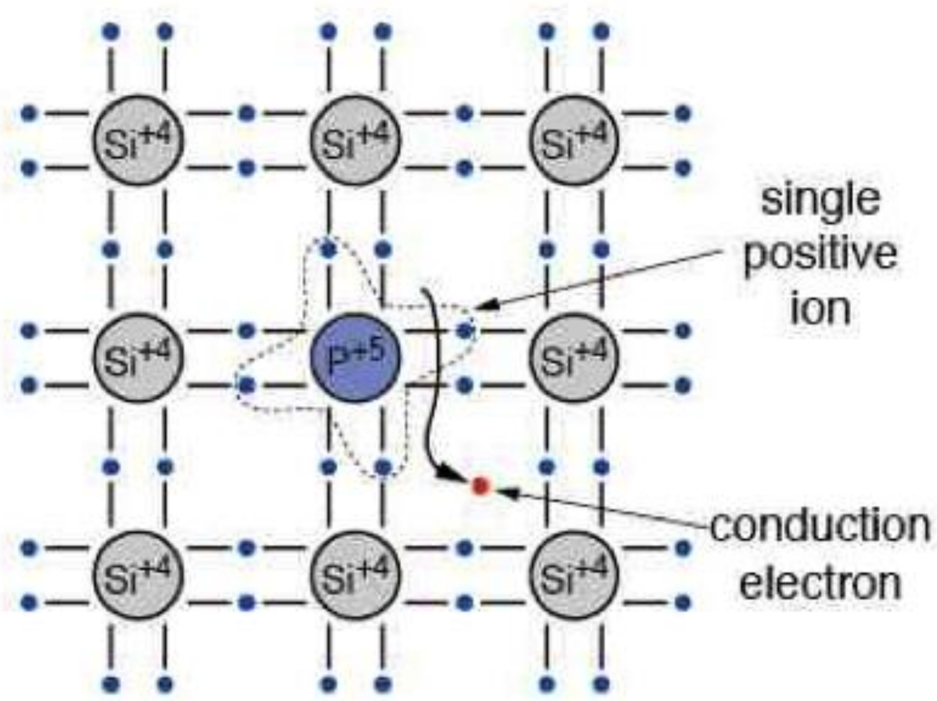

Si doping: n-dope bond model II

- Energy level of donor is below edge of conduction band
  - Most electrons enter conduction band at room temperature
  - Fermi level moves up with respect to pure Si

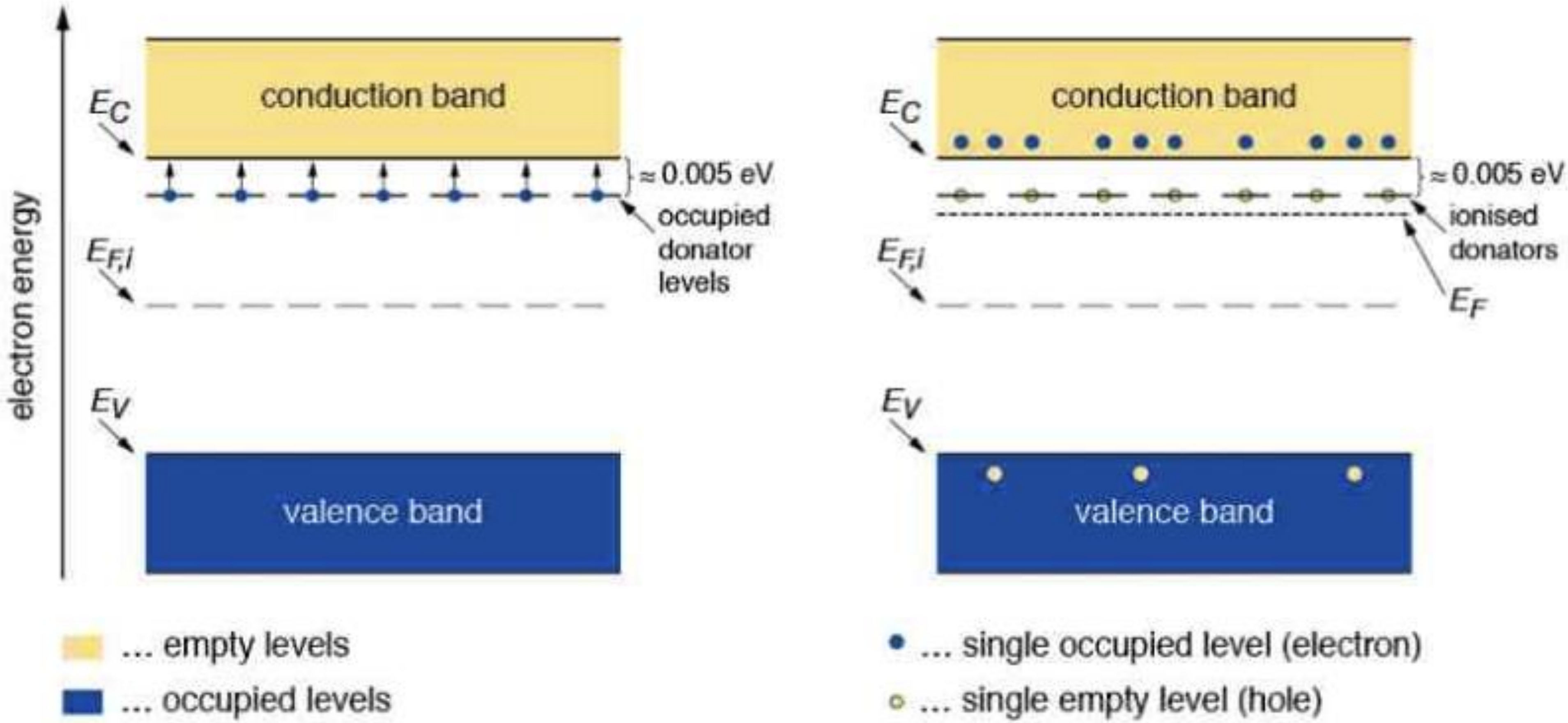

Si doping: p-dope bond model

- Doping with a group 3 atom (e.g. B, Al, Ga, In)
  - atom is an electron acceptor
  - open bond attracts electrons from neighbouring atoms
  - acceptor atom in the lattice becomes negatively charged

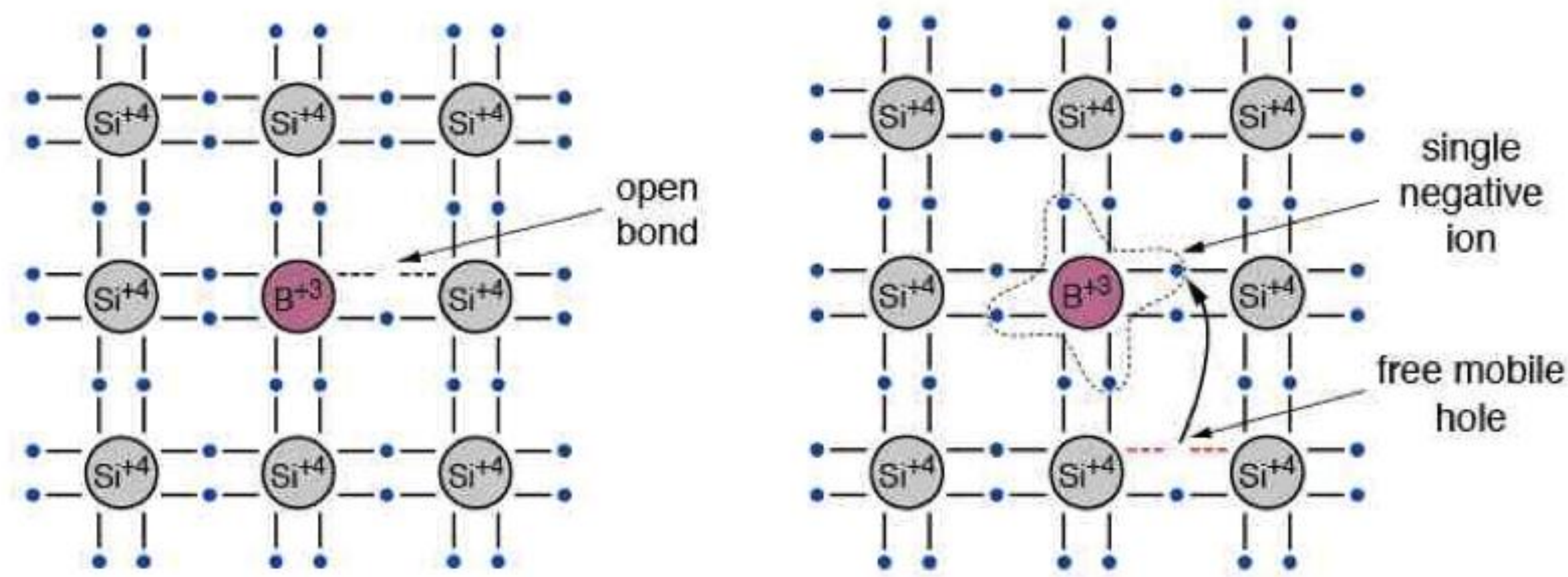

Si doping: p-dope bond model - II

- Energy level of acceptor is above edge of conduction band
  - Most levels are occupied by electrons → holes in the valence band
  - Fermi level moves down with respect to pure Si

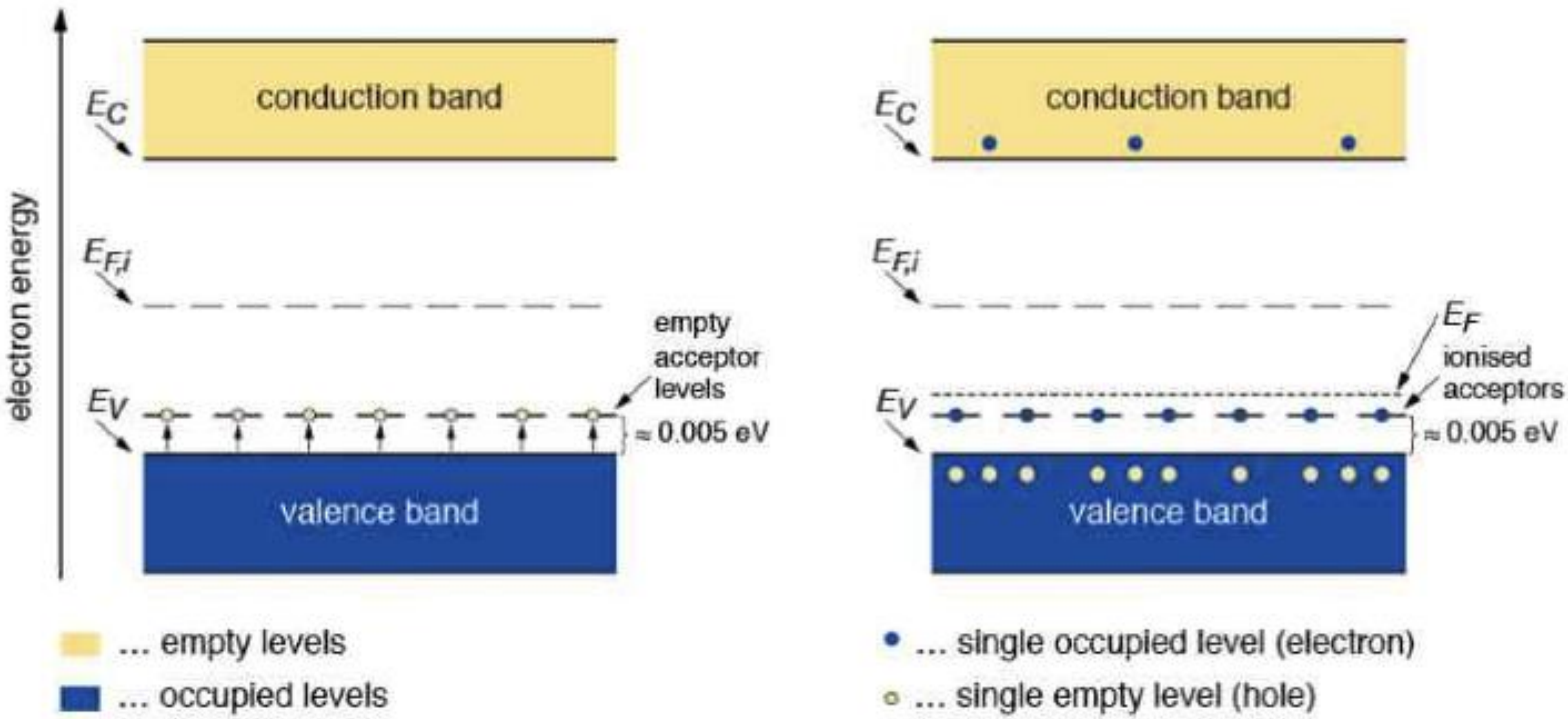

p-n junctions

- Difference in Fermi levels at the interface of n-type or p-type
  - diffusion of excess of charge carriers until thermal equilibrium (or equal Fermi level)
  - remaining ions create a depletion zone: electric field prevents further the diffusion

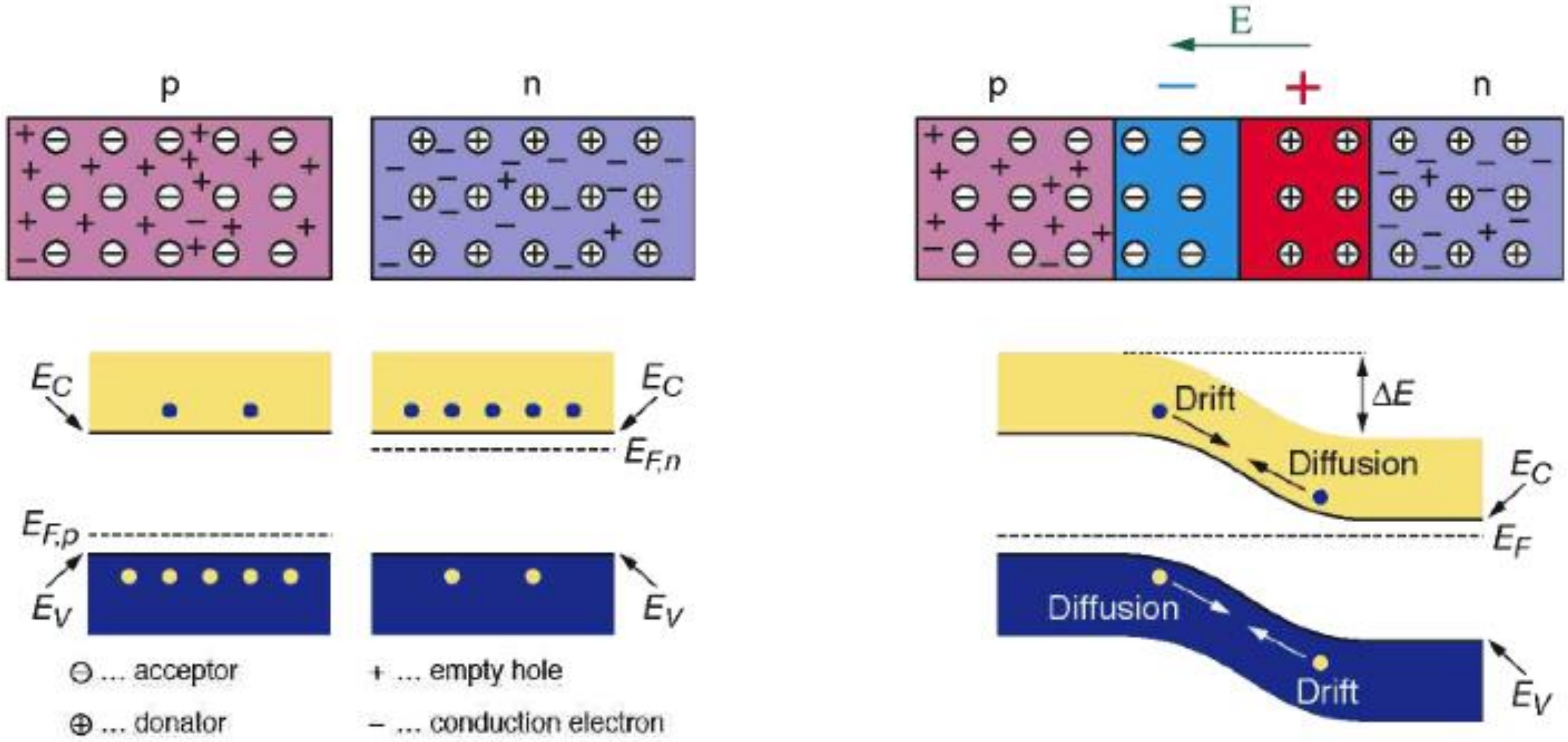

p-n junctions

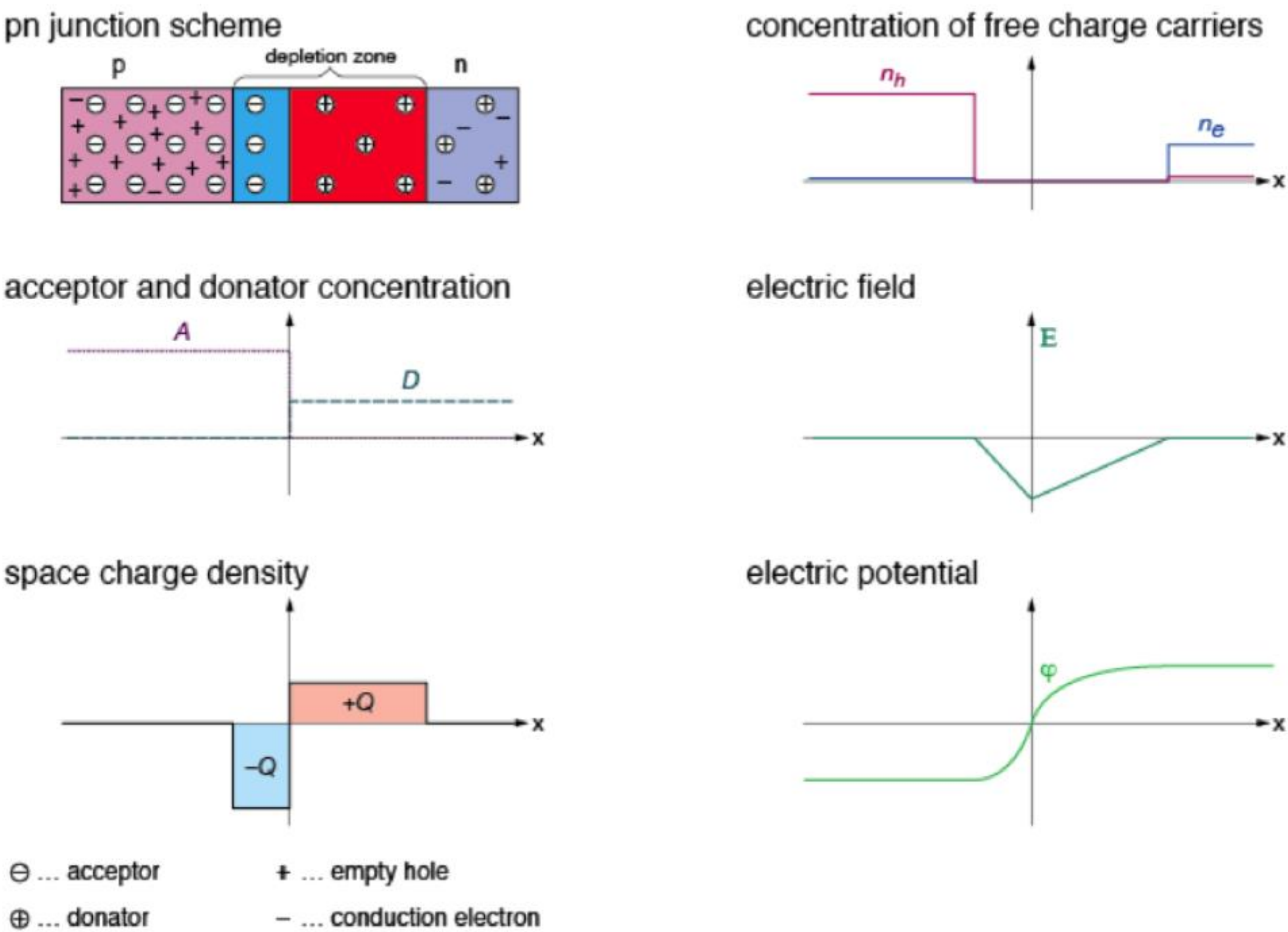

Biasing p-n junctions

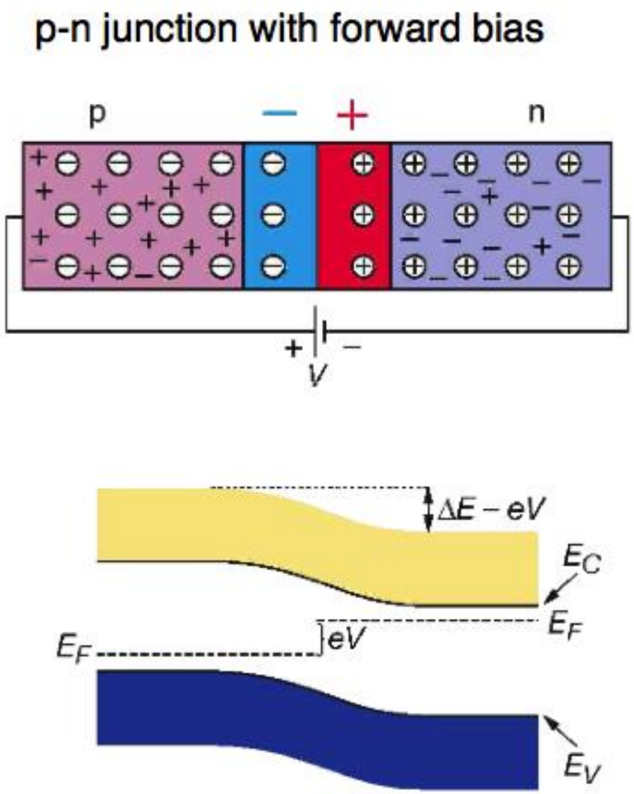

Forward-biased junction

- Anode to p, cathode to n
- Depletion zone becomes narrower
- Smaller potential barrier facilitates diffusion
- Current across the junction tends to increase

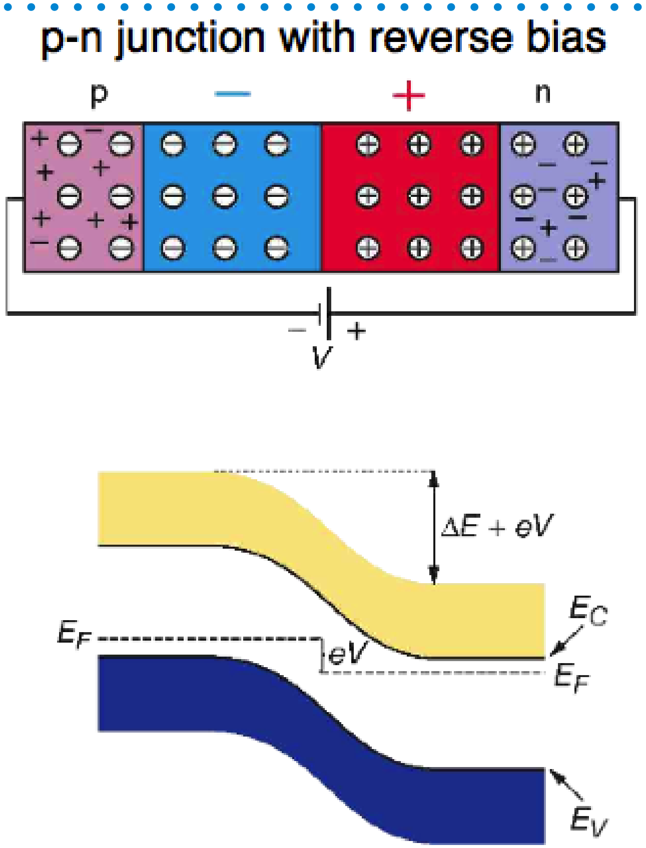

Reverse-biased junction

- Anode to n, cathode to p
- e,h pulled out of the depletion zone
- Potential barrier is suppressed
- Only leakage current across junction

Depletion zone width and capacitance

- Characterize depletion zone from Poisson equation with charge conserva $\nabla^2 \phi = -\frac{\rho_f}{\varepsilon}$
- Typically: $N_a = 10^{15}$ cm^{-3} (p+ region) >> $N_d = 10^{12}$cm^{-3} (n bulk)
- **Width of depletion zone** (n bulk): $W \approx \sqrt{\frac{2\varepsilon V_{\text{bias}}}{q} \cdot \frac{1}{N_d}}$

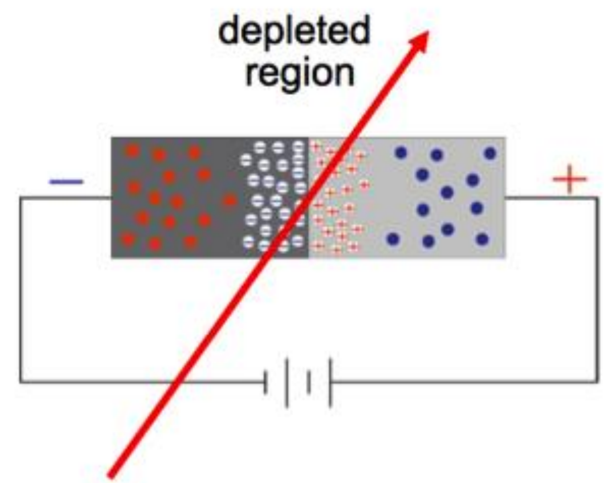

Reverse bias voltage (V)	W_p (μm)	W_n (μm)
0	0.02	23
100	0.4	363

- **Device is similar to a parallel-plate capacitor**

$$C = \frac{q}{V} = \frac{\varepsilon A}{d} = A\sqrt{\frac{\varepsilon q N_d}{2V_{\text{bias}}}}$$

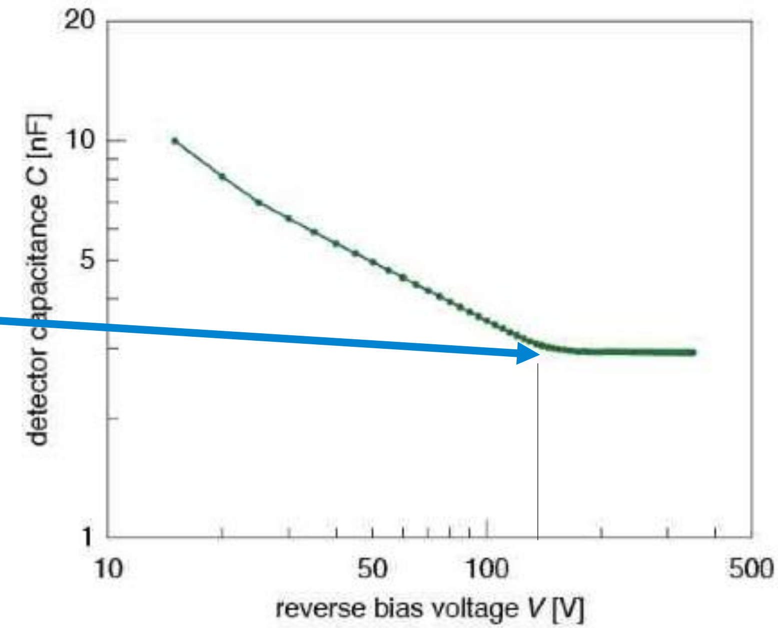

  - Depletion voltage saturates the capacitance
  - Typical curve obtained for CMS strip detector

Leakage current

- Thermal excitation generates eh pairs
- Reverse bias applied separates pairs
- eh pairs do not recombine and drift

⇒ leakage current

- Depends on purity, defects and temperature

$$j_{\text{gen}} \propto T^{3/2} e^{\frac{1}{\kappa_B T}}$$

⇒ usually require detector cooling for stable operation (-30°-10°C)

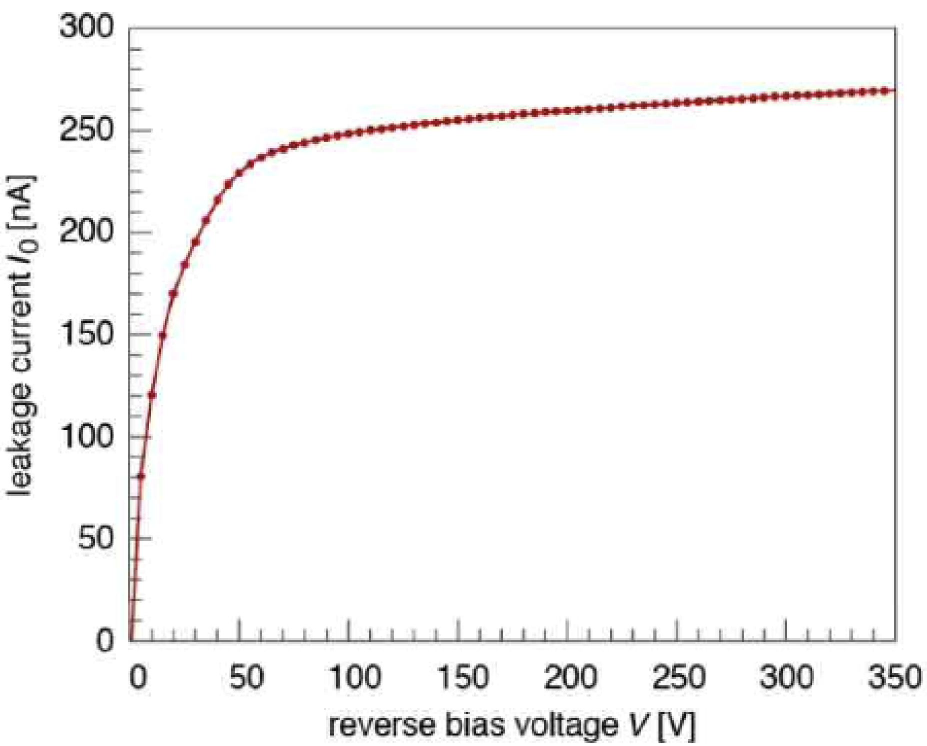

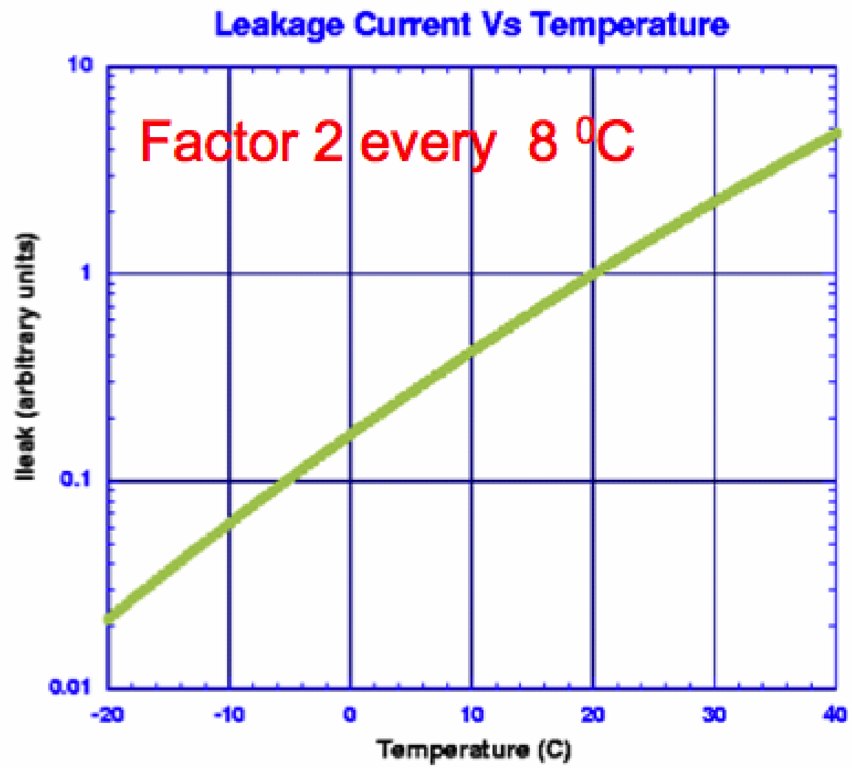

Charge collection

- eh pairs move under the electric field
  - larger biases smaller collection times
  - typically smaller than LHC bunch crossing

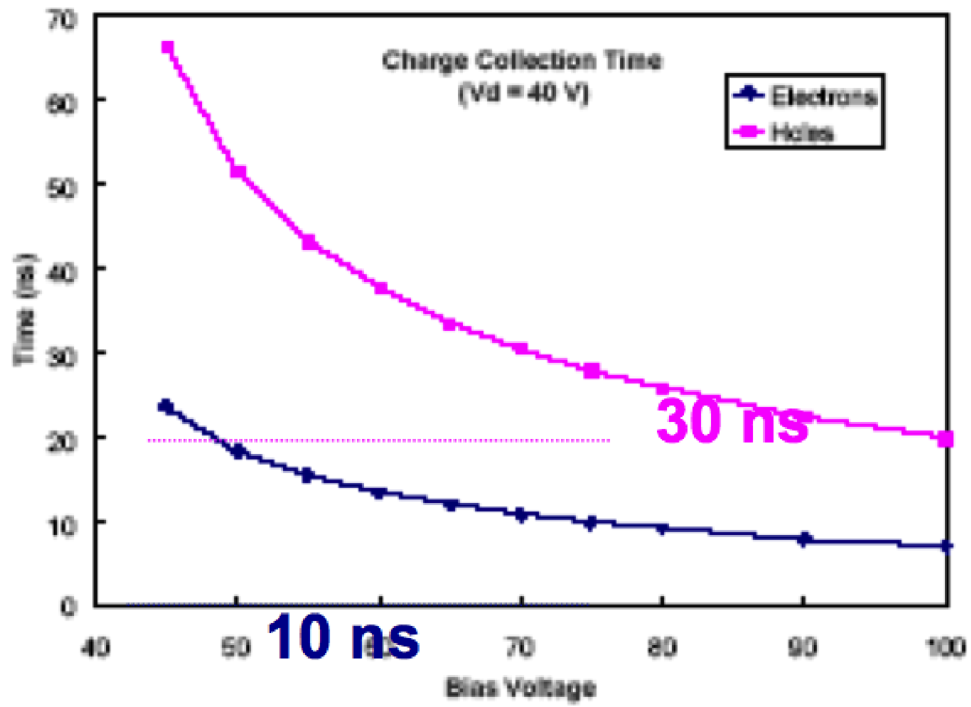

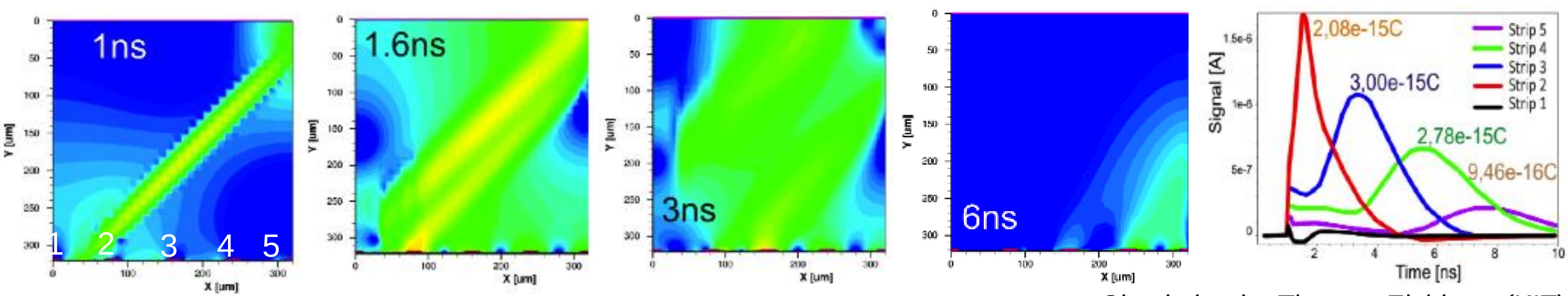

Simulation by Thomas Eichhorn (KIT)

charge collection simulation for a 45^0 incident particle

Position resolution (DC coupled)

- Segmentation of the implants determines precision in position reconstruction

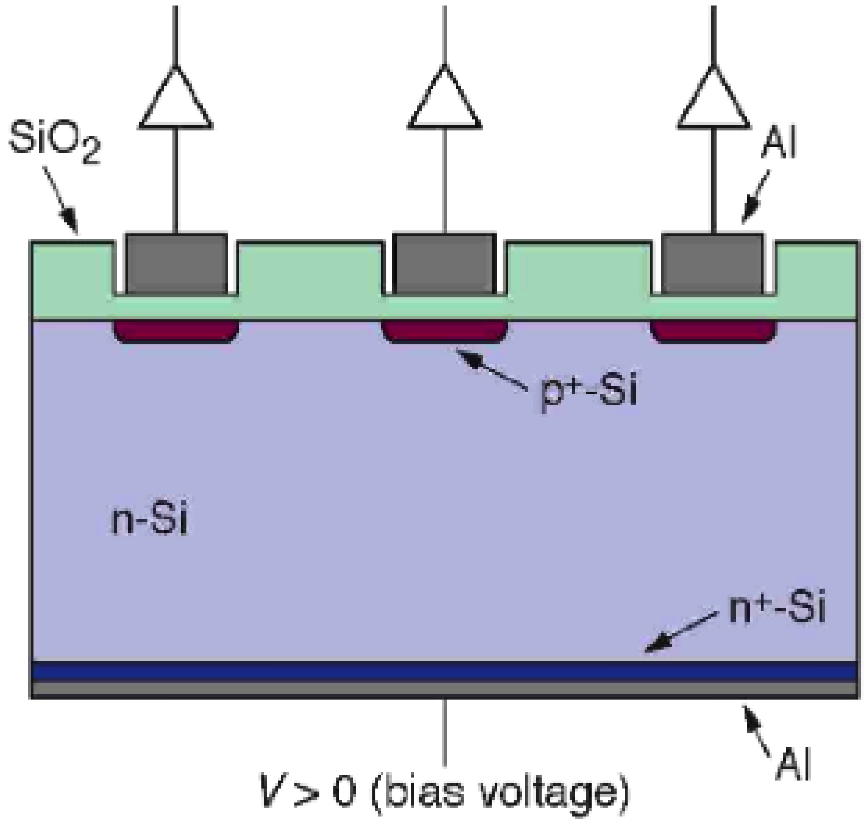

- Typical configuration
  - p implants in strips
  - n-doped substract ~300µm (2-10kΩcm)
  - depletion voltage <200 V
  - backside P implant establishes ohmic conta
  - Al metallisation

- Field is closest to the collecting electrodes (where most of the signal is)

Position resolution (AC coupled)

- AC coupling blocks leakage current from amplifier
- Deposit SiO_2 between p^+ and Al strip
  - Capacitance ~32 pF/cm
  - Shorts through pinholes may be reduced with a second layer of Si_3N_4
- Use large poly silicon resistor (R>1MΩ) connecting the bias voltages to the strips

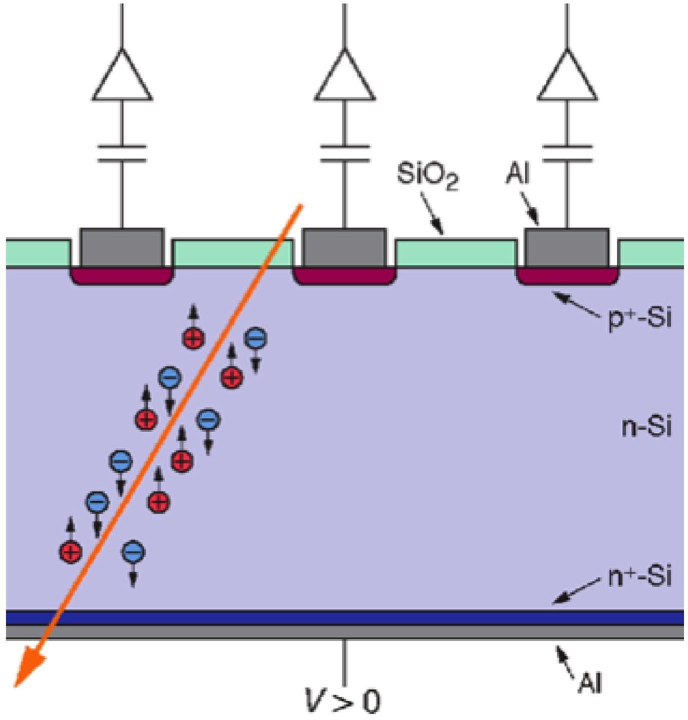

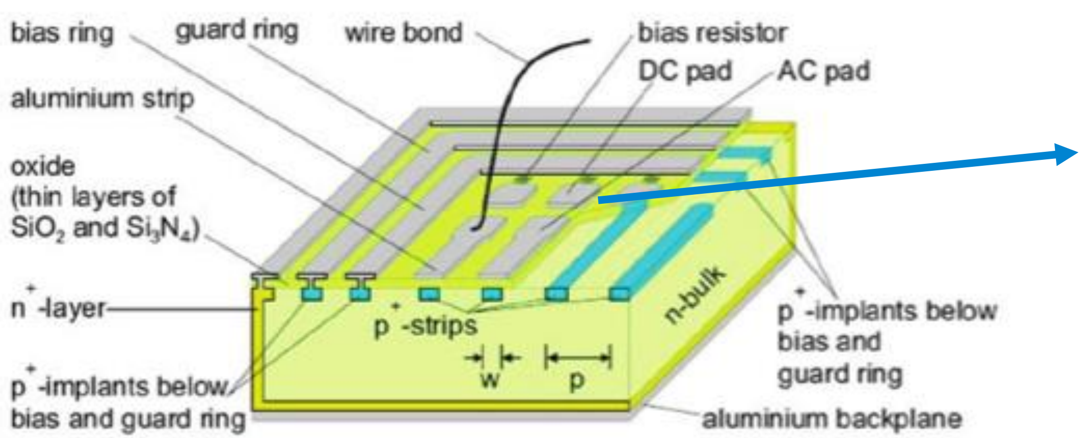

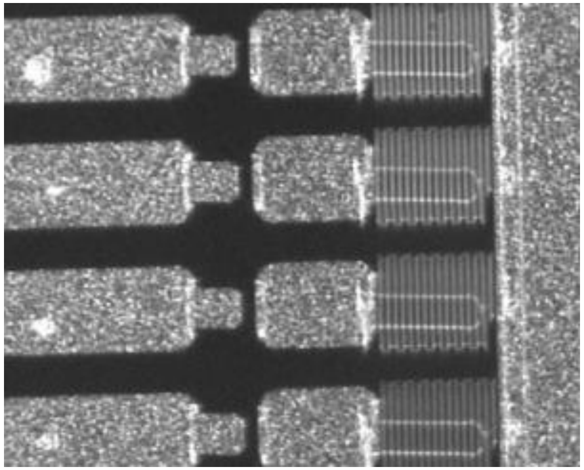

CMS module

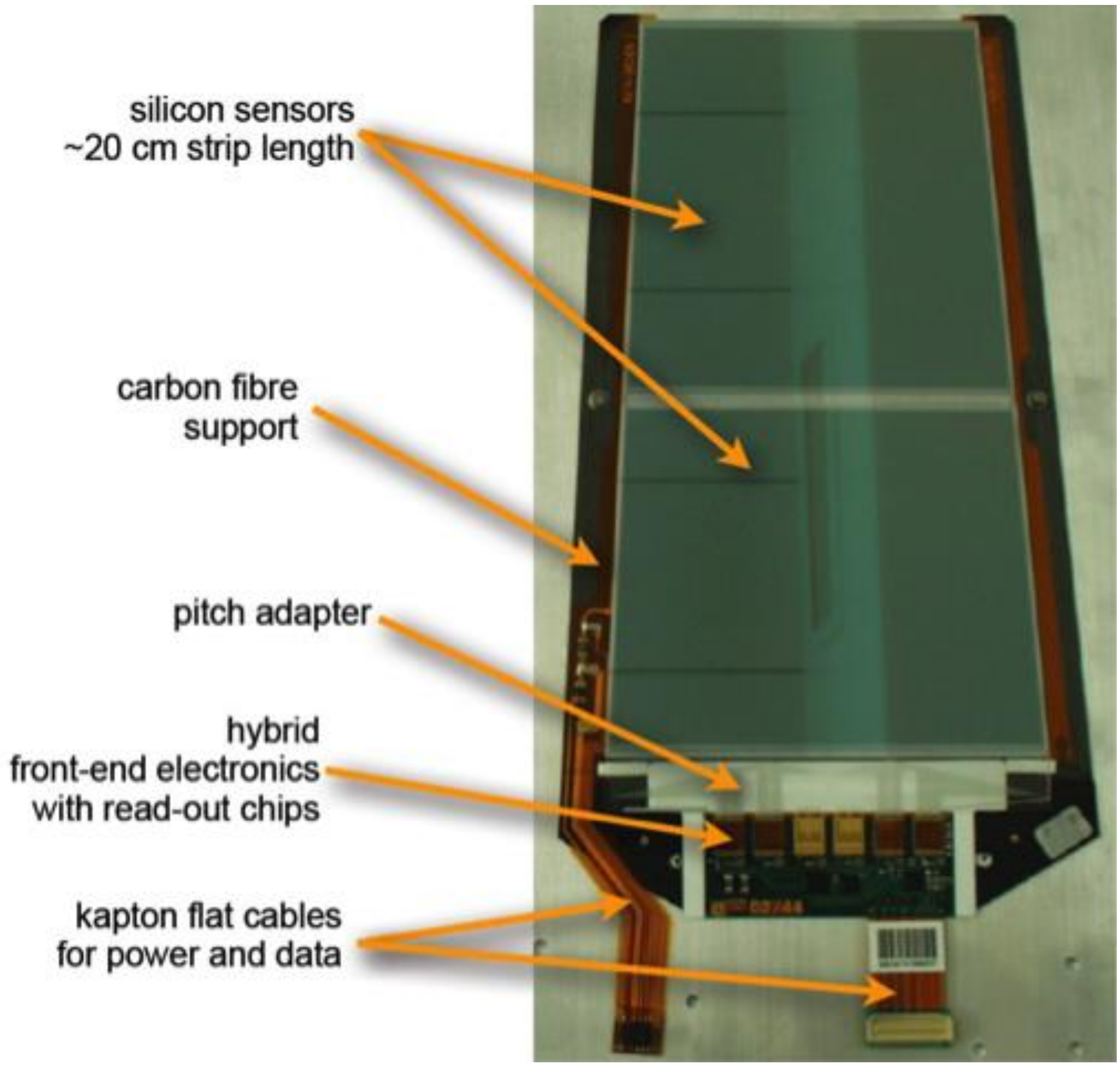
silicon sensors
~20 cm strip length
carbon fibre
support
pitch adapter
hybrid
front-end electronics
with read-out chips
kapton flat cables
for power and data

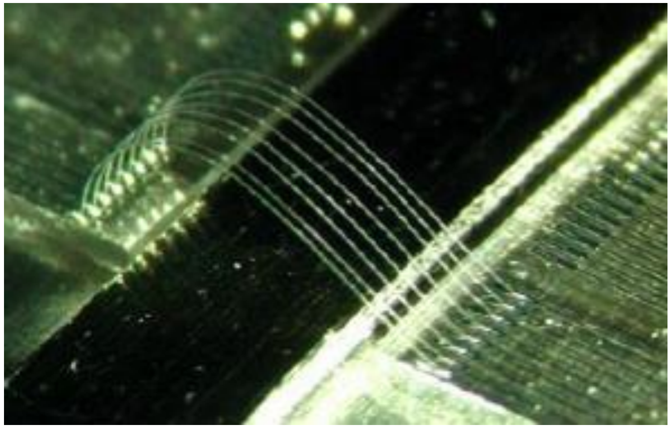

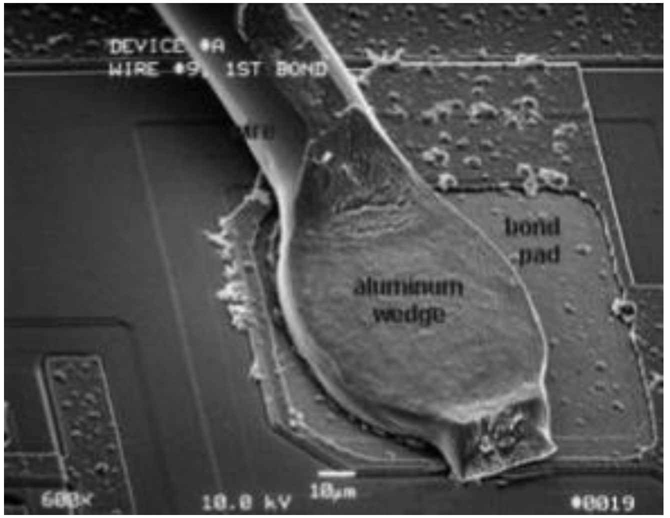
bond
pad
aluminum
wedge
10.0 kV

Pixel sensors

- High track density better resolved with 2D position information
  - back-to-back strips for 2D position information → yields “ghost” hits
- Hybrid pixel detectors with sensors and bump-bonded readout chips

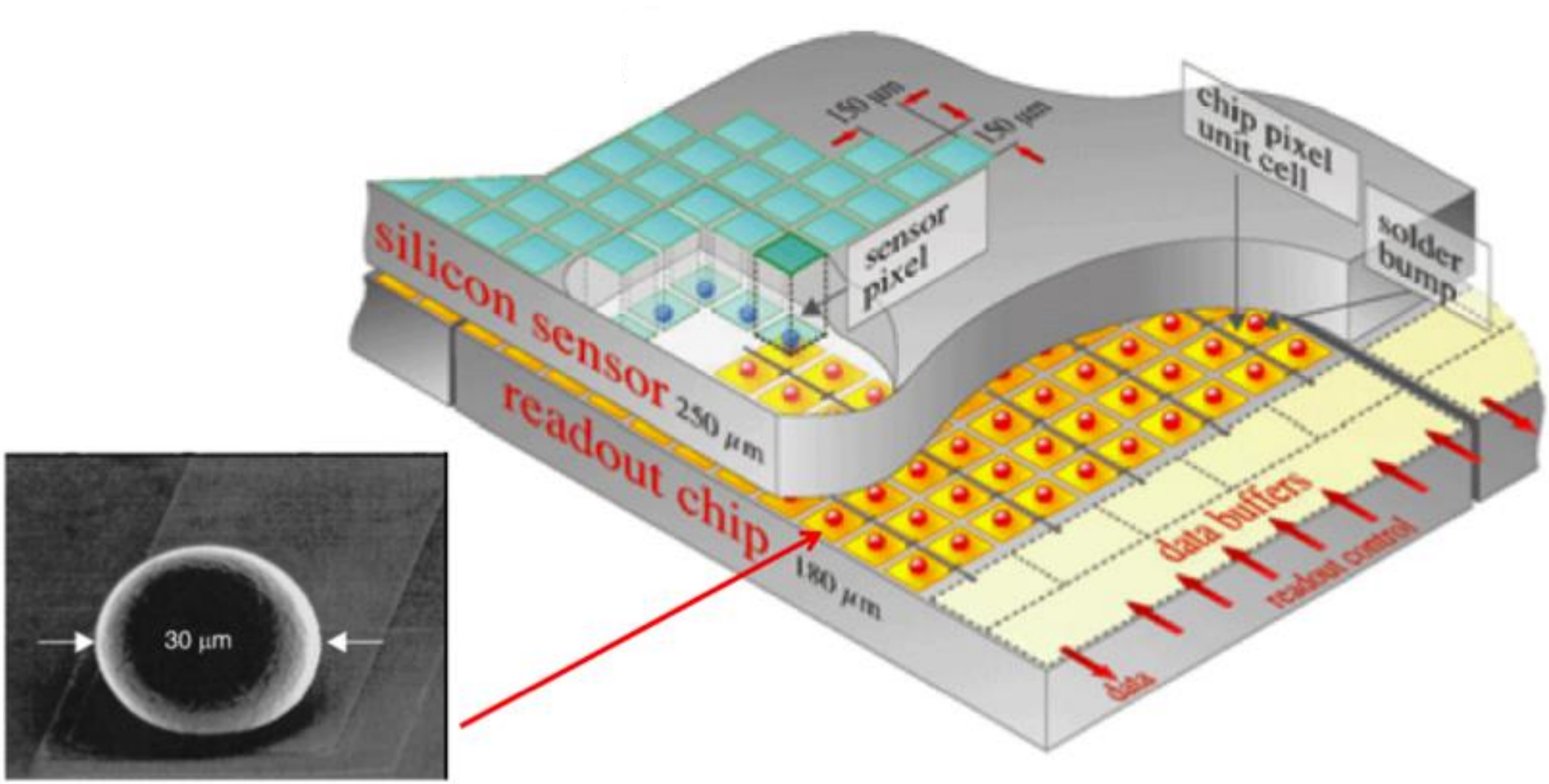

one sensor, 16 front-end chips and 1 master controller chip

Hybrid Pixel Module for CMS

Sensor:

- Pixel Size: 150mm x 100mm
  - Resolution $\sigma_{r-\varphi}$ ~ 15µm
  - Resolution σ_z ~ 20µm
- n+-pixel on n-silicon design
  - Moderated p-spray → HV robustness

Readout Chip:

- Thinned to 175µm
- 250nm CMOS IBM Process
- 8" Wafer

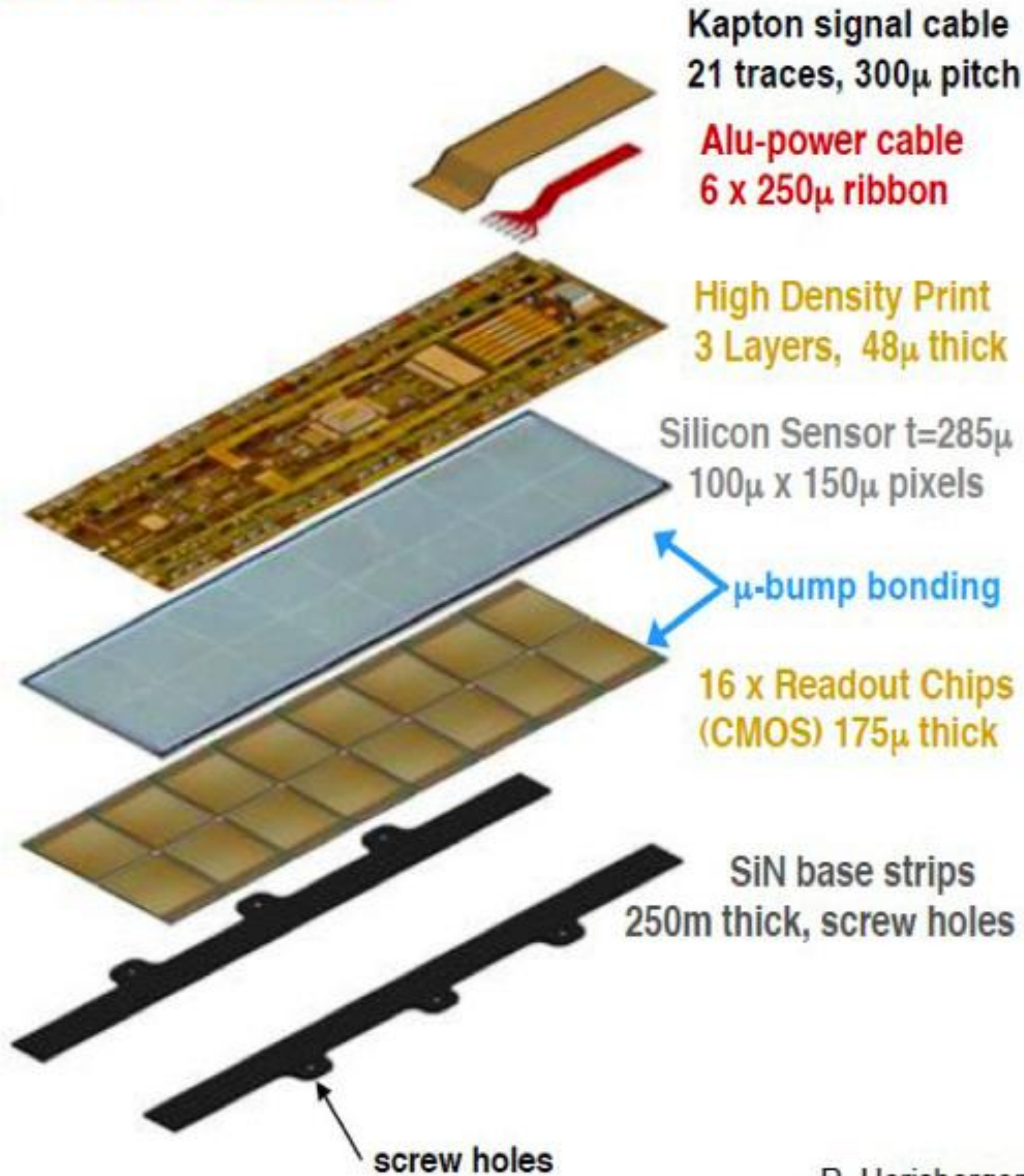

R. Horisberger

Performance: S/N

- Signal depends on the thickness of the depletion zone and on dE/dx of the particle

- Noise suffers contributions from:

$$\mathrm{ENC} = \sqrt{\mathrm{ENC}_\mathrm{C}^2 + \mathrm{ENC}_\mathrm{I}^2 + \mathrm{ENC}^2\mathrm{R}_{\parallel} + \mathrm{ENC}_{\mathrm{R}_\mathrm{series}}^2}$$

capacitance | leakage current | parallel resistor | series resistor

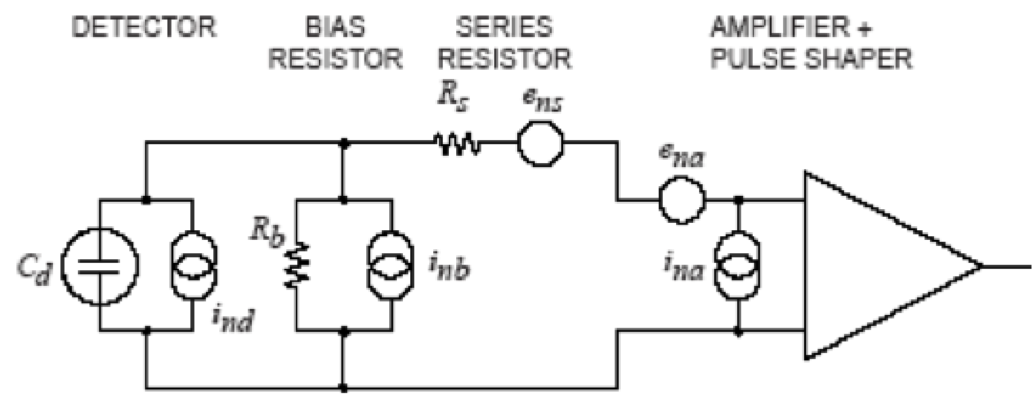

$$\mathrm{ENC}_\mathrm{peak} = (36.6 \pm 1.9)\, e^- /\mathrm{cm} \cdot L + (405 \pm 27)\, e^-$$
$$\mathrm{ENC}_\mathrm{dec} = (49.9 \pm 3.2)\, e^- /\mathrm{cm} \cdot L + (590 \pm 47)\, e^-$$

CMS strips

- Optimizing S/N
  - N_{ADC}>thr, given high granularity most channels are empty
  - decrease noise terms (see above)
  - minimize diffusion of charge cloud after thermal r
  - (typically ~8µm for 300µm drift)
  - radiation damage severely affects S/N (next slide

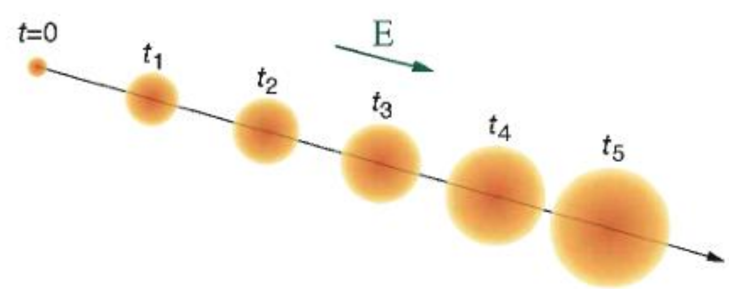

Influence of radiation

- Si is not fully robust against radiation
  - induced defects result in noise, inefficiency, leakage,…
  - need to increase depletion voltage at higher fluences
  - expected hit finding efficiency after 10 years of LHC operation: 95%

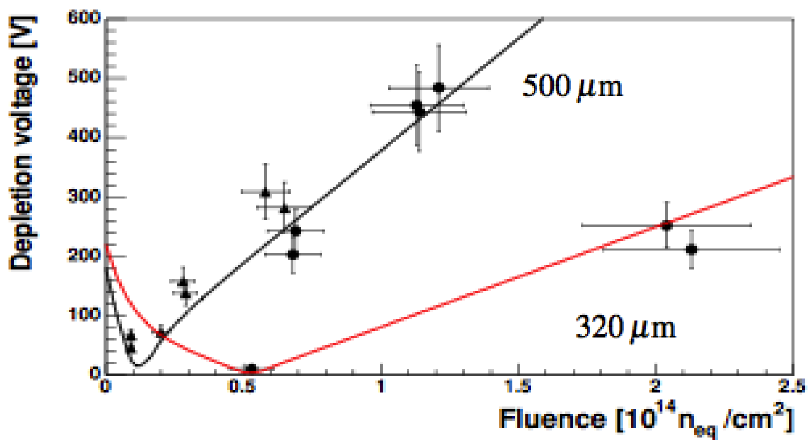

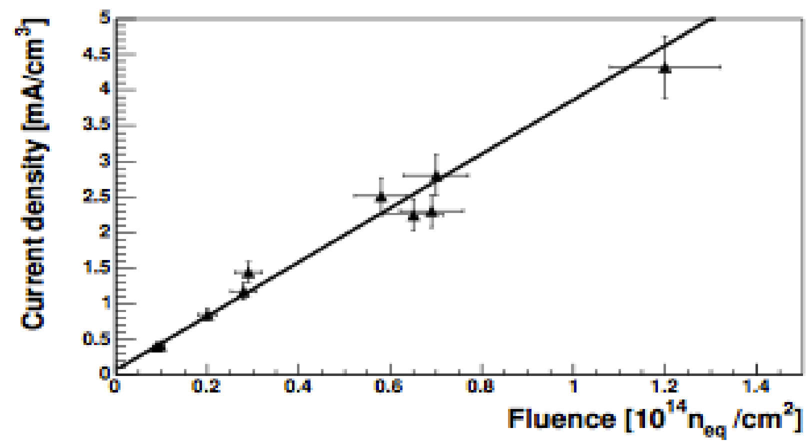

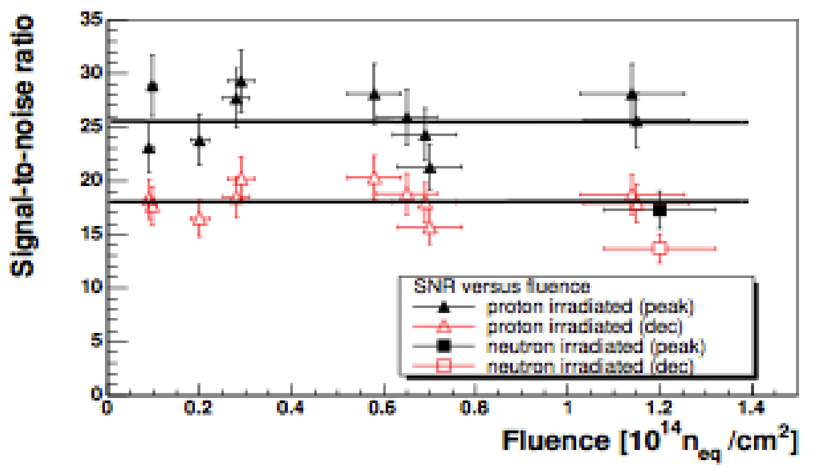

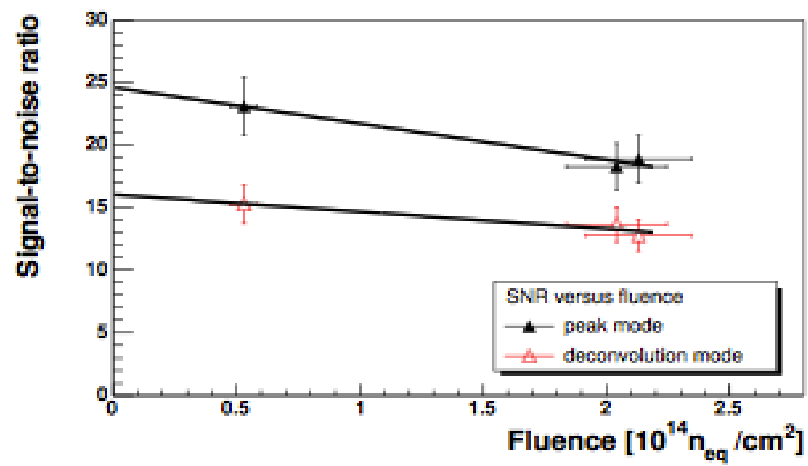

CMS tracker

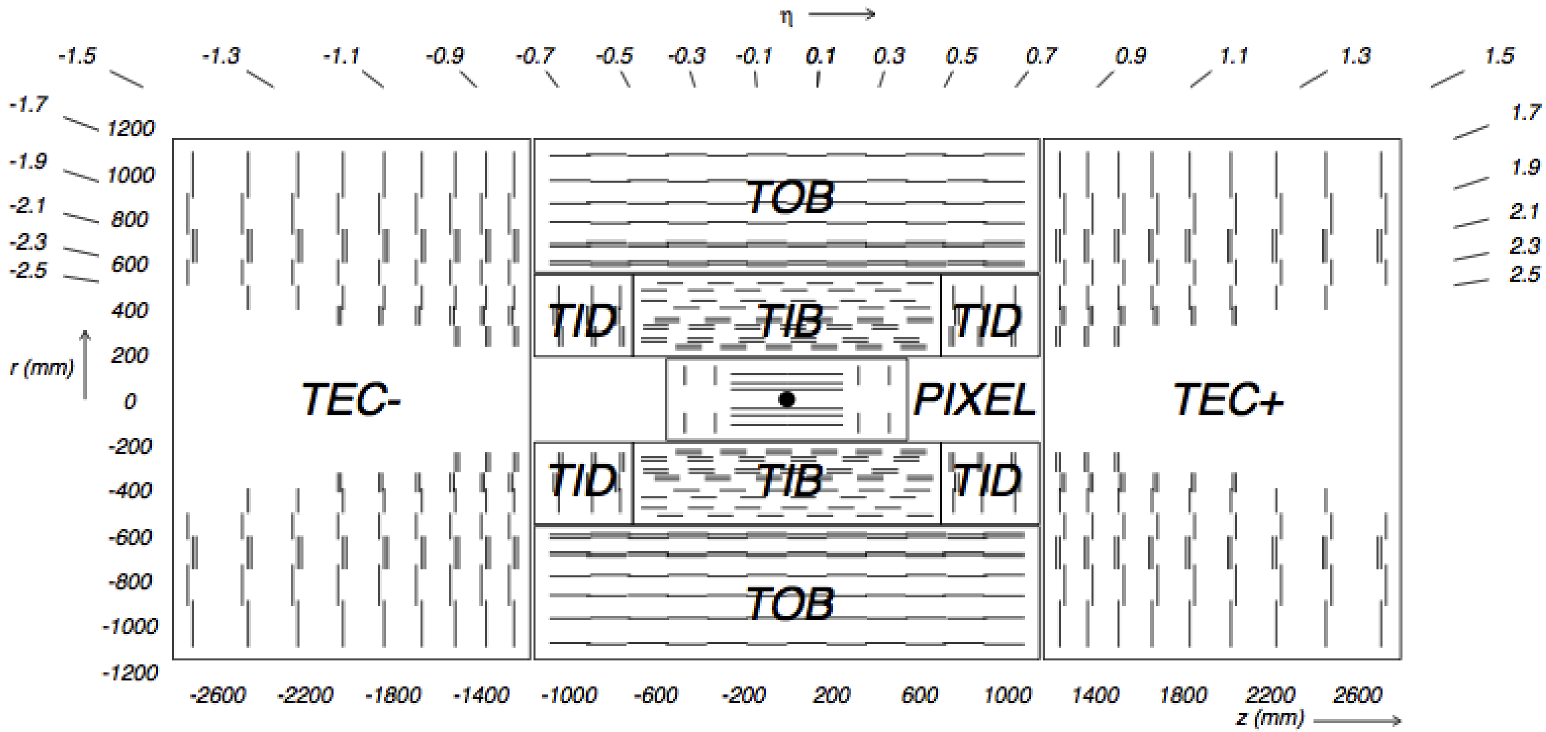

- Pixel detector: ~1m^2 area
  - 1.4k modules ⇒ 66M pixels
- Strips: ~200m^2 area
  - 24k single sensors, 15k modules
  - 9.6M strips = electronics channels
  - 75k readout chips

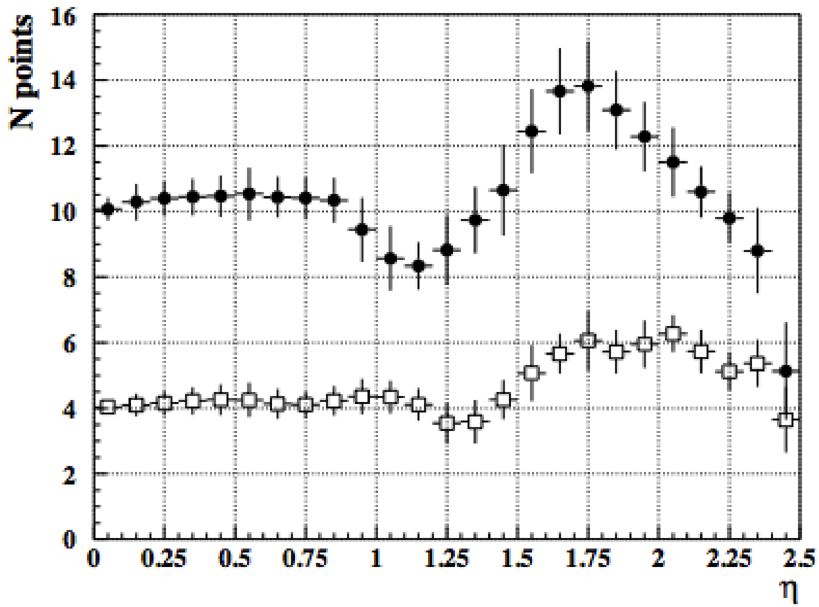

CMS tracker budget

- In some regions can attain $1.8X_0$
  - often photons will convert, electrons will radiate :(
  - use for alignment and material budget estimation :)
- Precise knowledge is crucial, e.g. for Higgs with γ and electrons in the final state

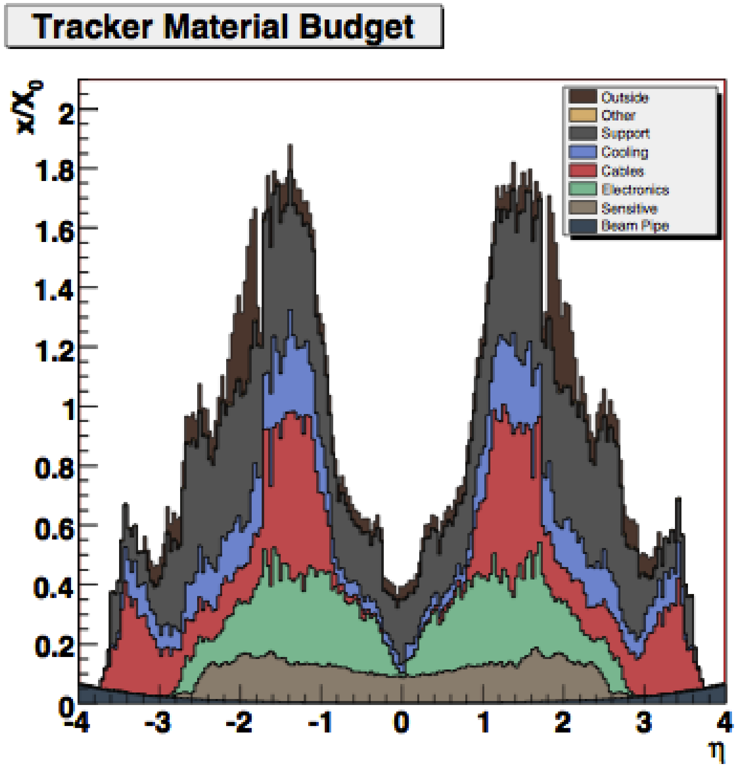

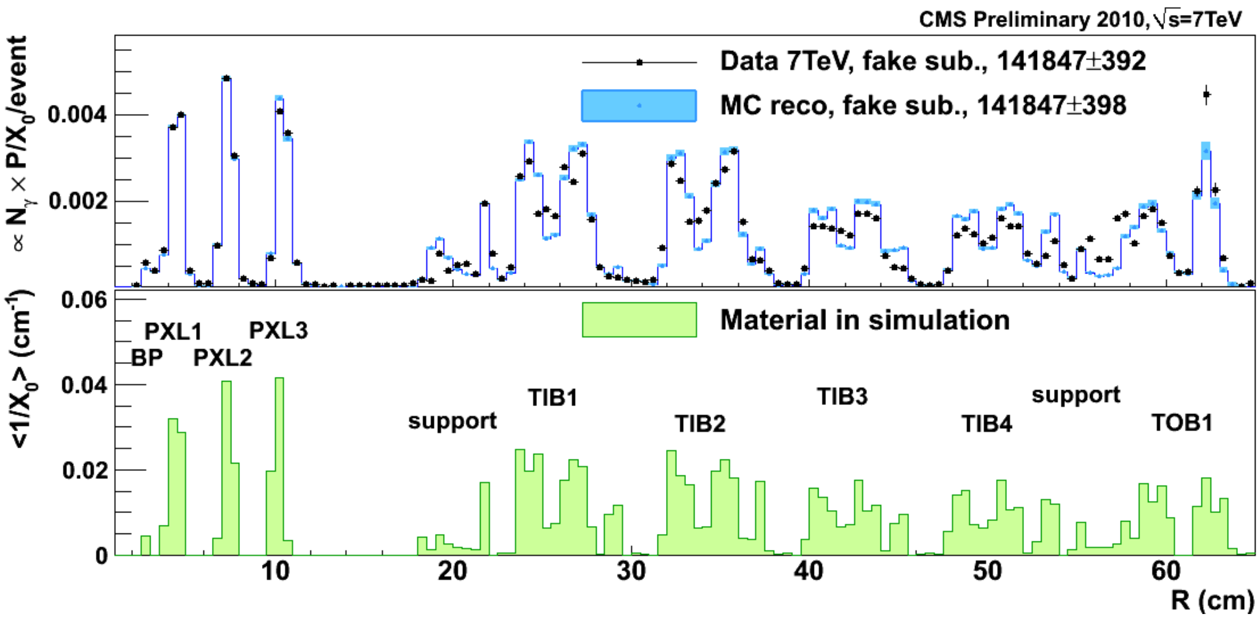

X-ray of the CMS tracker

- Use photon conversions ($\gamma \rightarrow e^+e^-$)
  - probability of interaction depends on the transversed material ($1-e^{-x/X0}$)
  - 54% of the H → γγ events have are expected to have at least one conversion

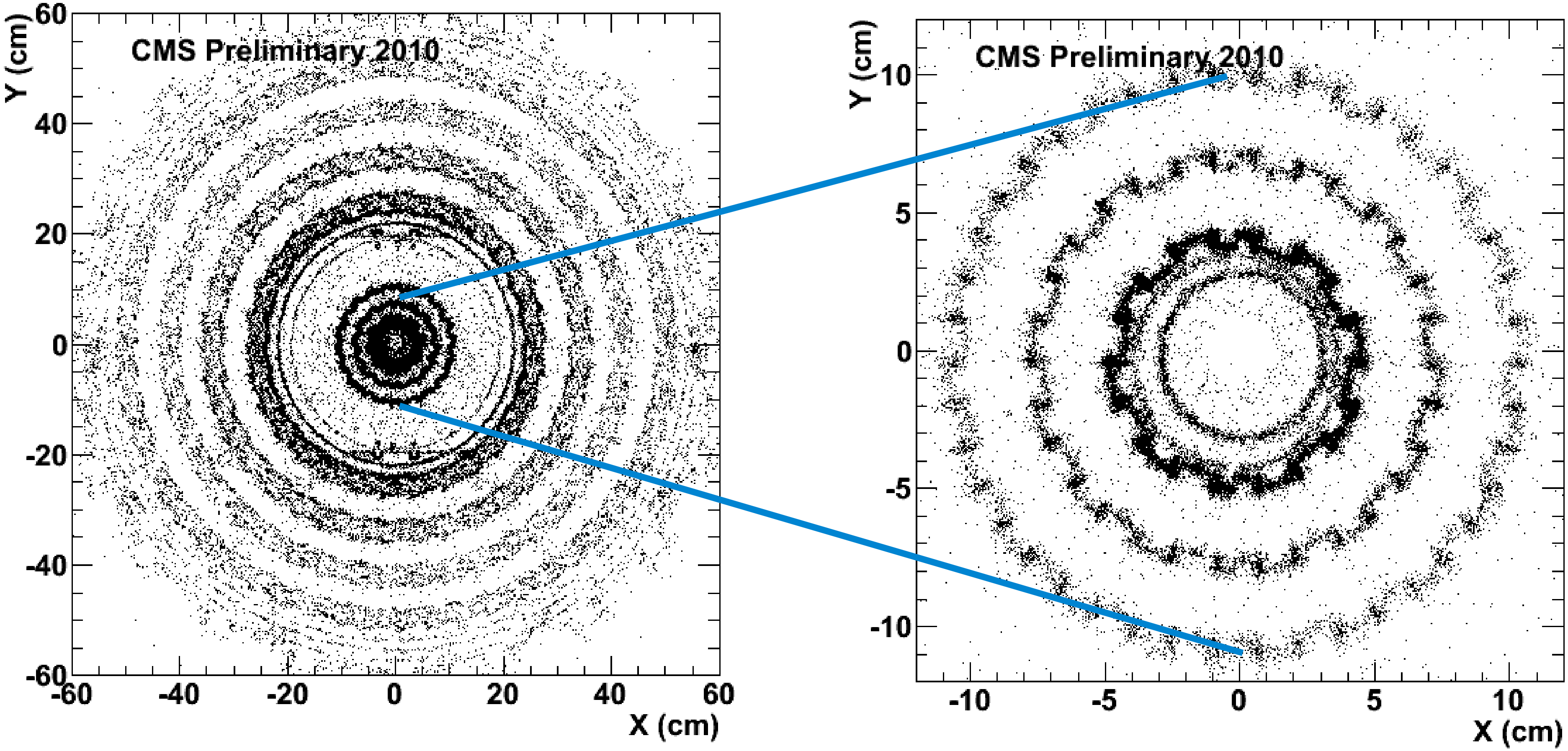

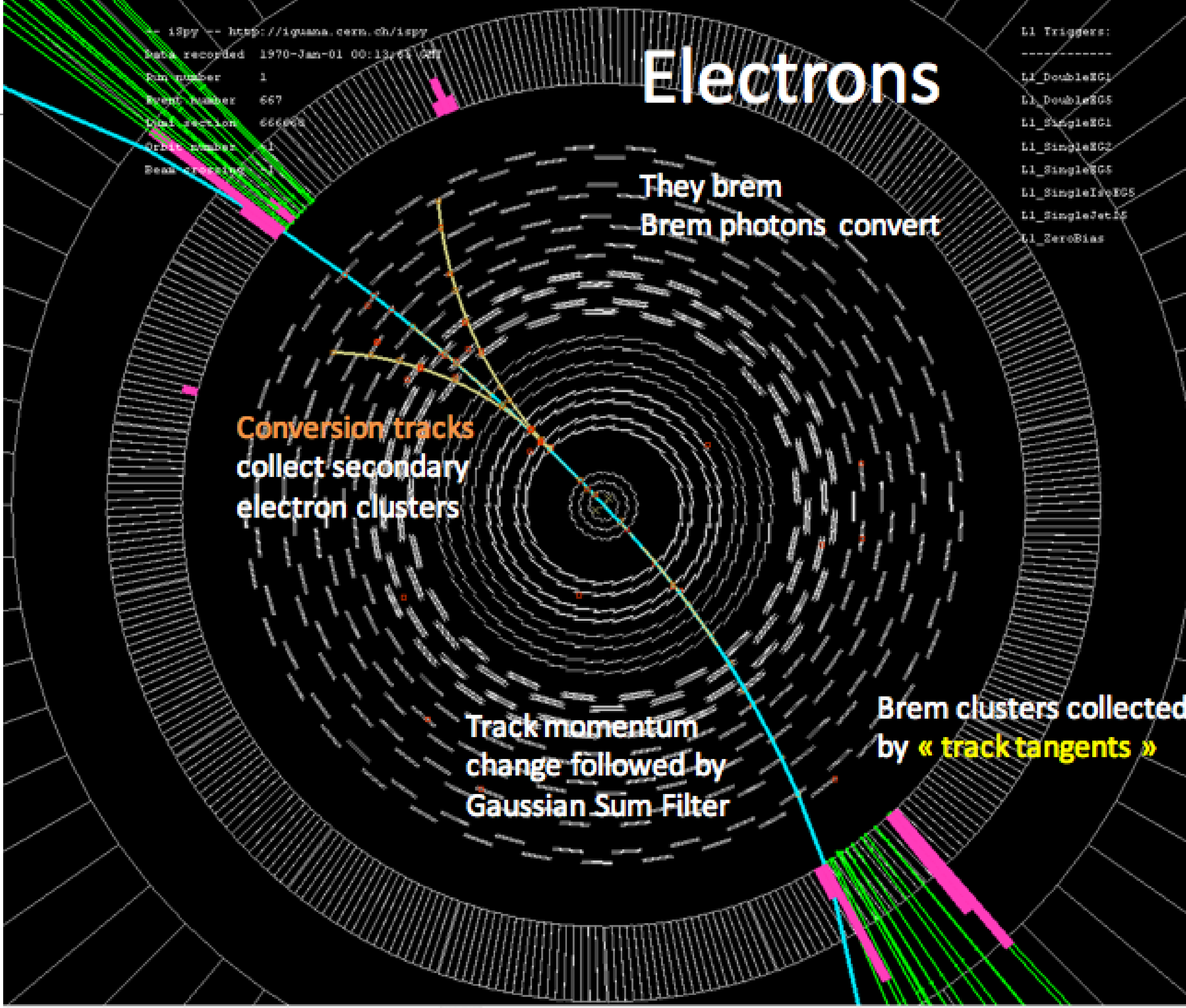
Electrons
They brem
Brem photons convert
Conversion tracks
collect secondary
electron clusters
Track momentum
change followed by
Gaussian Sum Filter
Brem clusters collected
by « track tangents »

Calorimetry for pedestrians

Recall: we measure what collapses in the detector

- Particles need to interact in matter ⇒ destructive interaction
  - dE/dx is converted in a signal
  - collect: charge, light, heat

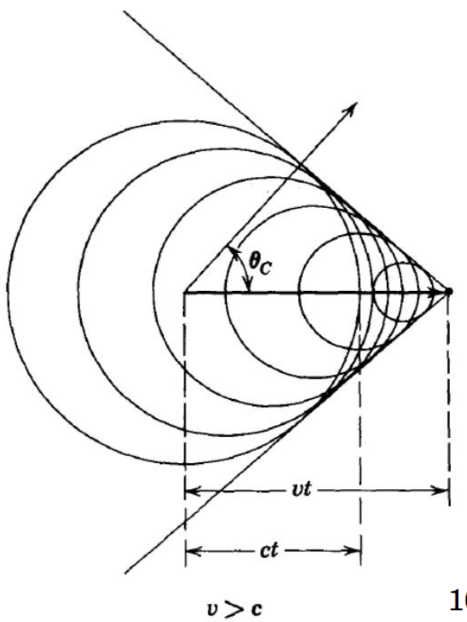

Cerenkov radiation

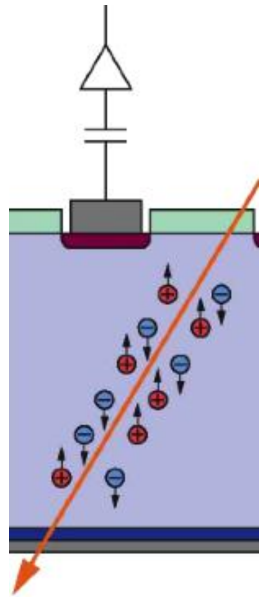

ionization

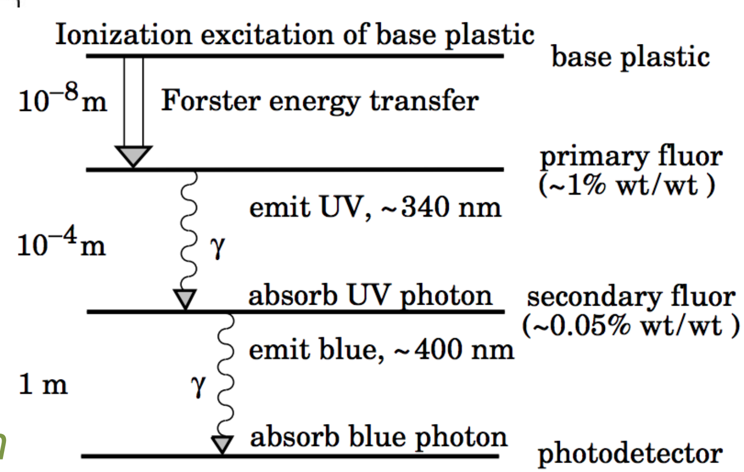

scintillation

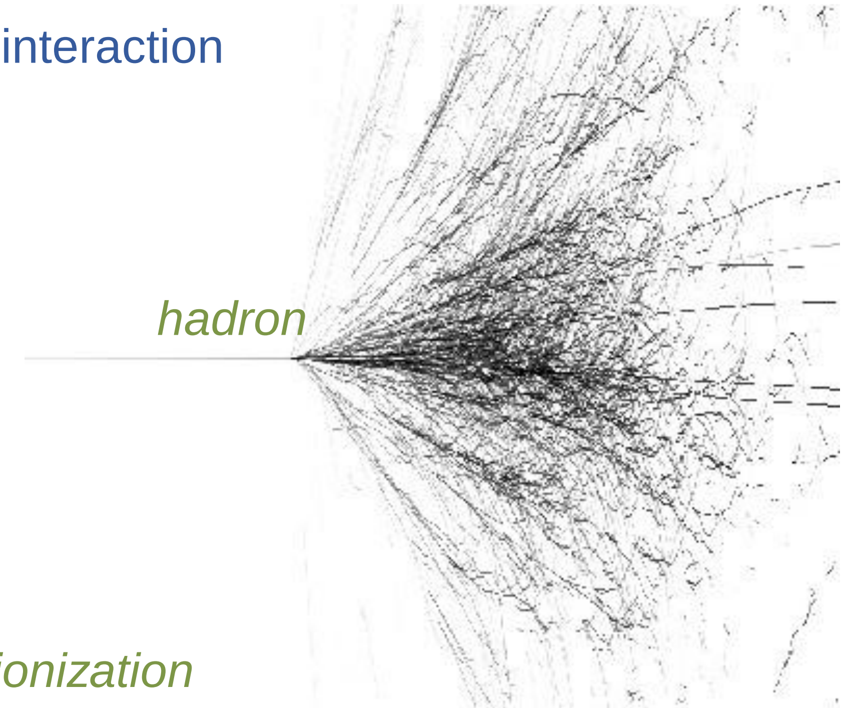

hadron

e/γ

Purpose of a calorimeter

- Primarily they measure the total energy of a particle, but they are versatile
  - can measure position, angle and timing
  - infer energy of neutrinos after energy balance

- General properties
  - length of showers induced in calorimeters increase logarithmically with E
  - energy resolution improves with E
  - fast signals, easy to reconstruct (unlike tracking) $\Rightarrow$ trigger

- Almost impossible to do high energy physics without calorimeters

A very brief historical overview

- Nuclear Physics in the 50's usage of semi-conductor devices improving the energy measurement of radiation energy
- Cosmic Rays (1958) - the first sampling calorimeter
- Particle Physics: adoption of electromagnetic and some times hadronic calorimeters as crucial components in experiments
  - Uranium/compensation (1975) - uniformize response to e/γ and hadrons to improve resolution
  - 4π calorimeters
  - High precision calorimetry with crystals, liquid Argon, scintillating fibers
- Particle flow calorimeters for HL-LHC, CLIC/ILC

  (weighing more on reconstruction than hardware…)

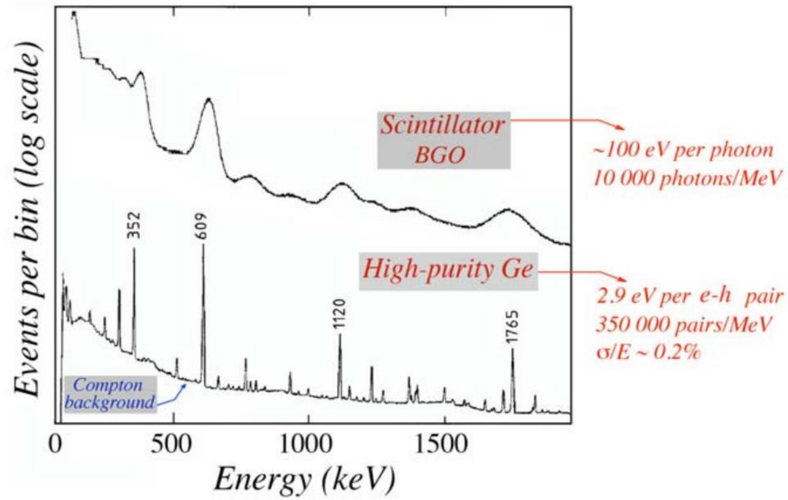

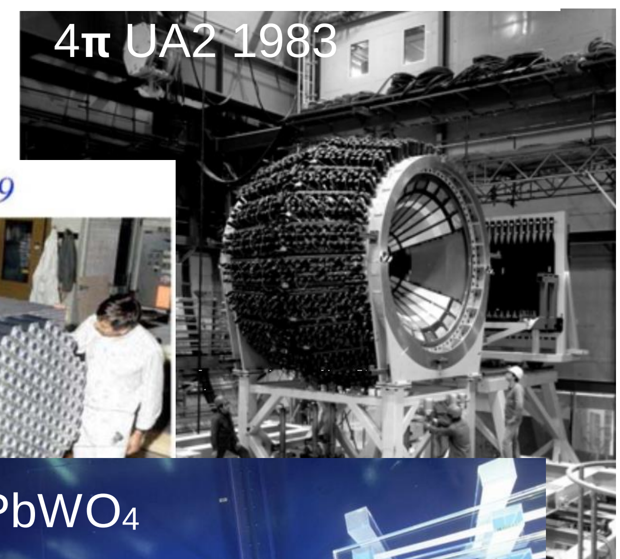

ATLAS calorimetry system

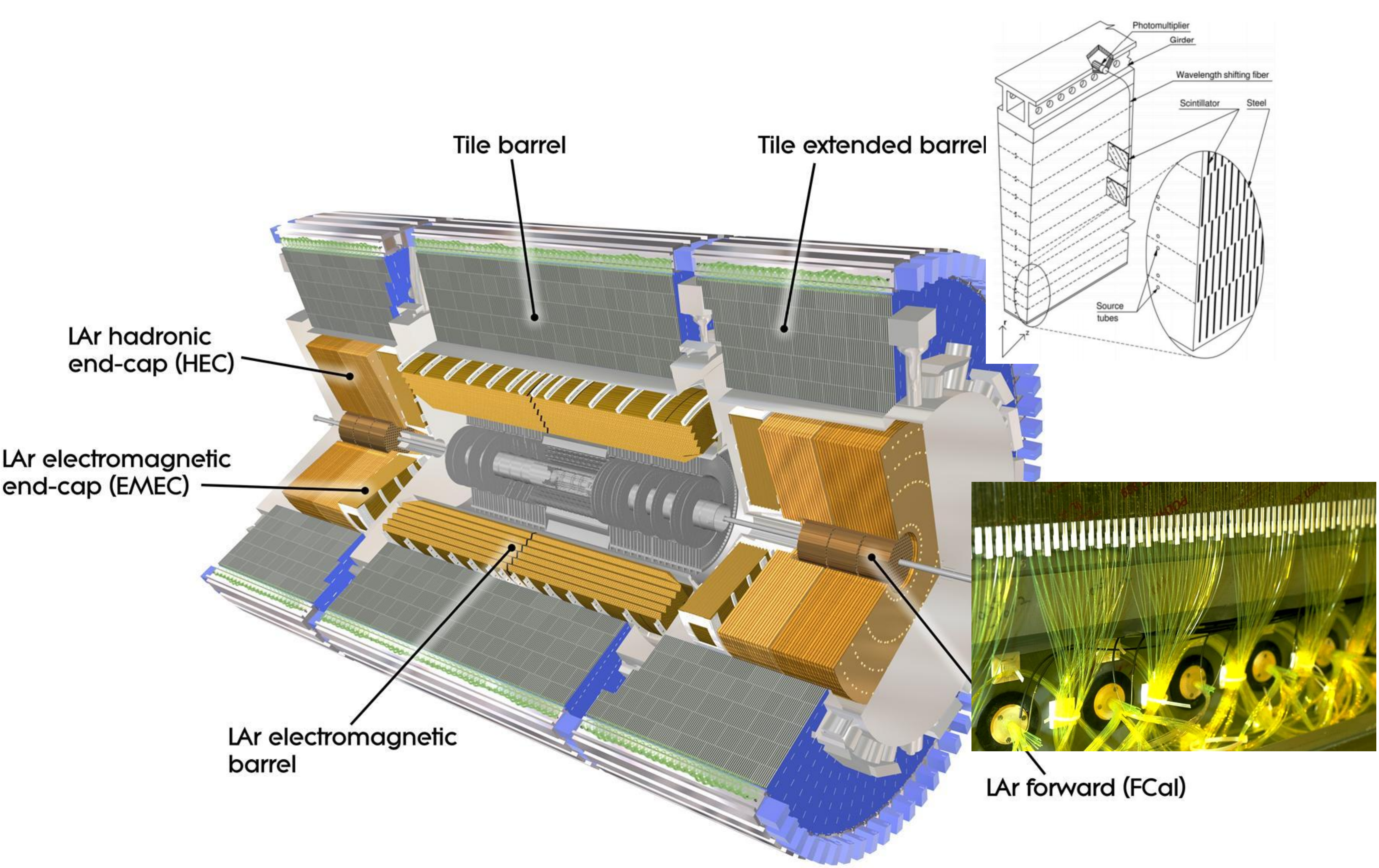

CMS calorimetry system

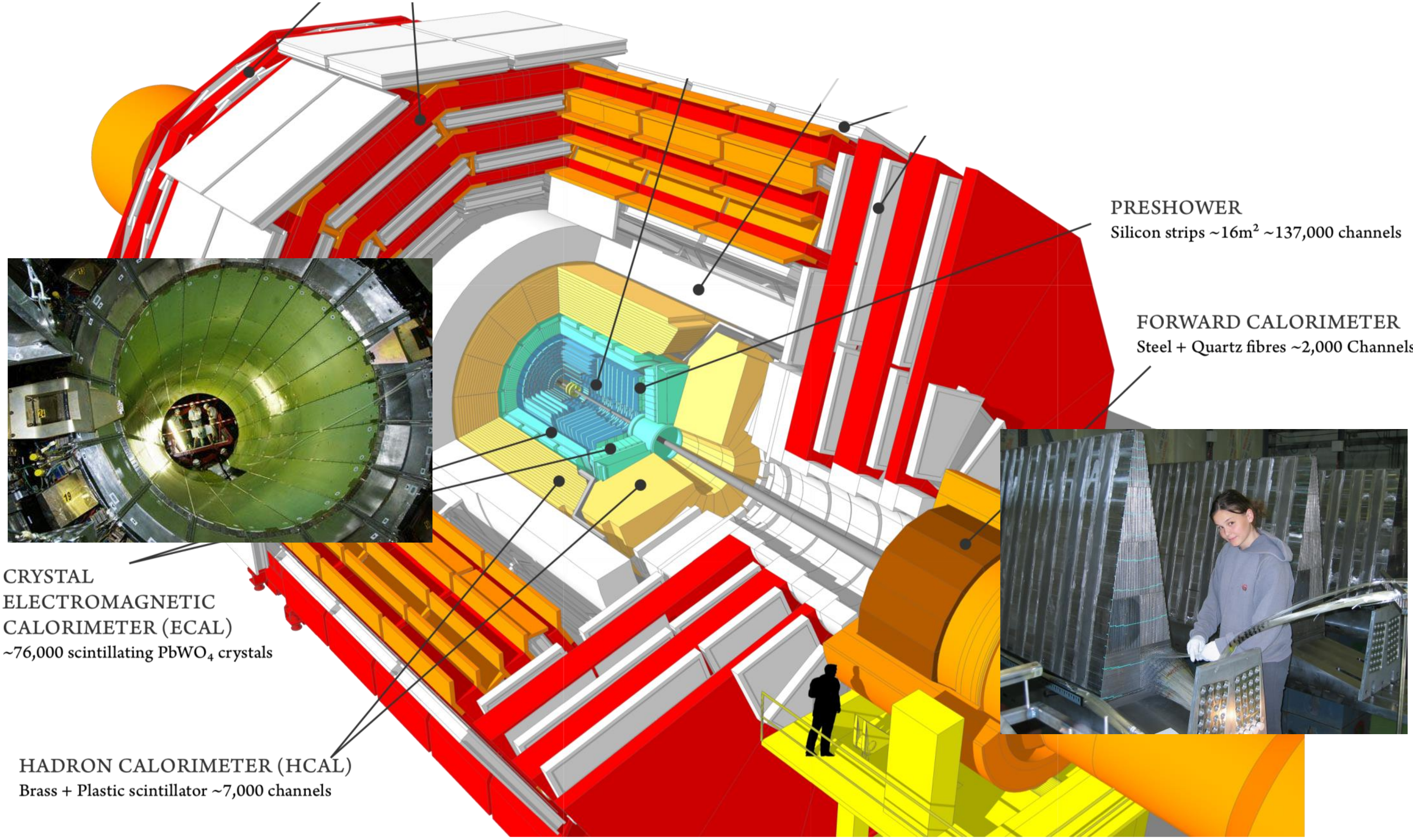

Calorimetry in LHCb

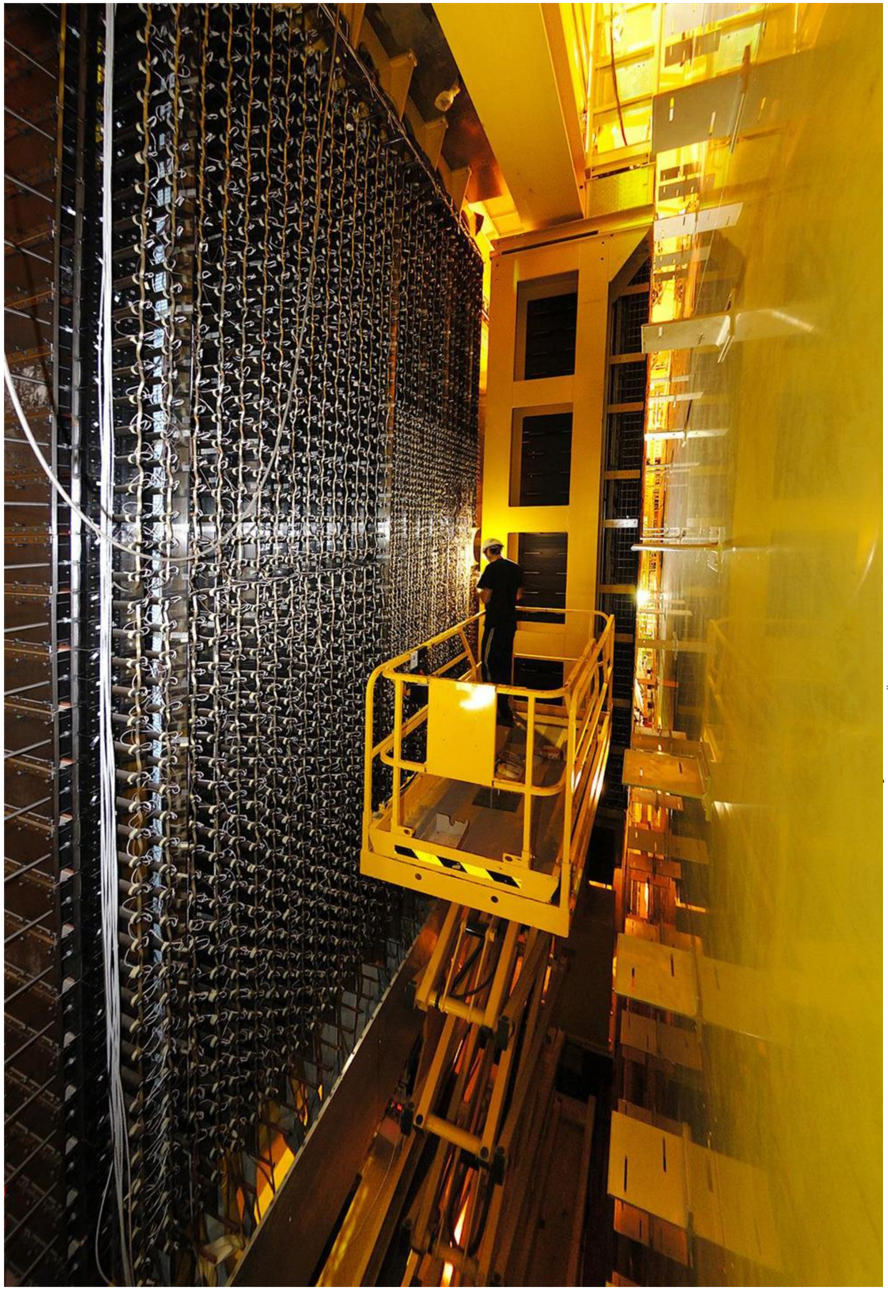

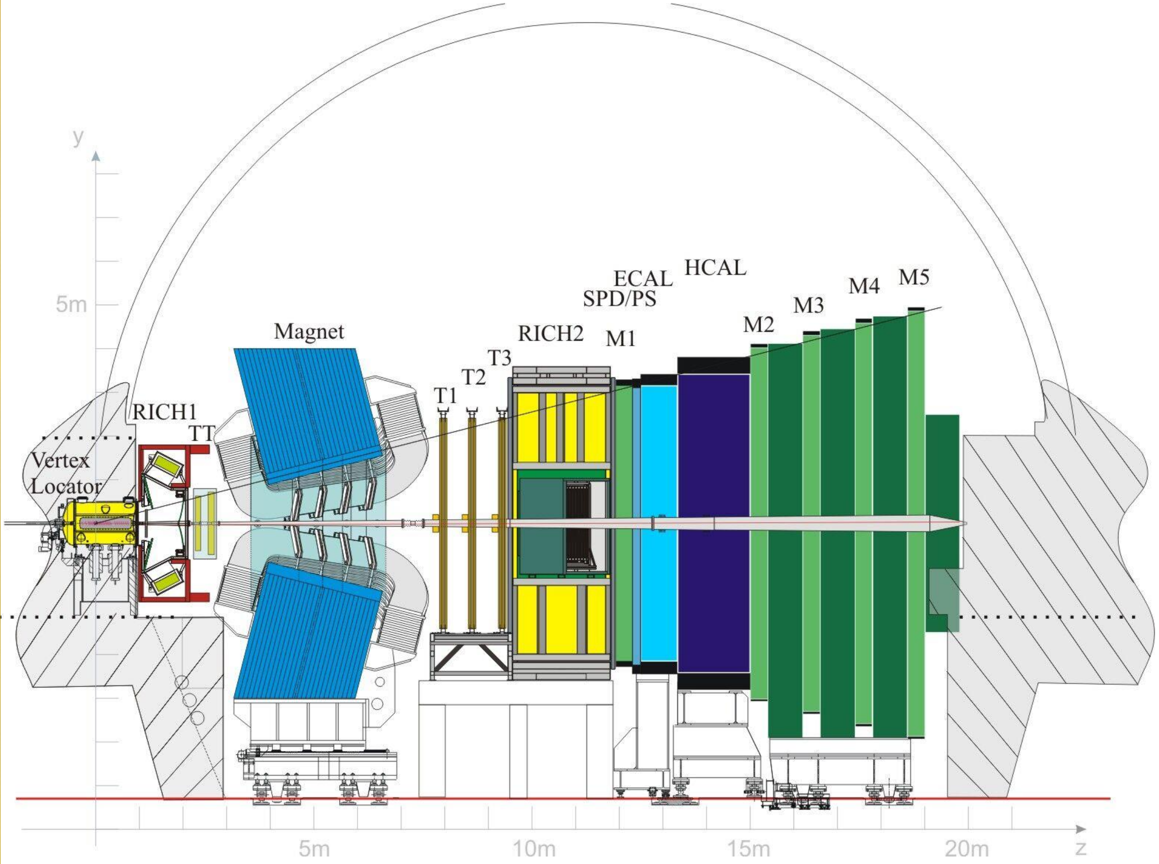

Plastic+metal sandwiches

Calorimetry in ALICE

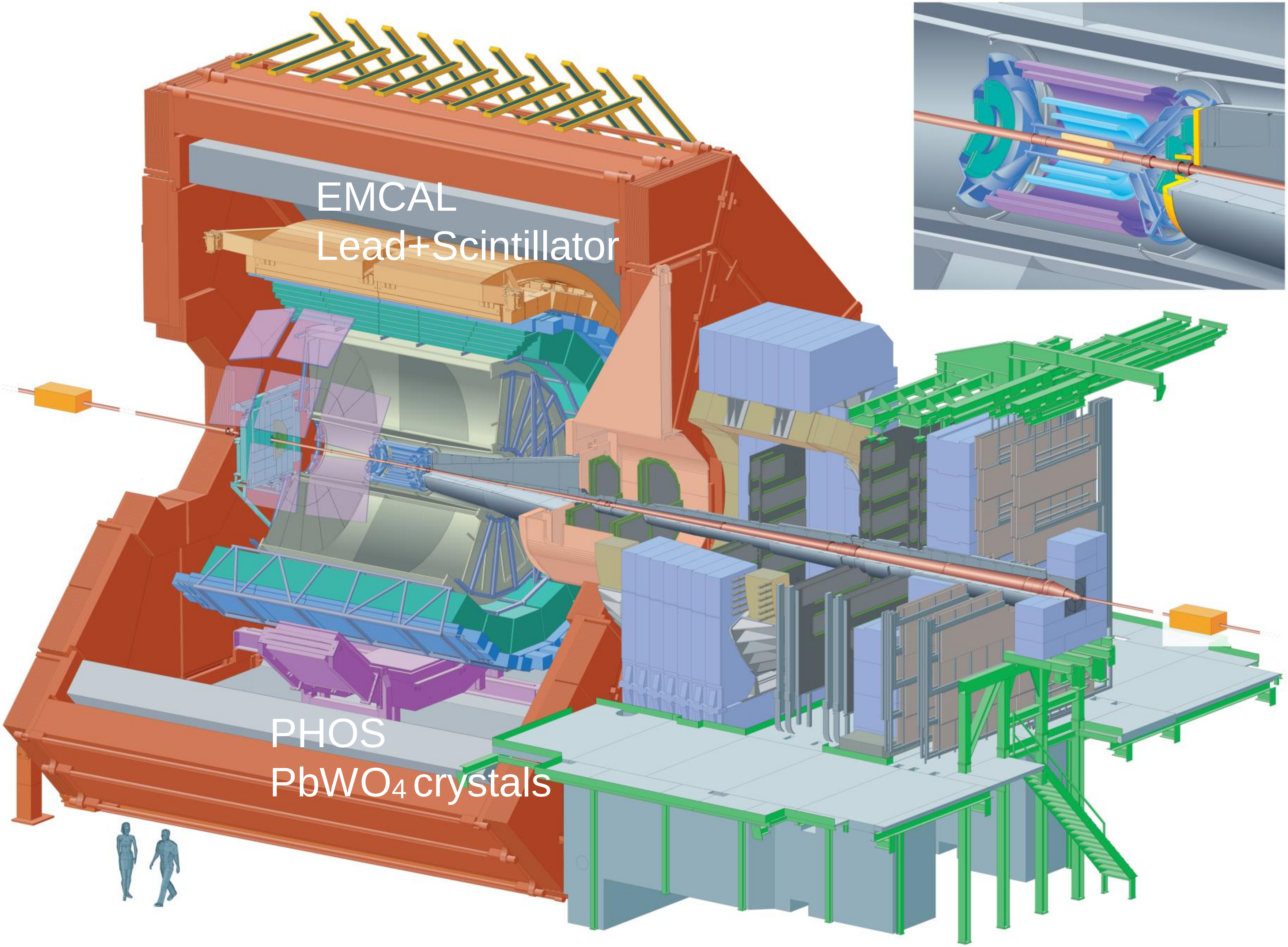

Electromagnetic calorimeters

- e/γ loose energy interacting with nuclei and atomic electrons

e
- ionization
- bremmstrahlung

γ
- photoelectric effect
- Compton scattering
- pair production

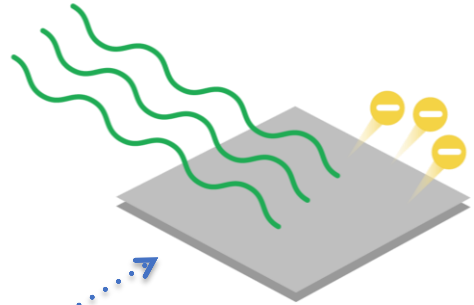

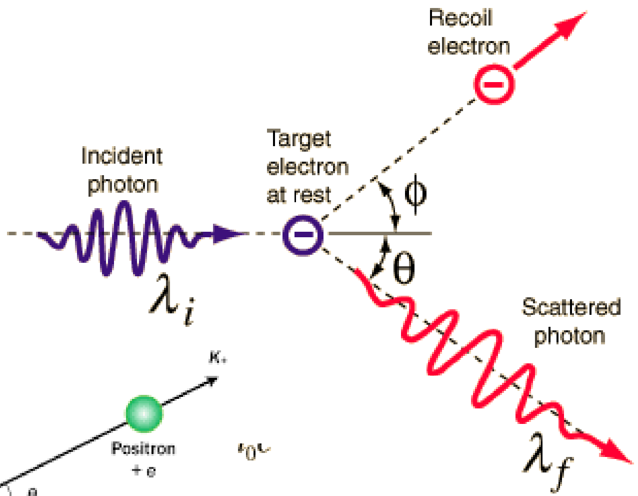

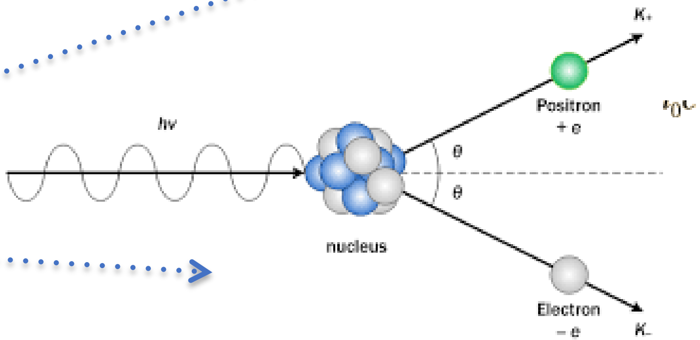

- e.m. showers will evolve very similarly independently on how they start
  - subsequent e or γ will branch according to these interactions

Processes initiated by electrons

Critical energy (E_c):
ionization and radiation are at the same level

$$E_c \propto \frac{1}{Z + \mathrm{cte}}$$

7 MeV for Lead

Radiation length (X_0):
quantifies by how much the energy flux is reduced by 1/e

$$X_0 \approx \frac{716\ [\mathrm{gcm}^{-2}]\ A}{Z(Z+1)\ln(287/\sqrt{Z})}$$

0.56cm for Lead

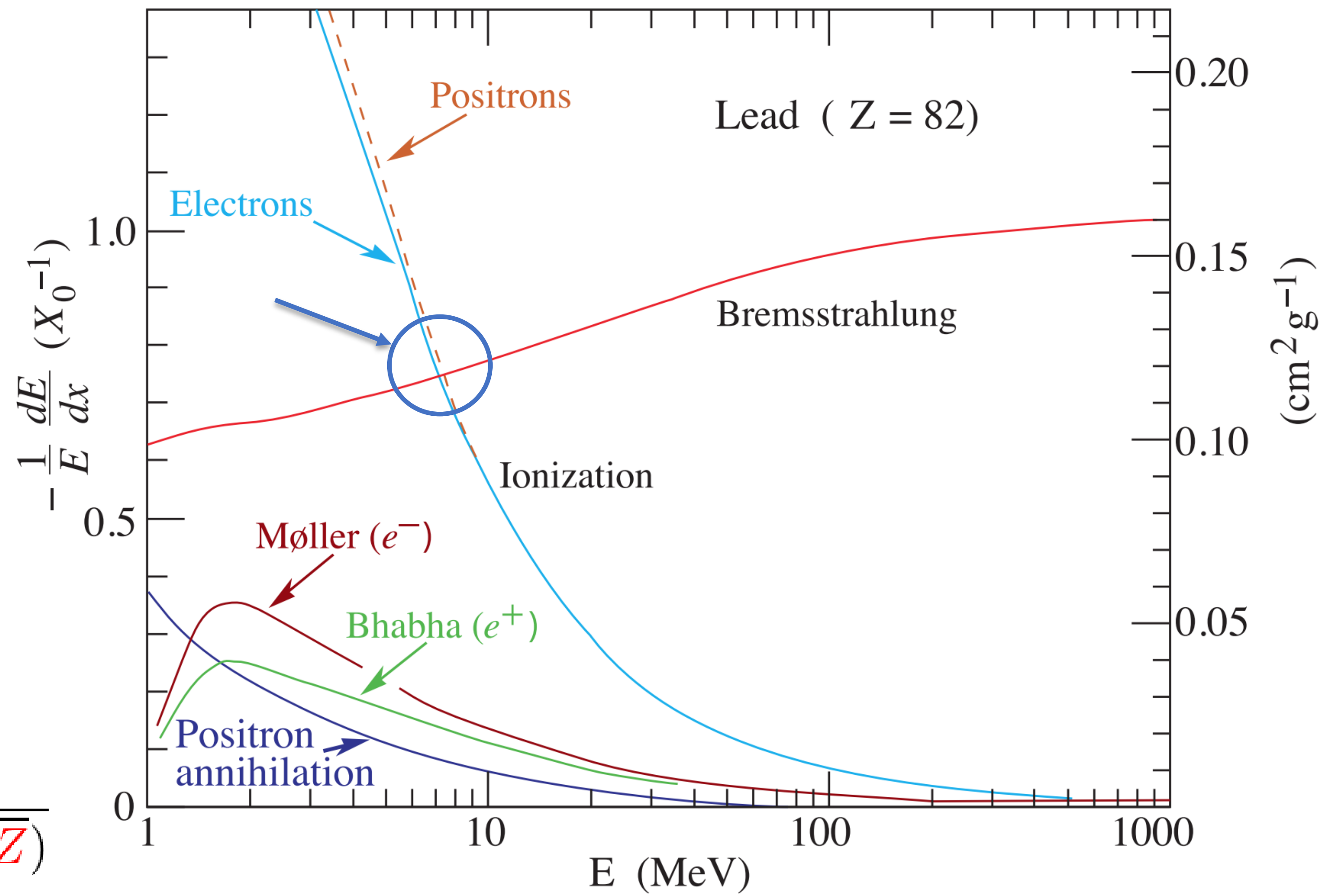

Processes initiated by photons

- Photo-electric effect

$$\sigma \approx Z^5 \alpha^4 \left(\frac{m_e c^2}{E}\right)^{-7/2}$$

- Compton scattering

$$\sigma \approx Z \frac{\ln E}{E}$$

- Pair production

$$\sigma \approx \frac{7}{9} \frac{A}{N_A} \frac{1}{X_0} \propto Z(Z+1)$$

probability to convert after $1X_0$ is $e^{-7/9}$

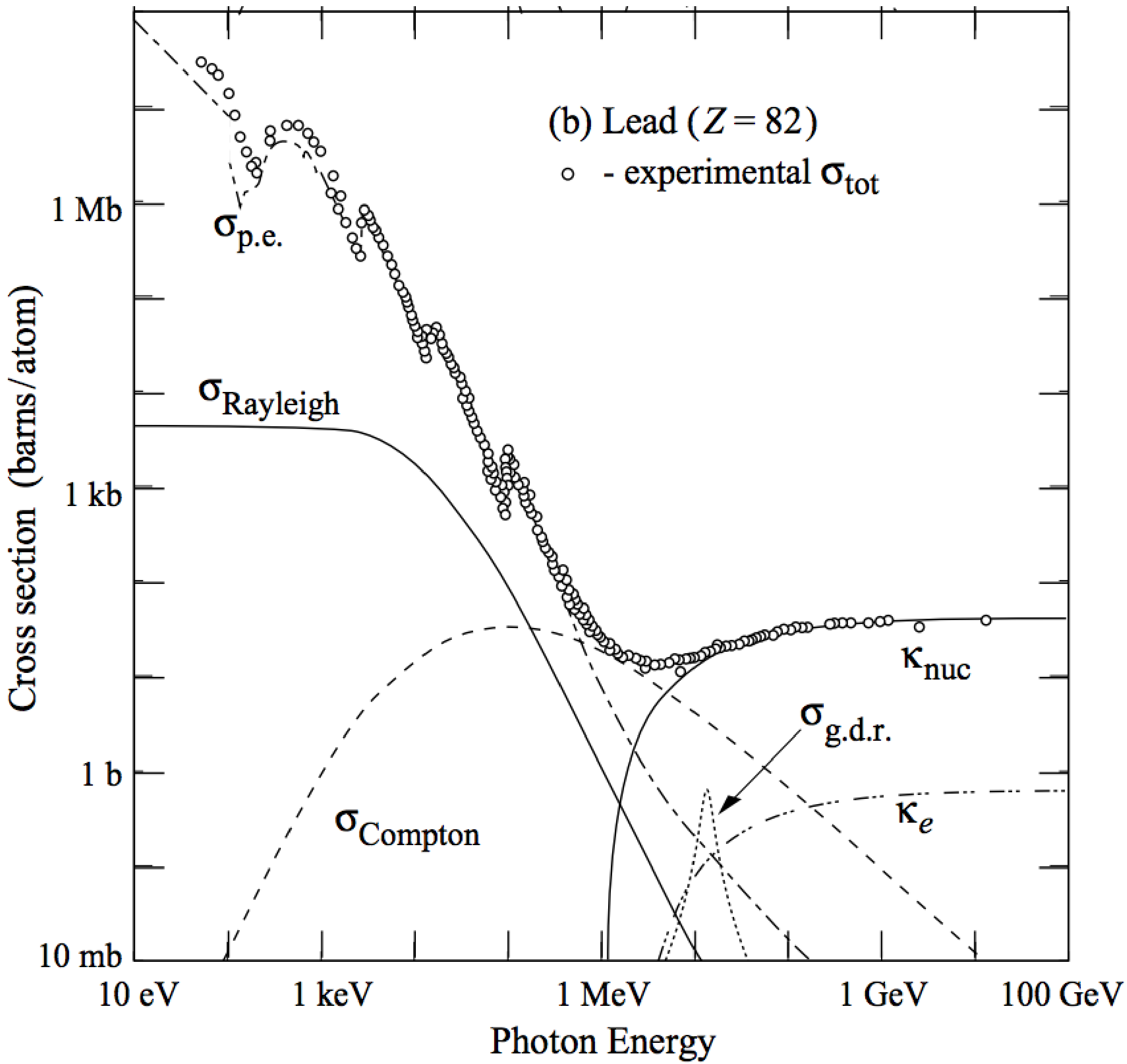

Electromagnetic showers

- High energy e/γ will start a cascade of pair production and bremmstrahlung
    - multiplicative regime until secondaries start falling below E_c

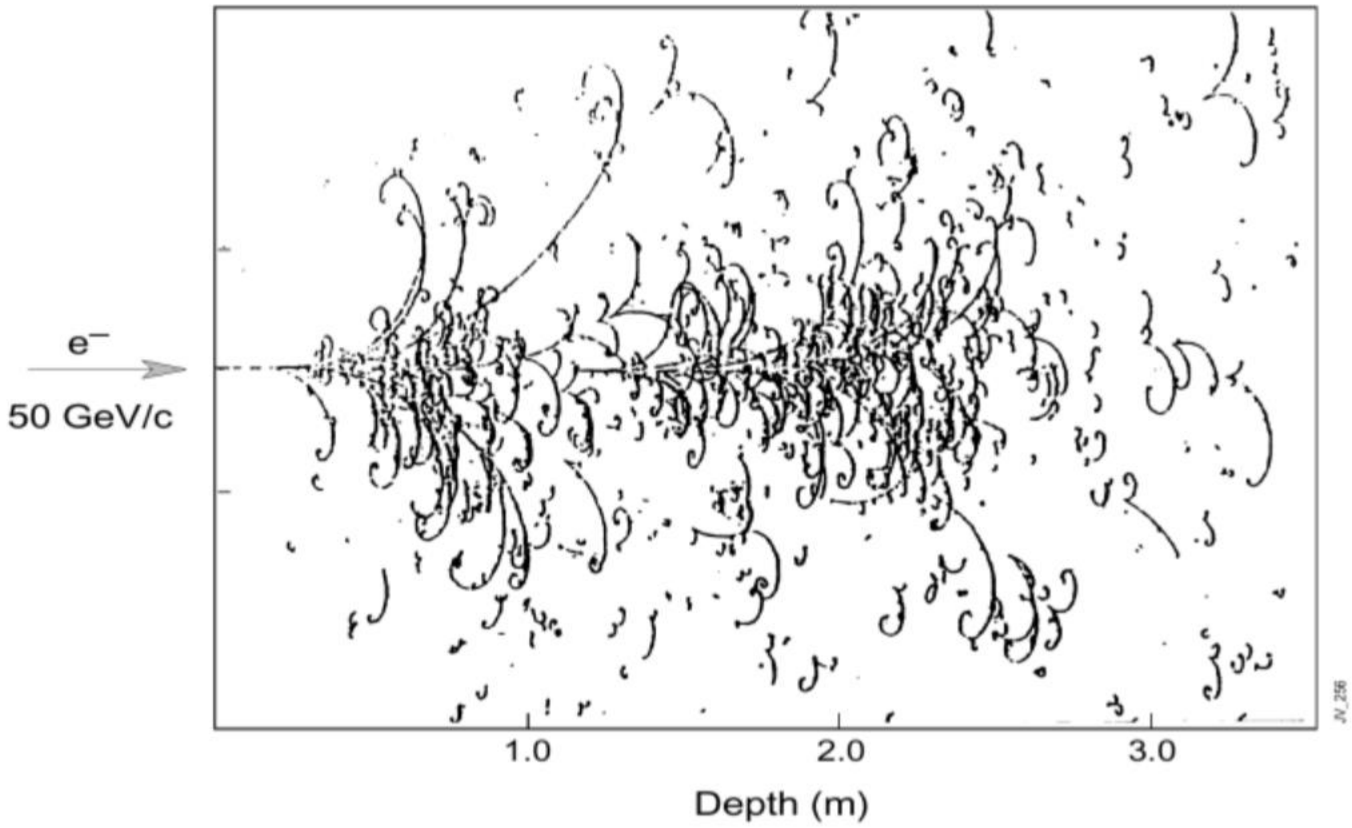

e- in bubble chamber (70% Ne: 30% H_2) under 3T field

Electromagnetic showers

- High energy e/γ will start a cascade of pair production and bremmstrahlung
  - multiplicative regime until secondaries start falling below E_c

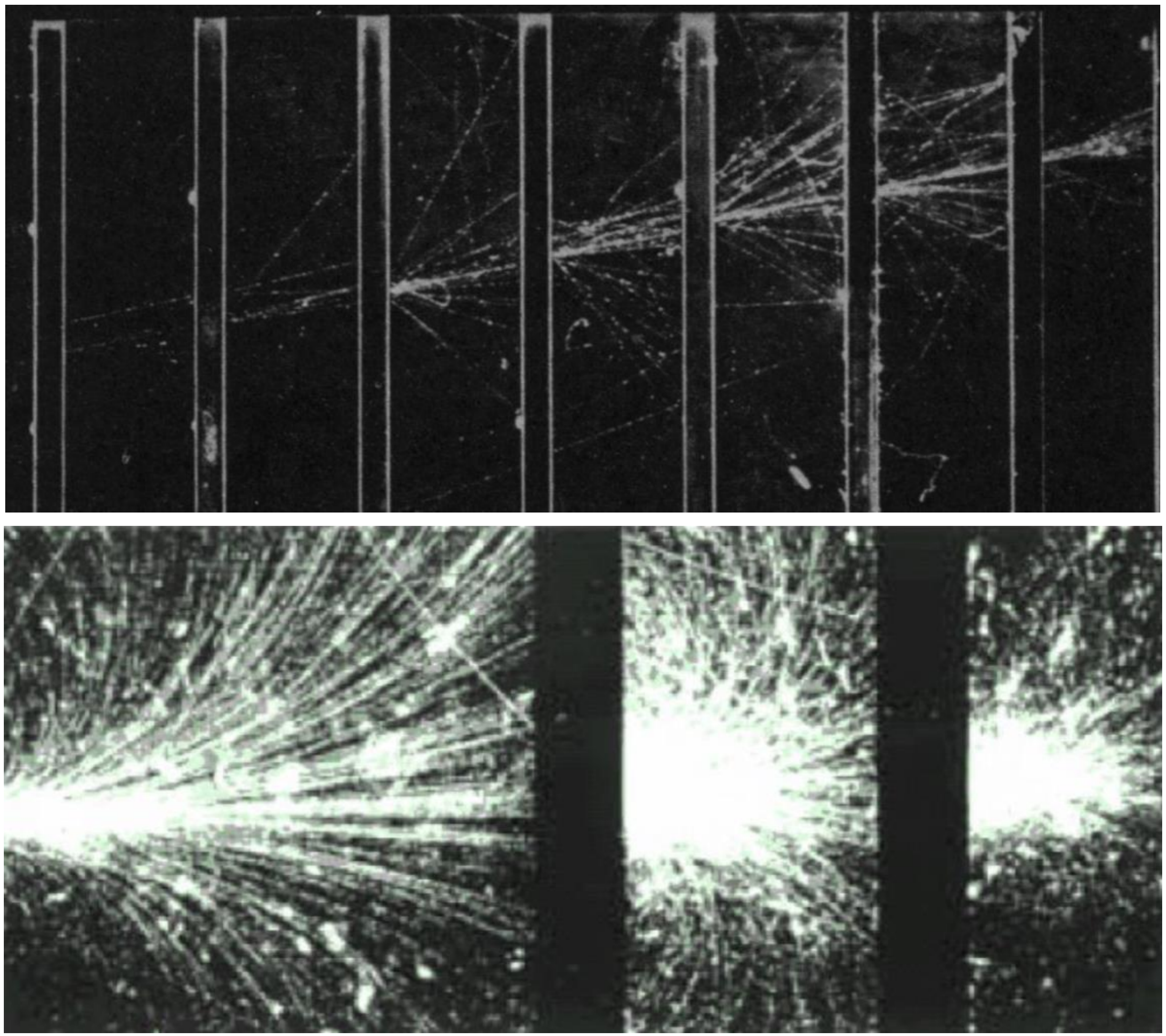

showers from two different energy photons in bubble chambers

A toy model for electromagnetic showers

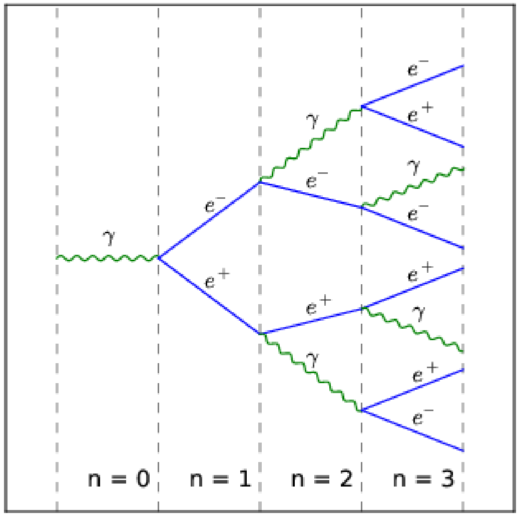

- Start with a pair conversion followed by radiation,… E → E/2 → E/4 → …

- Scaling properties $N(x) = 2^{x/X_0}$ $E(x) = E_0/2^{x/X_0}$

- Splitting energy reaches E_C limit, shower starts to be absorbed

$$x_{max} = X_0 \ln_2 \frac{E}{E_c} \qquad N_{max} = \frac{E}{E_c}$$

not so far from reality

Detailed simulation of an electromagnetic shower

$$t_{\max} \sim \ln \frac{E}{E_c} \pm 0.5$$

$$t_{95\%} = t_{\max} + 0.08Z + 9.6$$

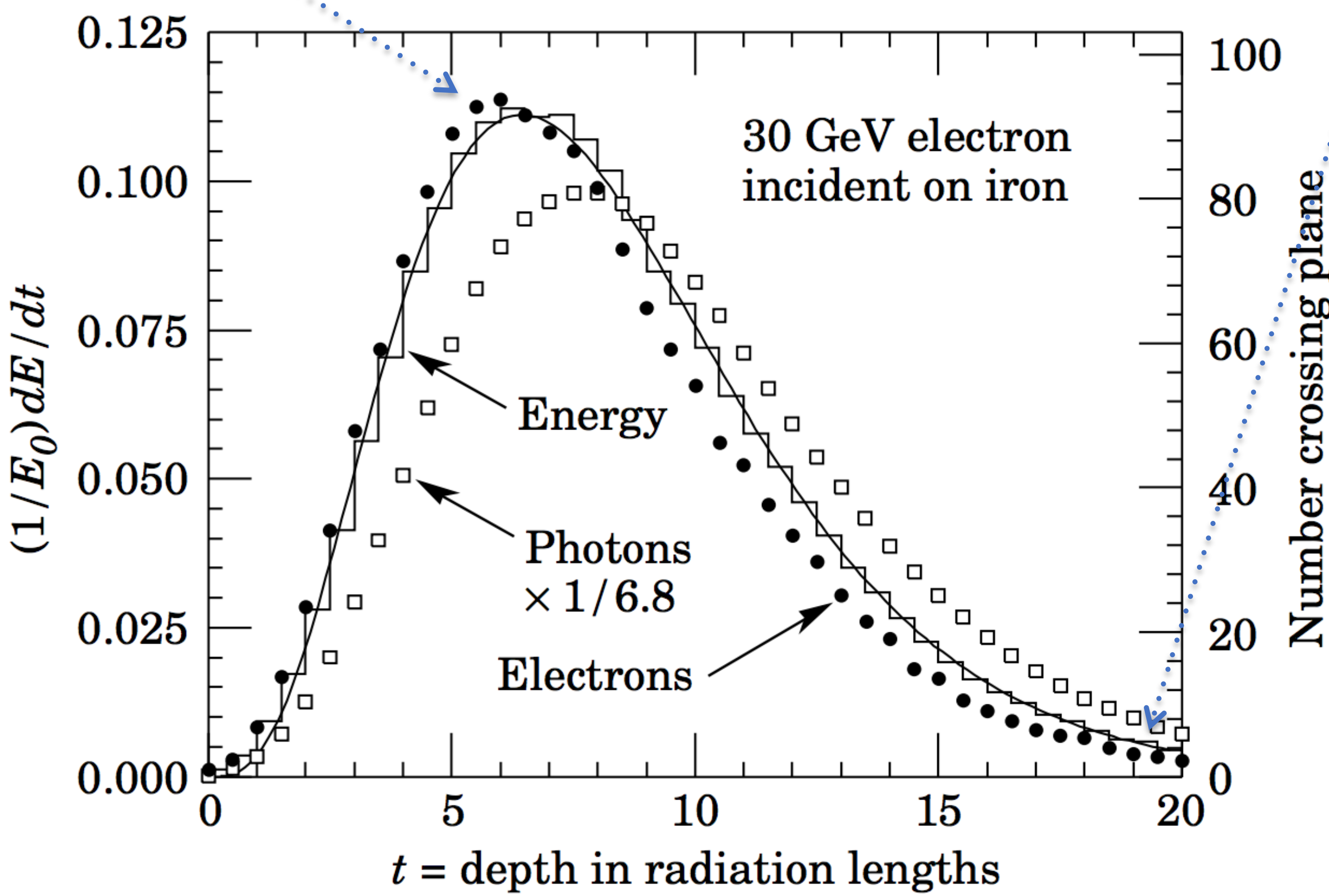

Spread in the transverse plane

- Particles disperse with respect to initial axis
  - decay openings
  - multiple scattering of charged particles
  - γ in the region of minimal absorption travelling longer

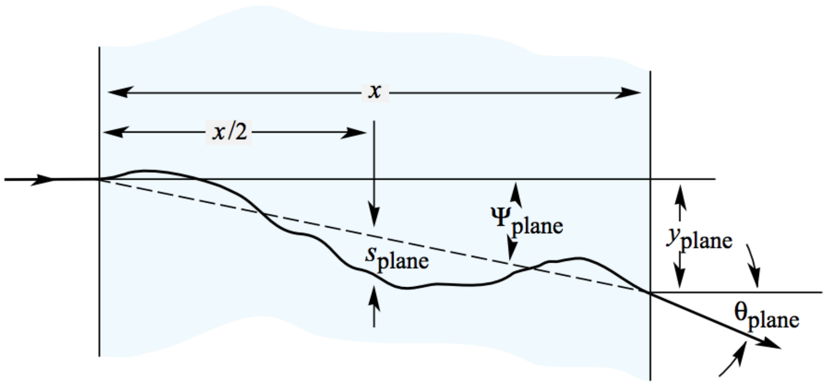

- Define the Moliere radius as

  lateral size containing 90% of the shower energy

$$R_M = \frac{21\ \mathrm{MeV}}{E_c} X_0 \propto \frac{A}{Z}$$

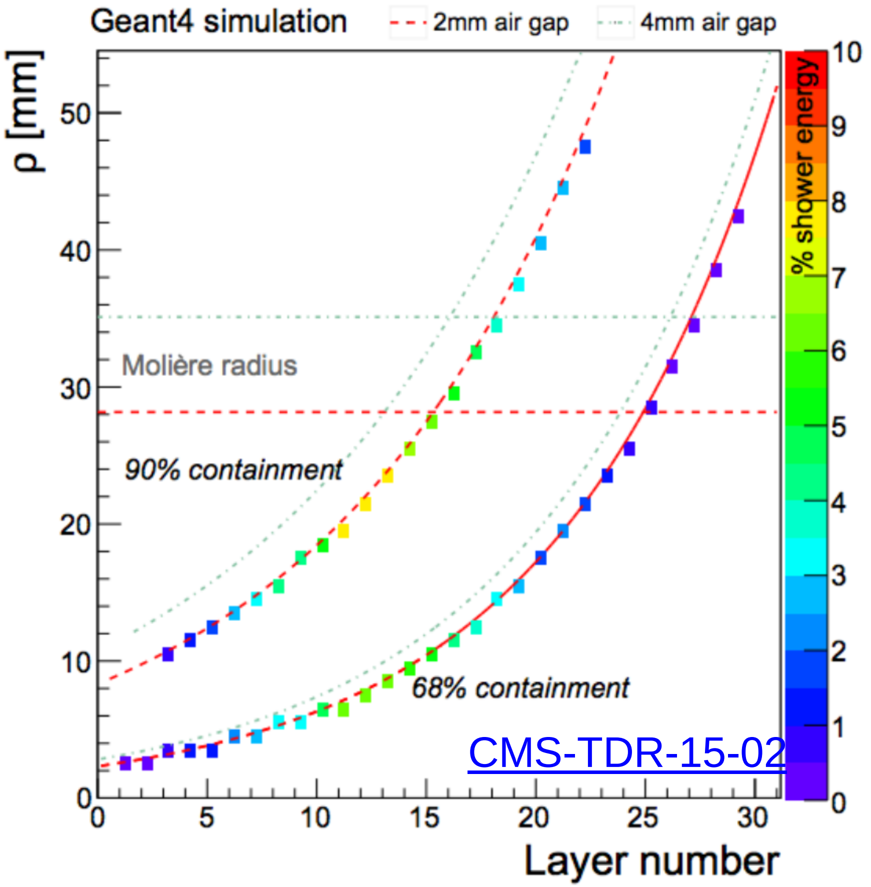

Electromagnetic energy resolutions

$$\frac{\sigma}{E} = \frac{a}{\sqrt{E}} \oplus \frac{b}{E} \oplus c$$

Stochastic term - fluctuations in the shower development, energy deposited. Enhanced if sampling is made, if Cerenkov radiation star later, etc.

Noise term - additional degradation at low energy due to electronics noise, pileup, etc.

Constant term - energy leakage, calibration, non uniformity, radiation damage, …

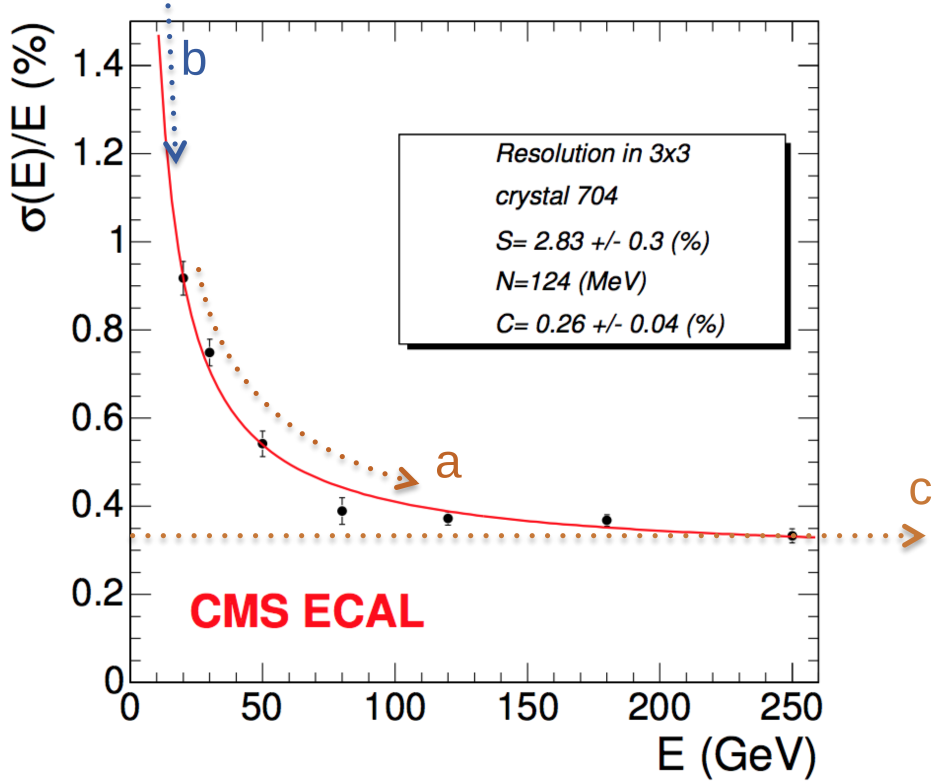

Some challenges in maintaining energy resolution

- Intercalibration between cells needs to attain 1% level or better
  - use η/$\boldsymbol{\pi}^0 \rightarrow \gamma\gamma$, Z→ee and ϕ symmetry in minimum bias
- Track radiation damage / recovery of the crystals with a laser
  - inject light into crystals and normalize to PN diodes

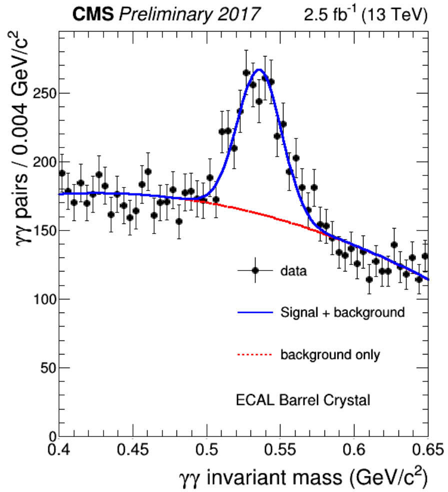

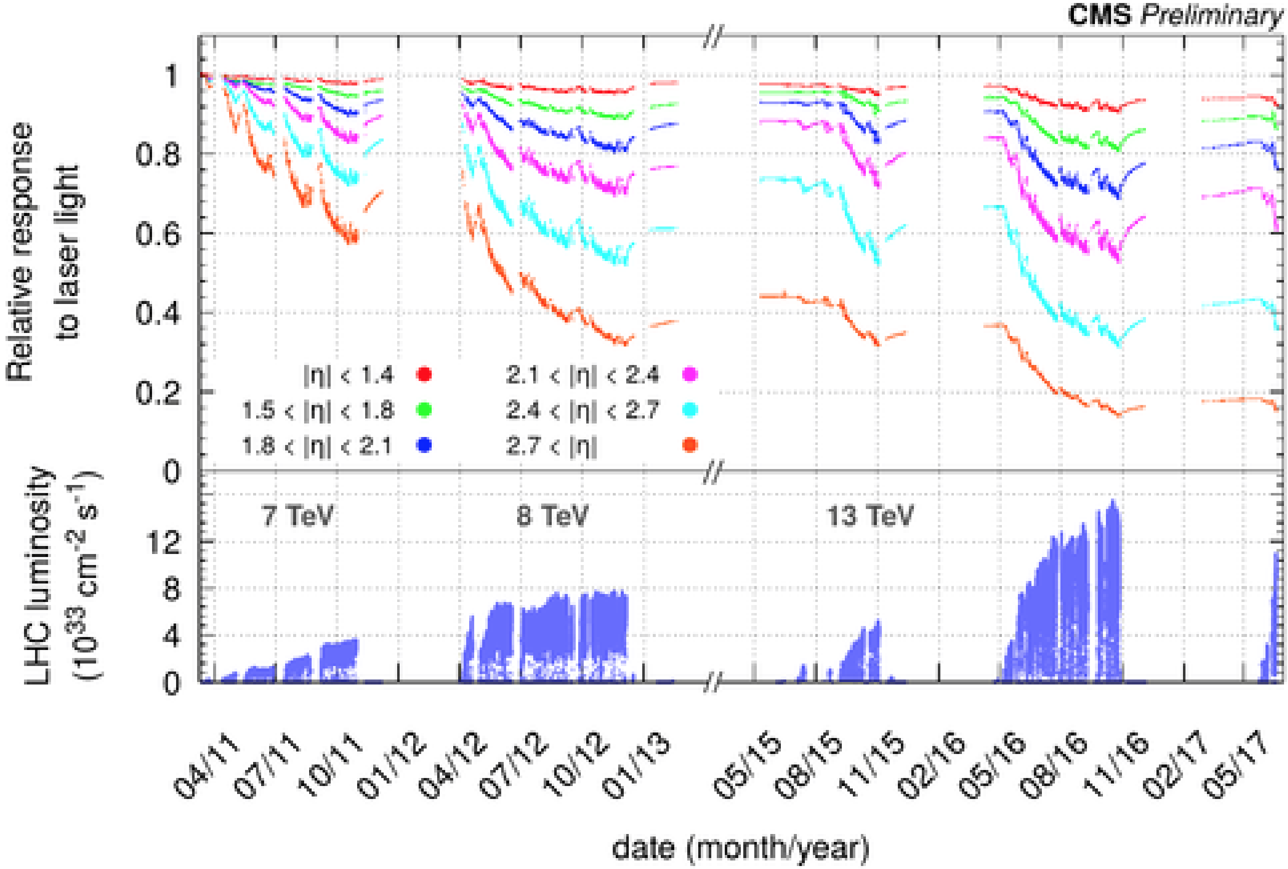

A comparison of different e.m. calorimeters

Technology (Experiment)	Depth	Energy resolution	Date
NaI(Tl) (Crystal Ball)	$20X_0$	$2.7\%/E^{1/4}$	1983
$Bi_4Ge_3O_{12}$ (BGO) (L3)	$22X_0$	$2\%/\sqrt{E} \oplus 0.7\%$	1993
CsI (KTeV)	$27X_0$	$2\%/\sqrt{E} \oplus 0.45\%$	1996
CsI(Tl) (BaBar)	16–$18X_0$	$2.3\%/E^{1/4} \oplus 1.4\%$	1999
CsI(Tl) (BELLE)	$16X_0$	1.7% for $E_\gamma > 3.5$ GeV	1998
$PbWO_4$ (PWO) (CMS)	$25X_0$	$3\%/\sqrt{E} \oplus 0.5\% \oplus 0.2/E$	1997
Lead glass (OPAL)	$20.5X_0$	$5\%/\sqrt{E}$	1990
Liquid Kr (NA48)	$27X_0$	$3.2\%/\sqrt{E} \oplus 0.42\% \oplus 0.09/E$	1998
Scintillator/depleted U (ZEUS)	20–$30X_0$	$18\%/\sqrt{E}$	1988
Scintillator/Pb (CDF)	$18X_0$	$13.5\%/\sqrt{E}$	1988
Scintillator fiber/Pb spaghetti (KLOE)	$15X_0$	$5.7\%/\sqrt{E} \oplus 0.6\%$	1995
Liquid Ar/Pb (NA31)	$27X_0$	$7.5\%/\sqrt{E} \oplus 0.5\% \oplus 0.1/E$	1988
Liquid Ar/Pb (SLD)	$21X_0$	$8\%/\sqrt{E}$	1993
Liquid Ar/Pb (H1)	20–$30X_0$	$12\%/\sqrt{E} \oplus 1\%$	1998
Liquid Ar/depl. U (DØ)	$20.5X_0$	$16\%/\sqrt{E} \oplus 0.3\% \oplus 0.3/E$	1993
Liquid Ar/Pb accordion (ATLAS)	$25X_0$	$10\%/\sqrt{E} \oplus 0.4\% \oplus 0.3/E$	1996

Hadronic showers

What is an hadronic shower?

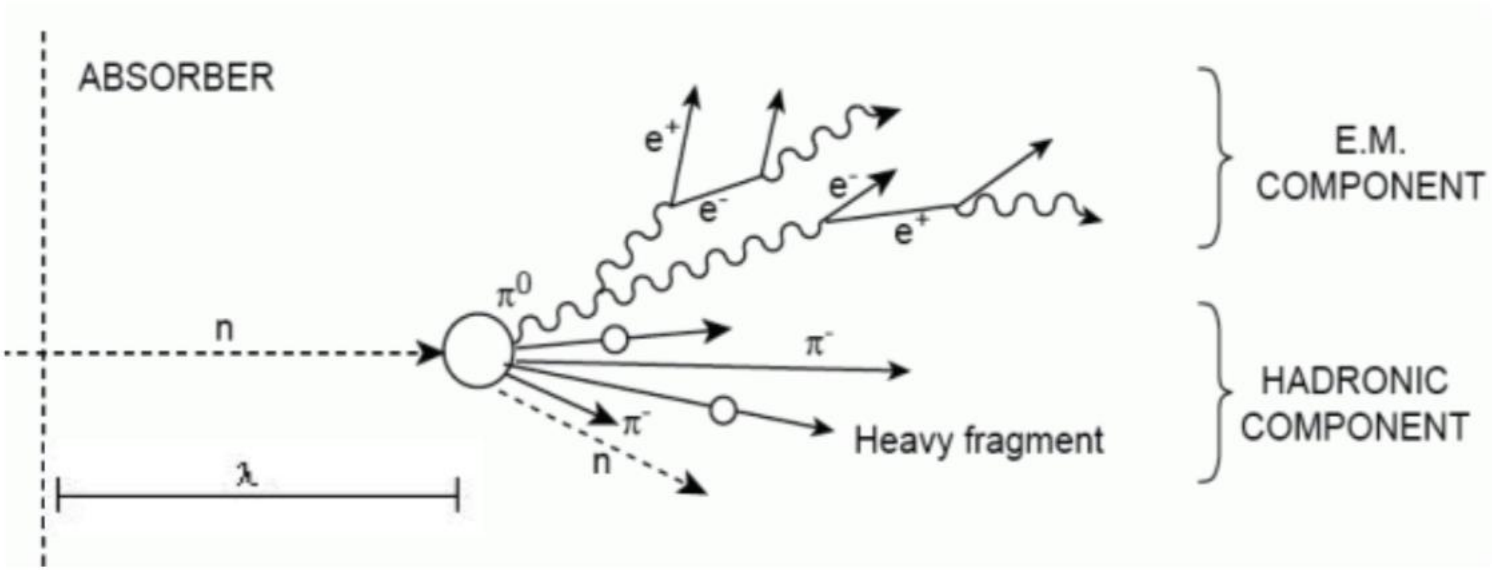

- Charged pions, kaons, protons, neutrons, etc…
- Products of strong interactions will start “mixed” showers
- Requires longer containment than e.m showers

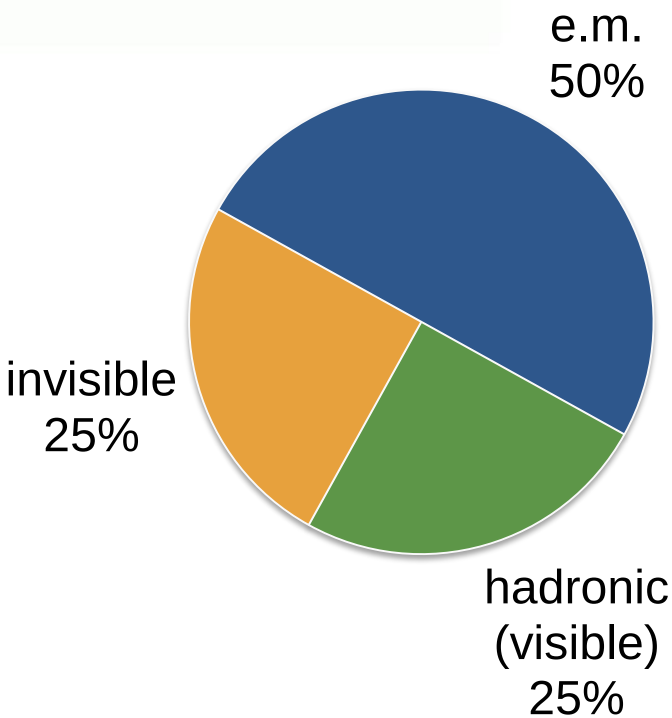

Particle spectra in a proton shower

Showers depend heavily on the incident particle…

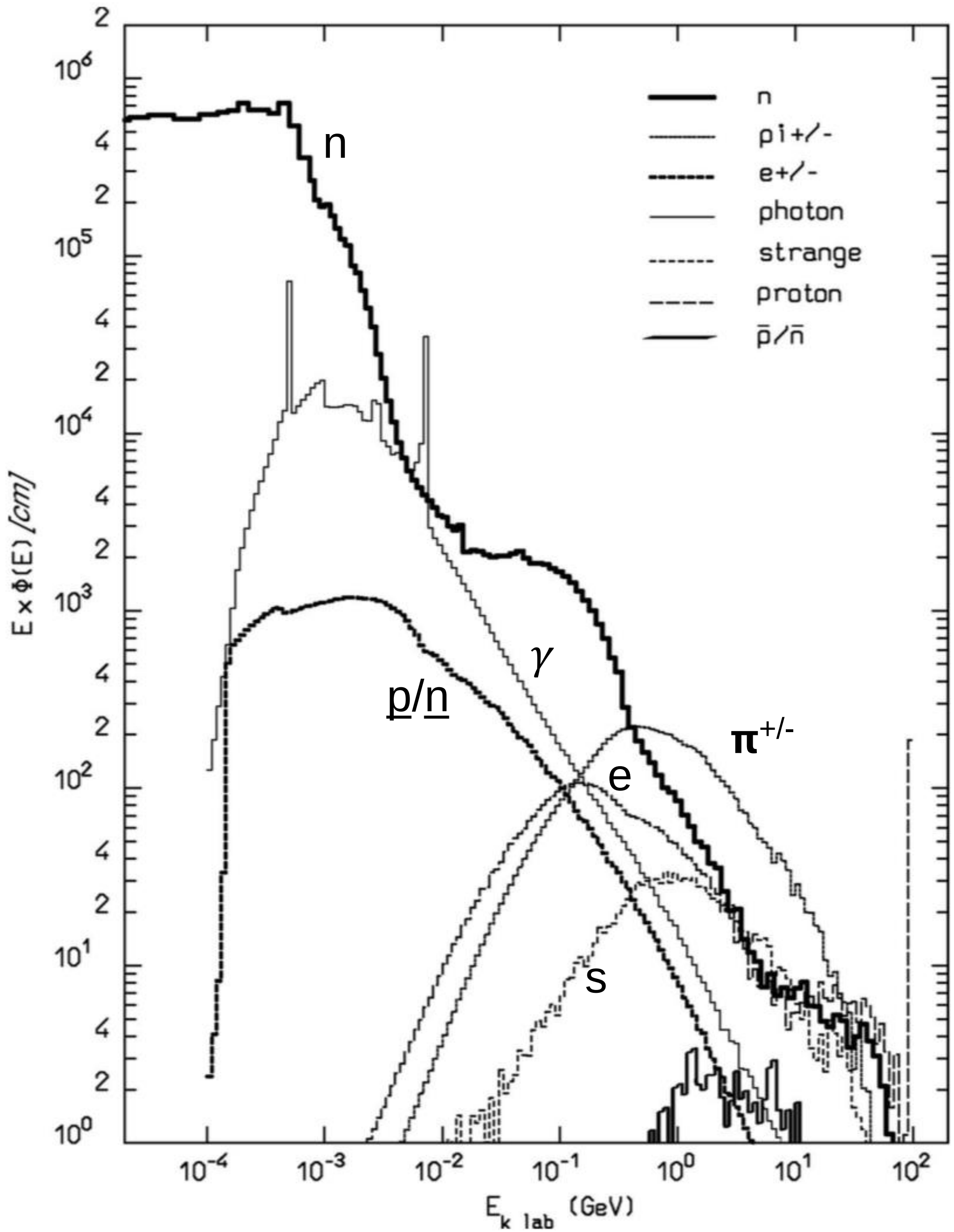

Based on simulation. The integral of each curve gives the relative fluence of each particle.

Particle spectra in a proton shower

Showers depend heavily on
the incident particle <u>and its energy</u>.

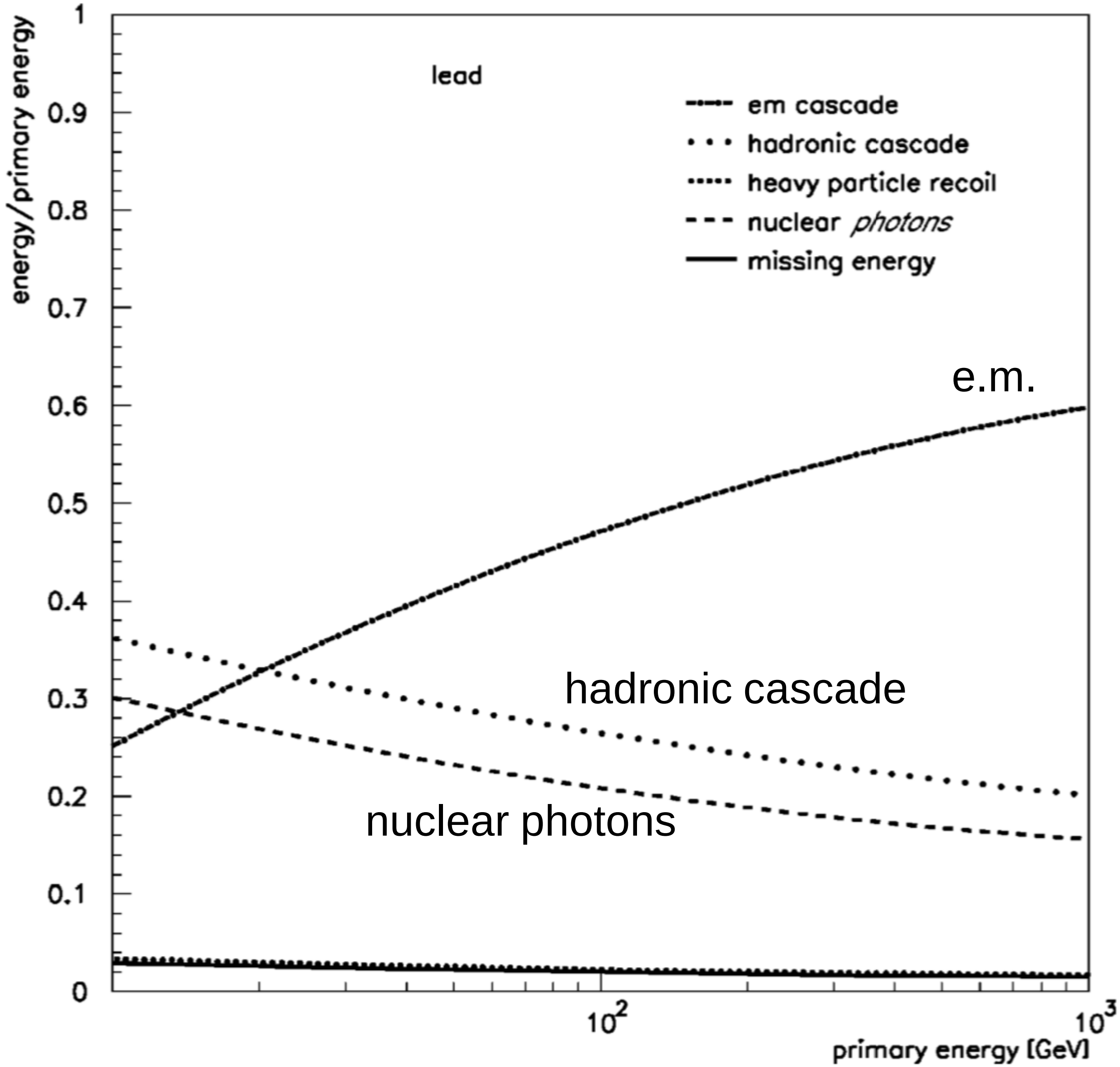

Based on simulation.

Particle spectra in a proton shower

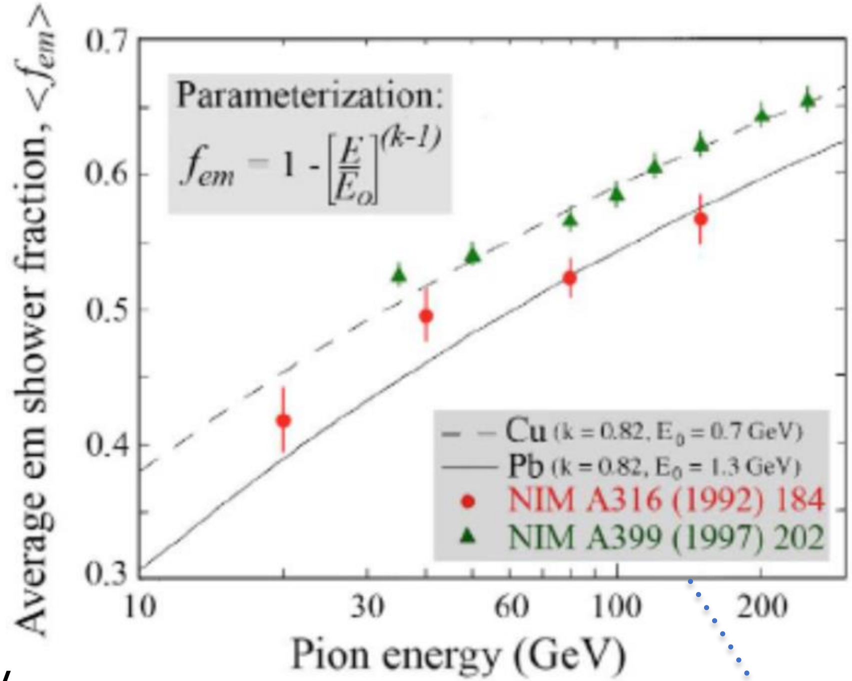

Showers depend heavily on
the incident particle and its energy…

…and fluctuations are non-gaussian!

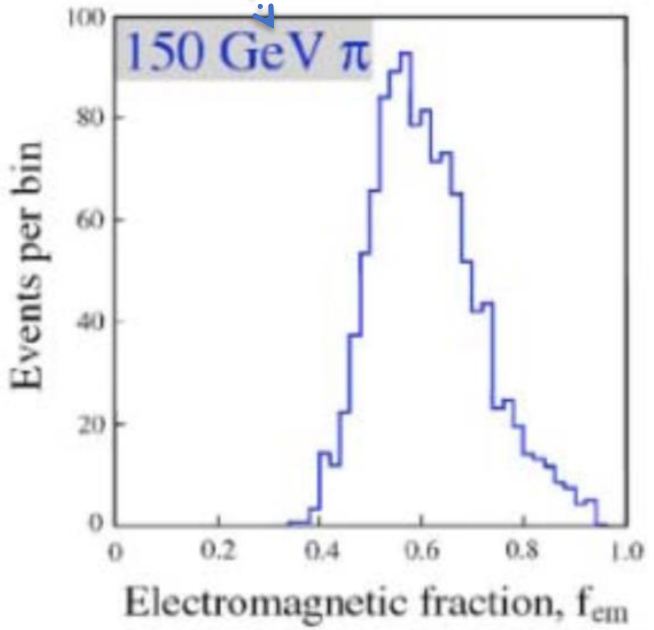

Hadronic showers are unique

- There are never two alike and need to be analyzed case-by-case
  - hardware compensation: enhance the nuclear energy through materials
  - high granularity calorimeter: enable feature extraction and cluster-by-cluster calibration
  - dual-readout: measure the e.m. energy fraction
  - particle flow: calorimeter identifies particle type, energy used only if no track

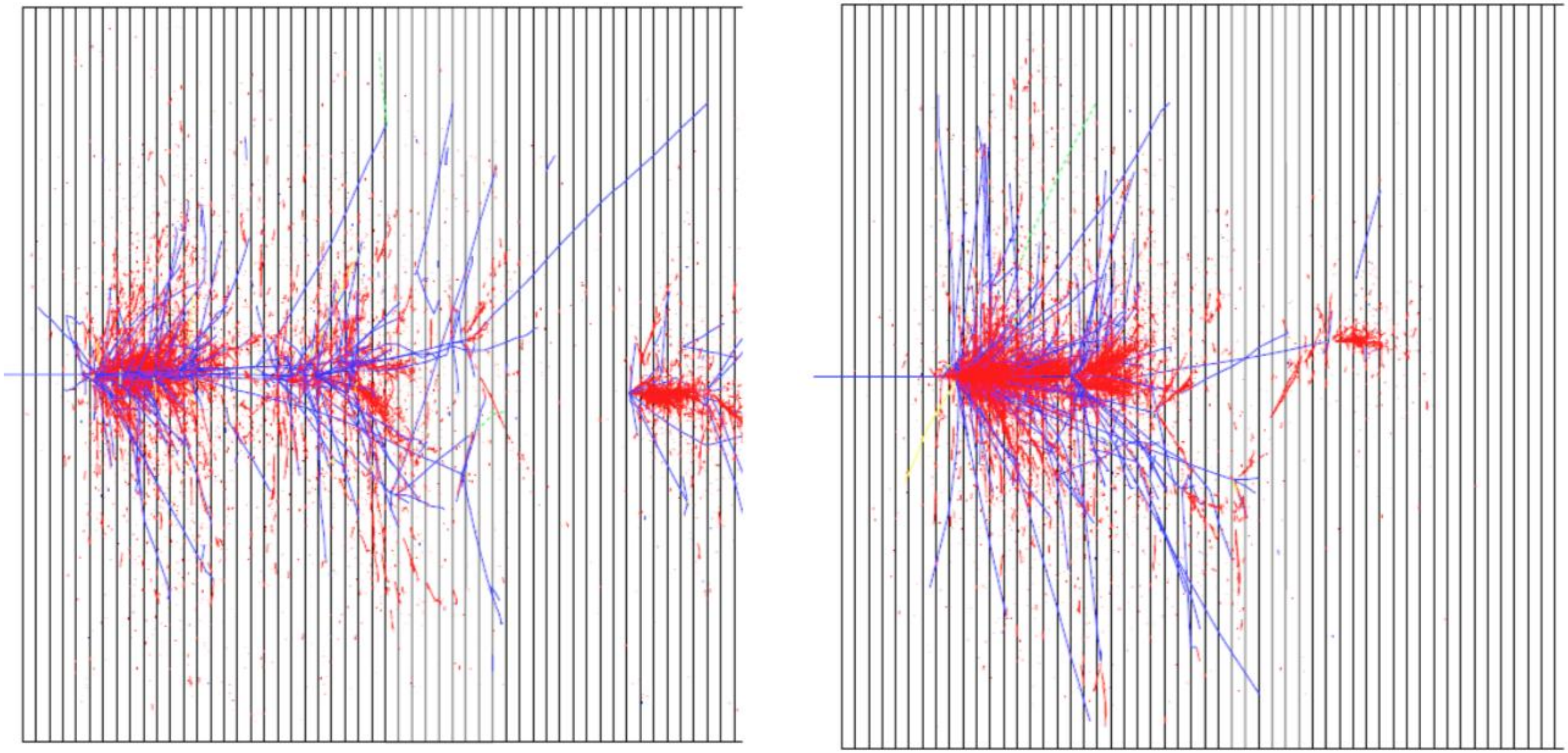

e.m. (hadronic) component is shown in red (blue)

Containment of an hadronic shower

- The interaction length quantifies the mean distance before undergoing a nuclear interaction
- Interaction length (λ) is significantly larger than the radiation length (X_0)

$$\lambda = 35\ A^{1/3} \mathrm{g/cm}^2$$

e.m. shower

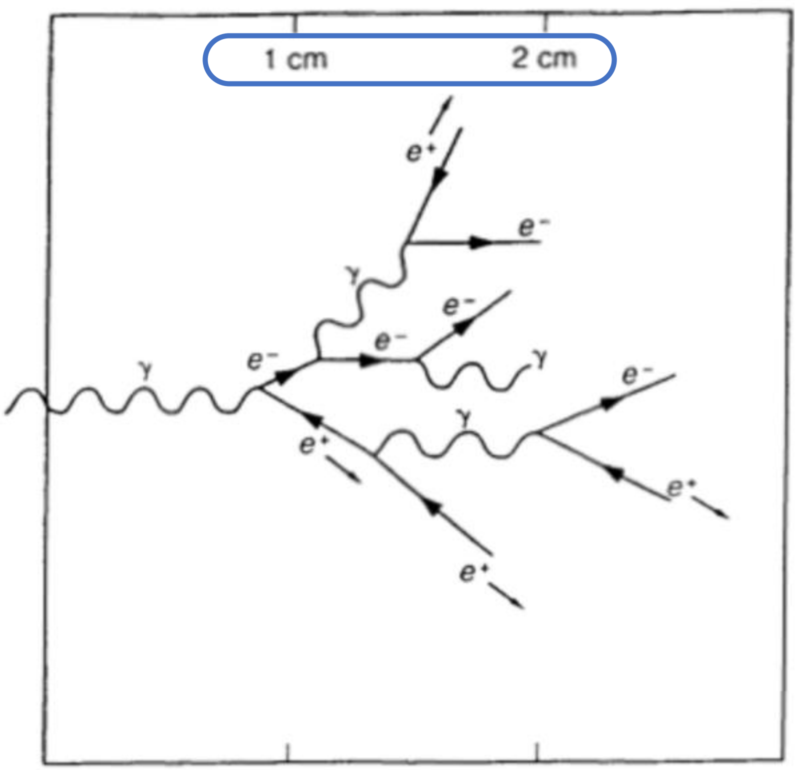

hadronic shower

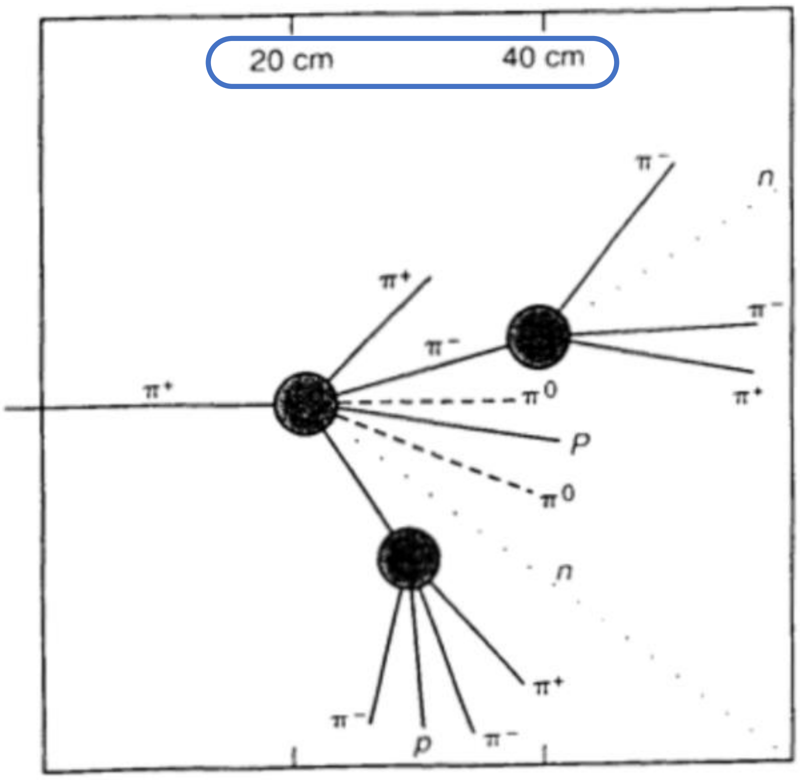

Characteristics of different materials

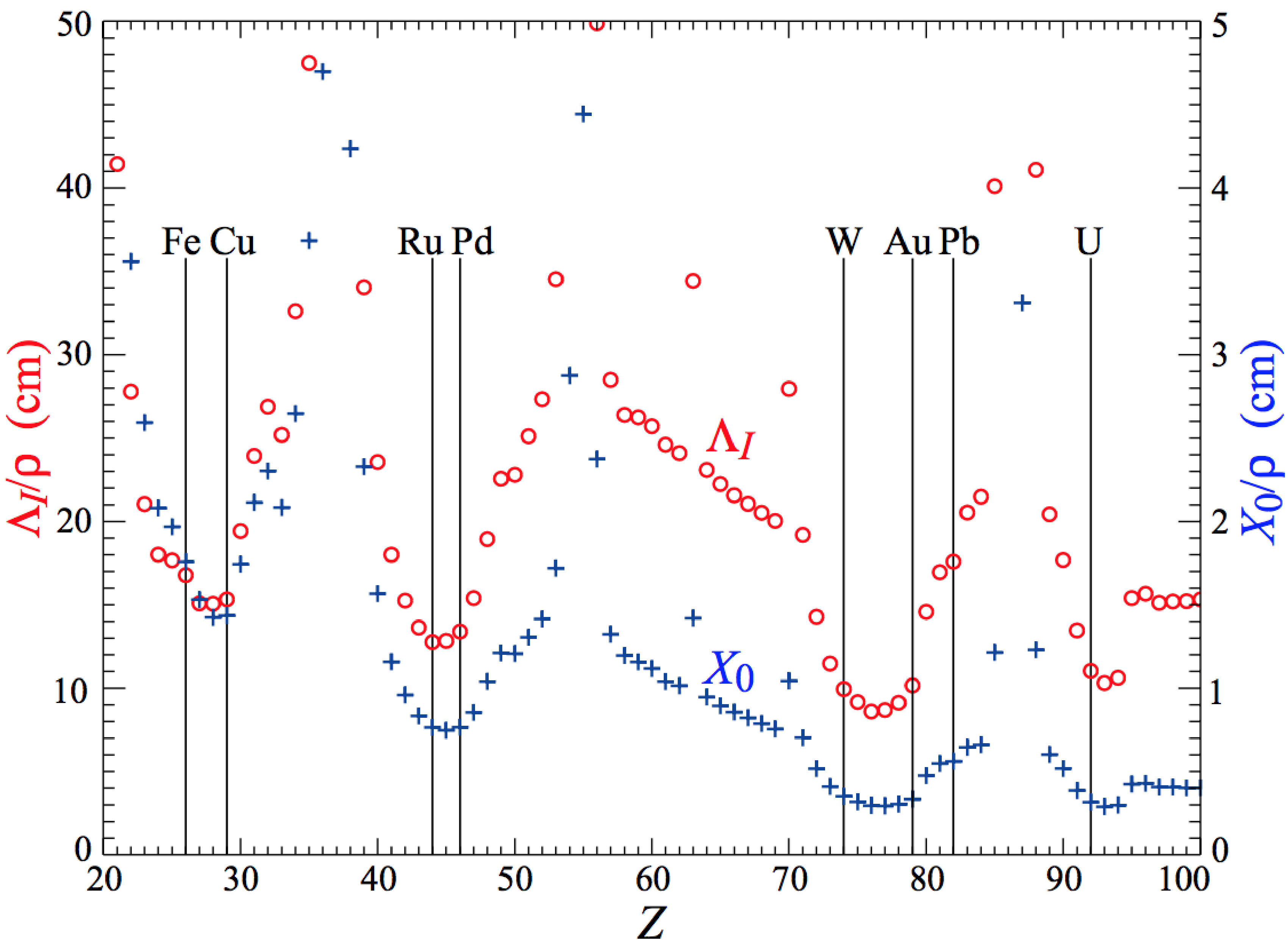

Energy reconstruction I

- Need to gather energy spread in **time**: integrate pulse shape by weighting / fitting
  - calorimeters often need more time to integrate signals with respect to tracking devices
  - hadron showers: slow neutron component can appear significantly delayed in time (>100ns)

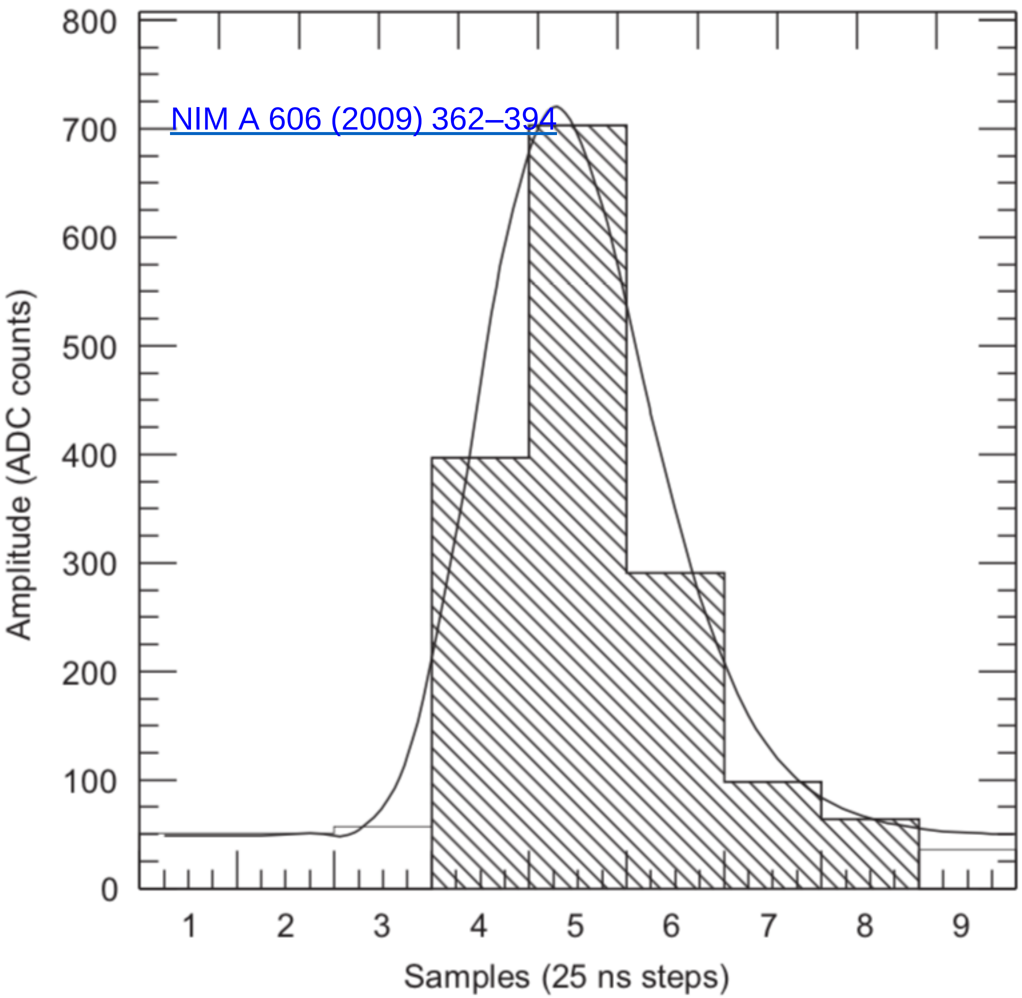

…and then there is pileup

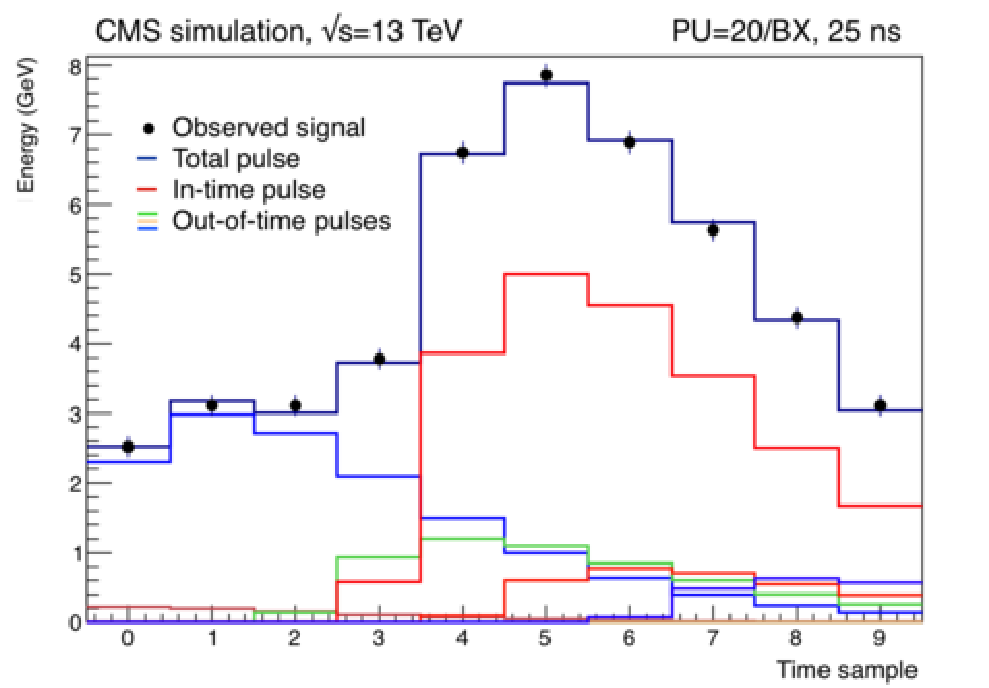

CMS DPS 2015-016

Energy reconstruction II

- Need to gather energy spread in space : clustering algorithms are needed
  - algorithm needs to be adapted to the particle, segmentation, material upfront, shower components
  - often several iterations needed, depending on how busy an event is

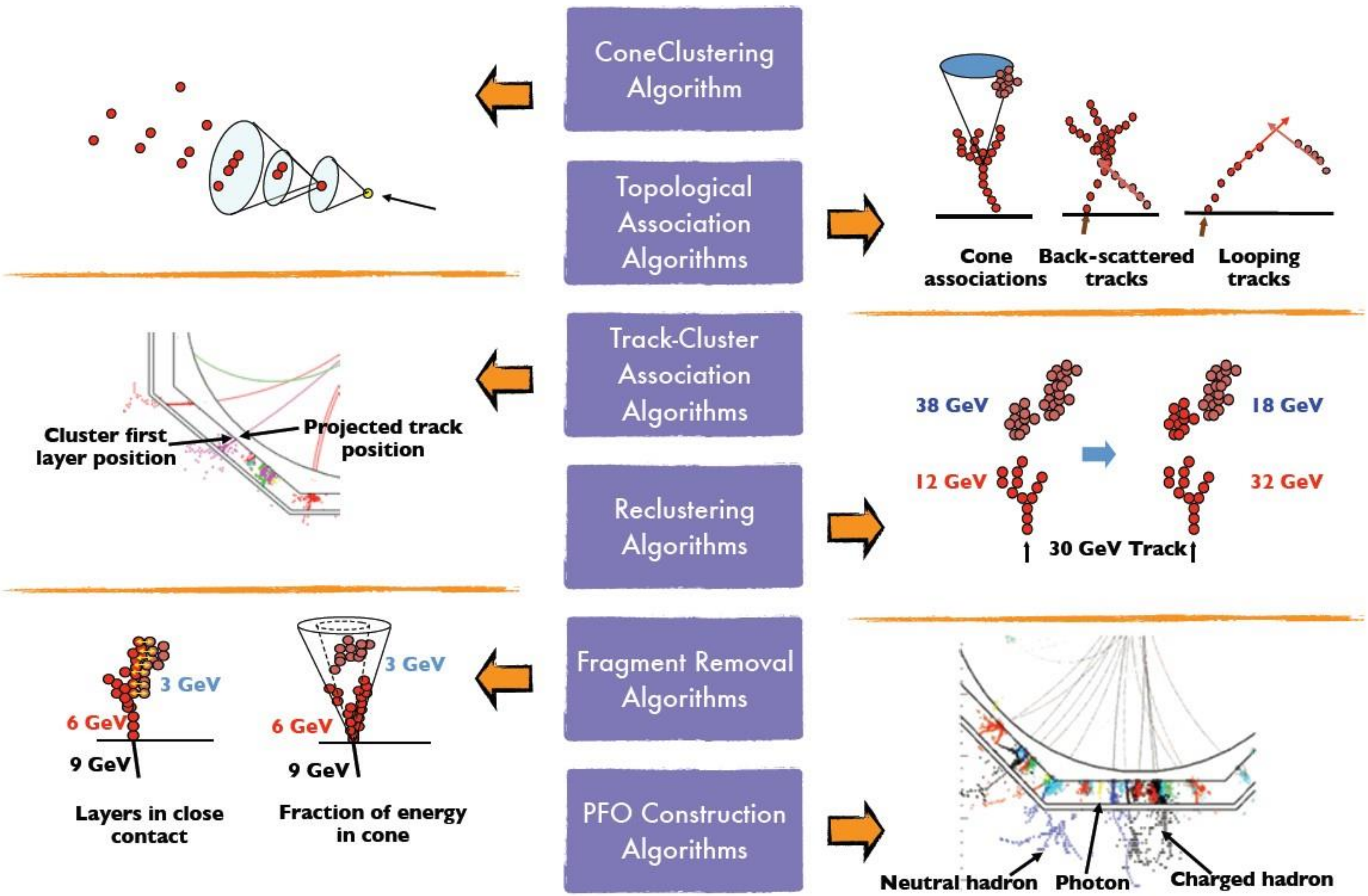

typical PF algorithms (implemented in Pandora)

Resolutions and response - ATLAS TileCal

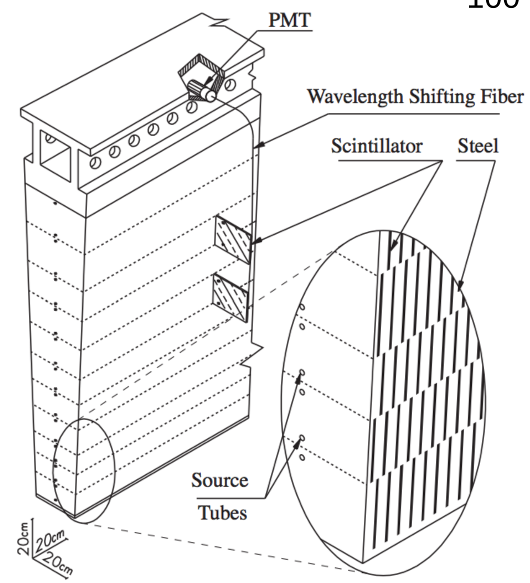

- Typically hadronic calorimeters exhibit
  - non-linearity, different response to e/γ and hadrons (compensation)
  - significantly poorer resolutions compared to e.m. calorimeters

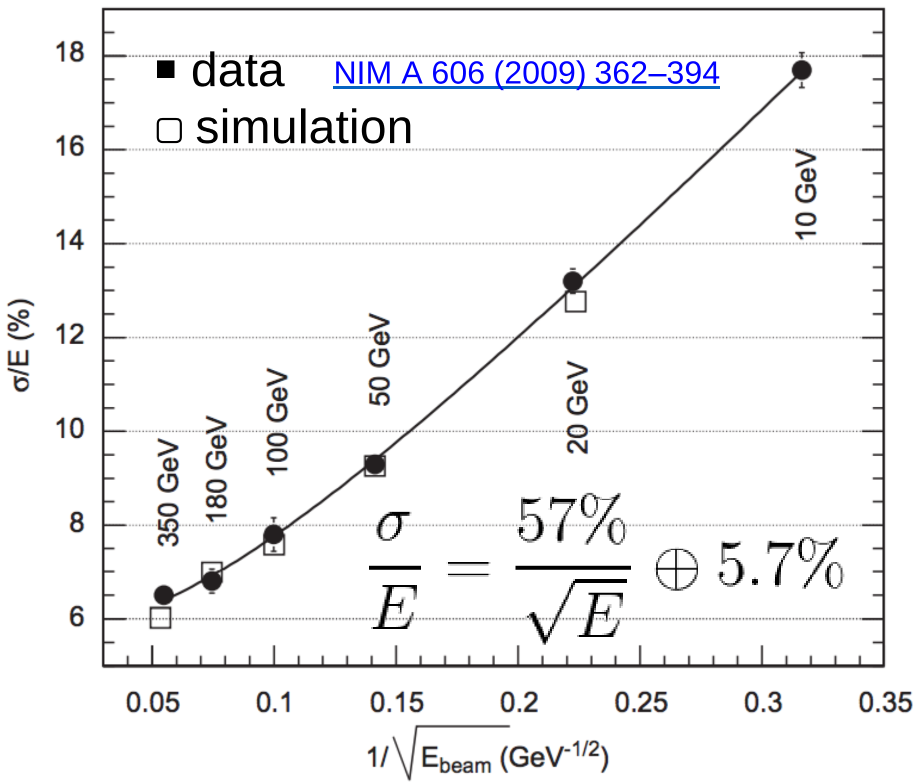

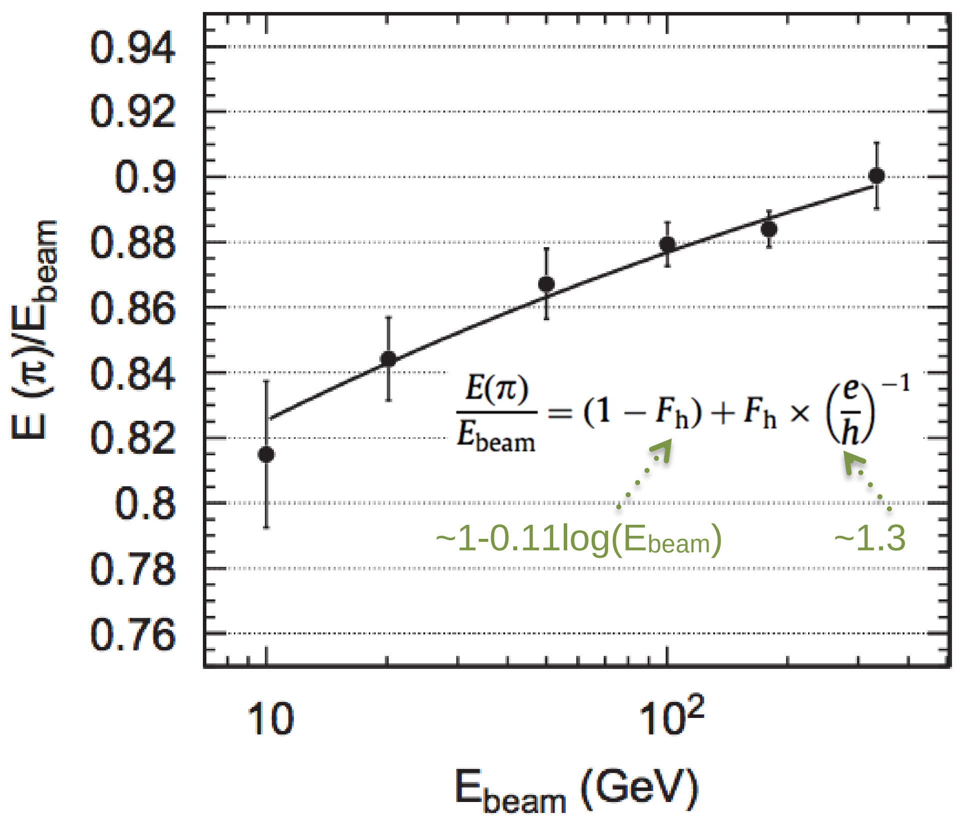

Resolutions and response - CMS HCAL

- Performance is mainly driven by materials used, segmentation, depth
  - but also material upfront and readout
  - partially compensated by reconstruction (next slide)

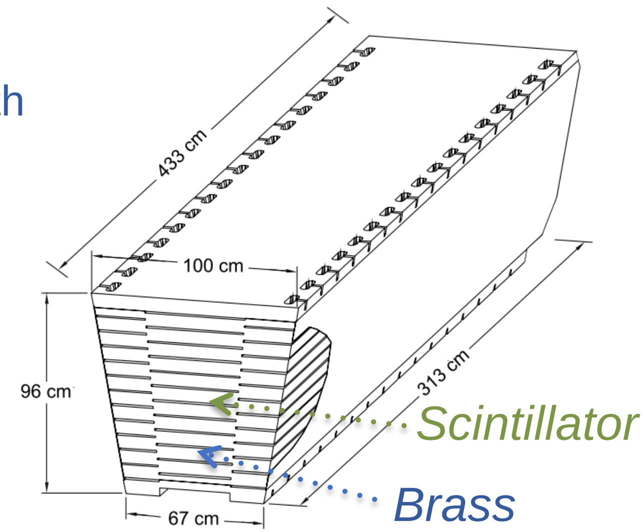

Eur. Phys. J. C (2009) 60: 359–373

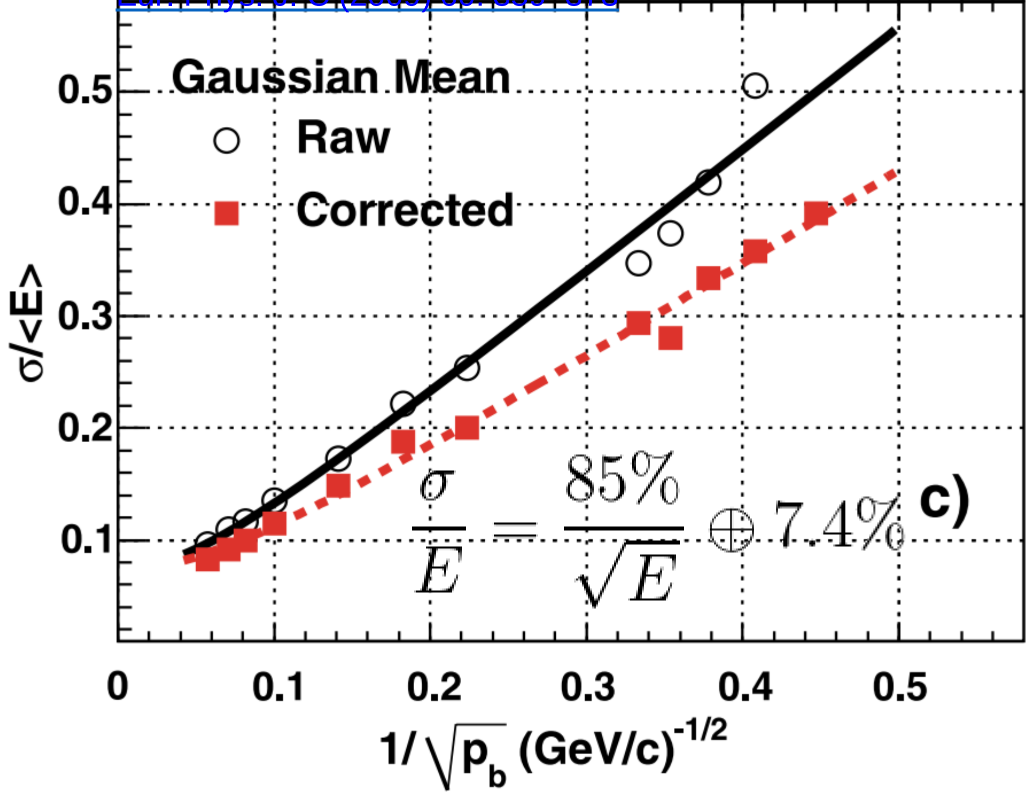

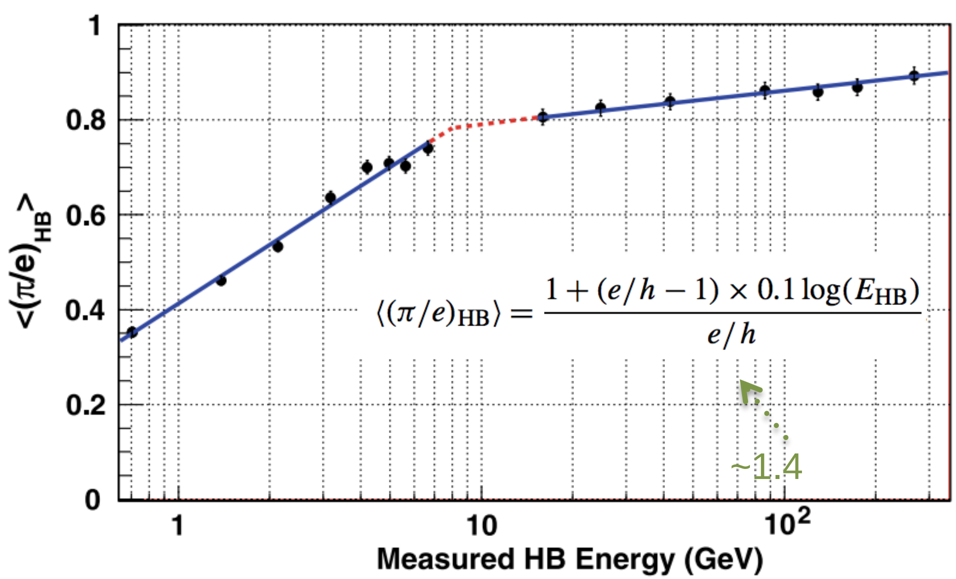

Particle flow algorithm is a reconstruction paradigm

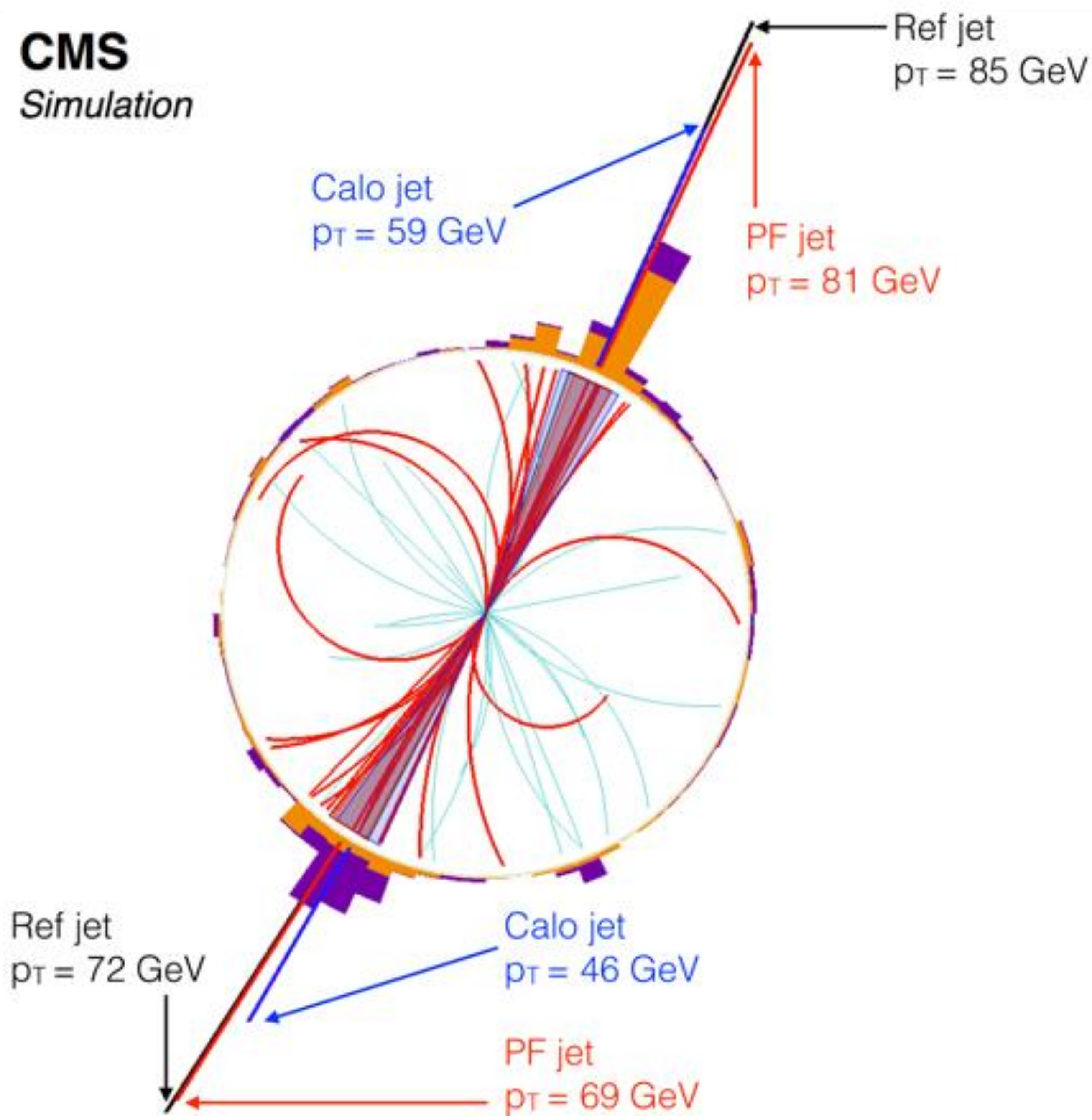

Compensating resolution performance with particle flow

- Particle flow optimizes the usage of the detector
  - most energy energy ends-up being estimated by tracks and the electromagnetic calorimeter
  - recover linearity and significantly improve in energy resolution

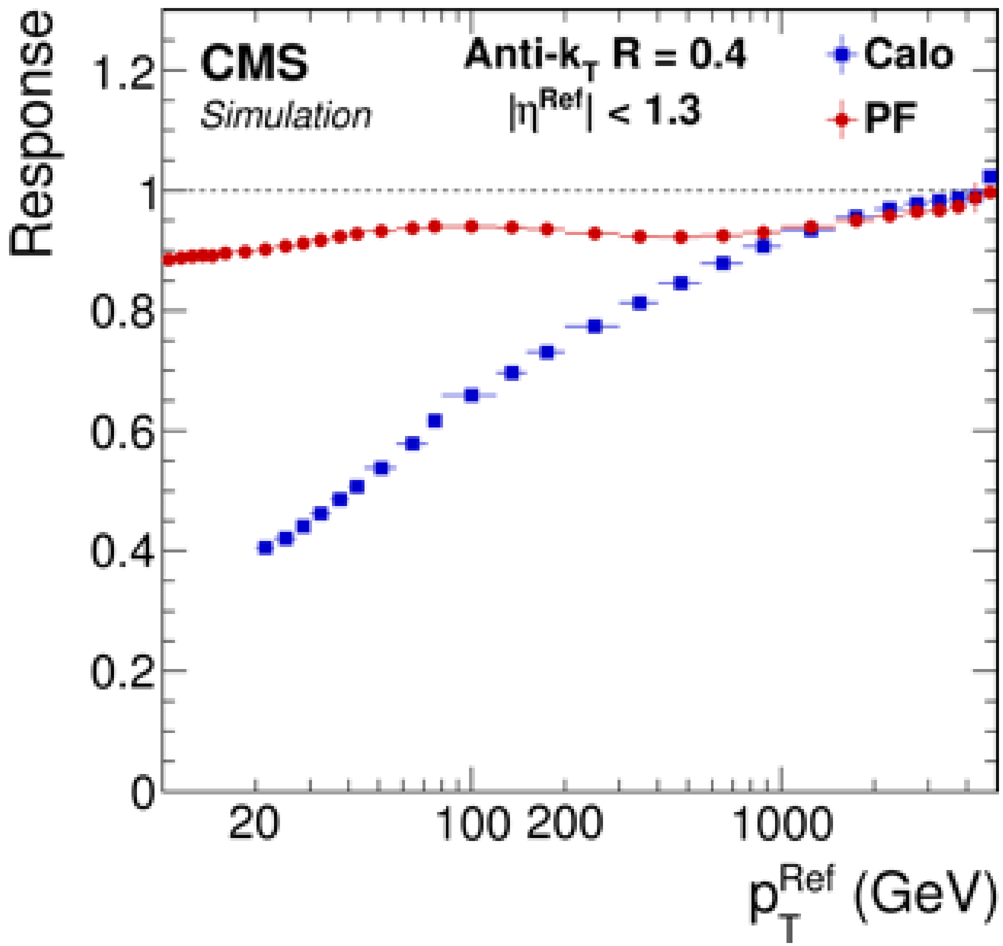

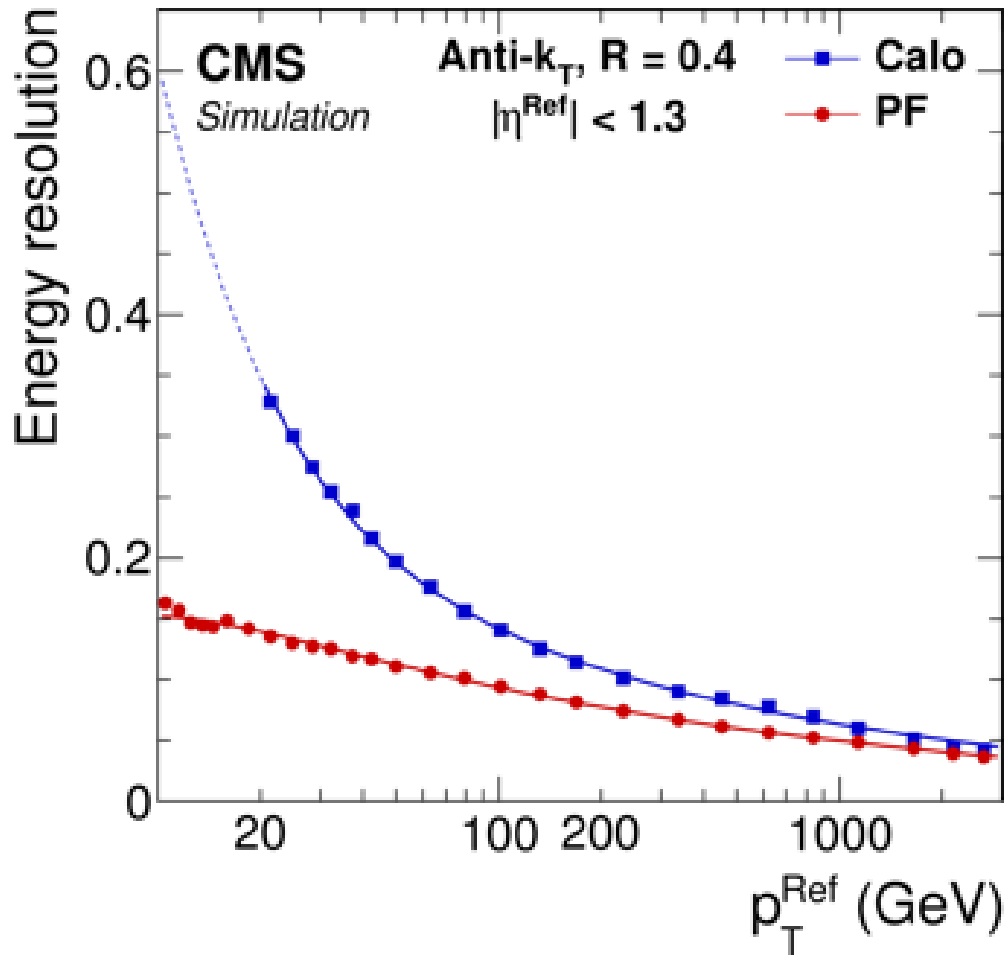

Possible directions in calorimetry: high granularity

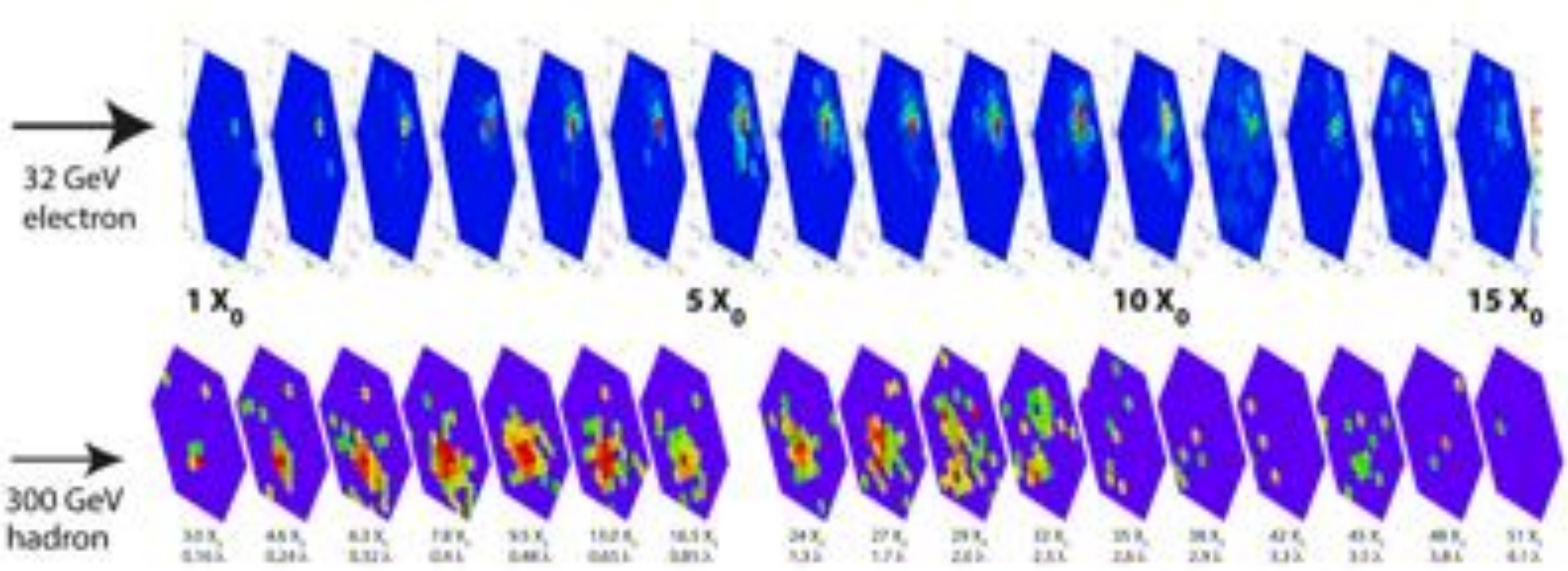

CMS HGCAL

- 52 Si sensor layers interleaved with Pb, Cu, stainless steel
  - small cell sizes (~0.5cm^2) to cope with 200 pileup and allow feature extraction
  - timing capabilities (~30-50ps) per cell to allow association to primary vertex

Possible directions in calorimetry: high granularity

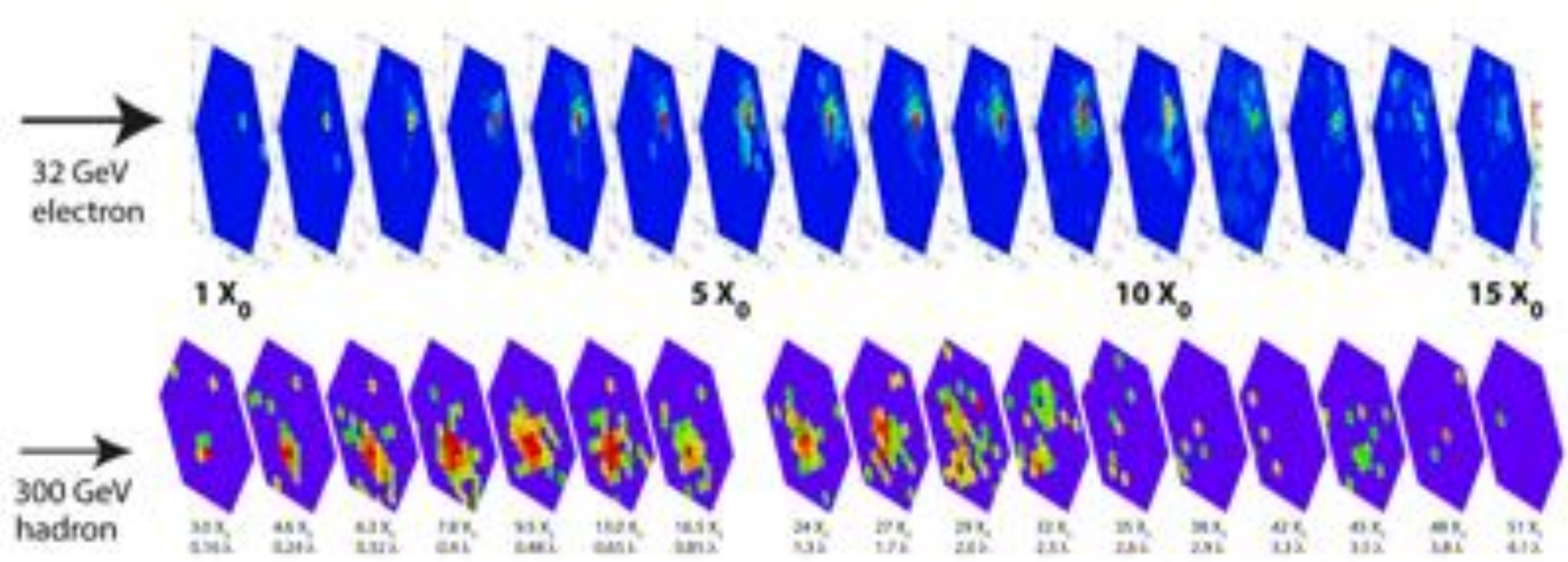

CMS HGCAL

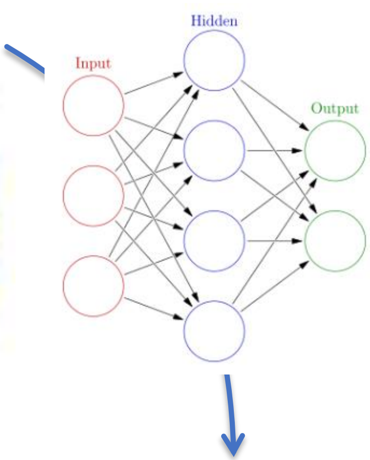

- Sampling limits energy resolution…

  … but can we see deposits in layers as images

  ⇒ machine-learned PFlow?

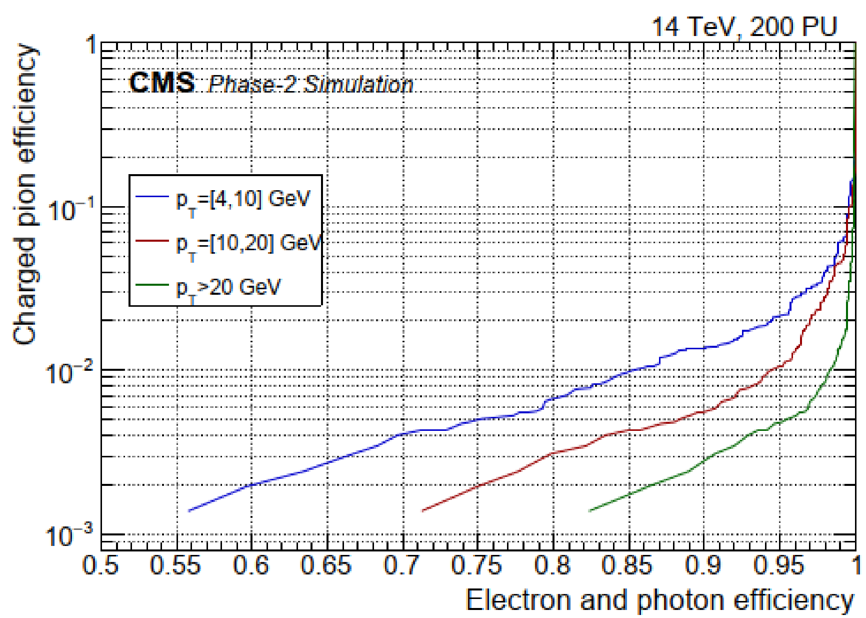

Getting data on tape: trigger systems

Recall: the proton-proton cross section

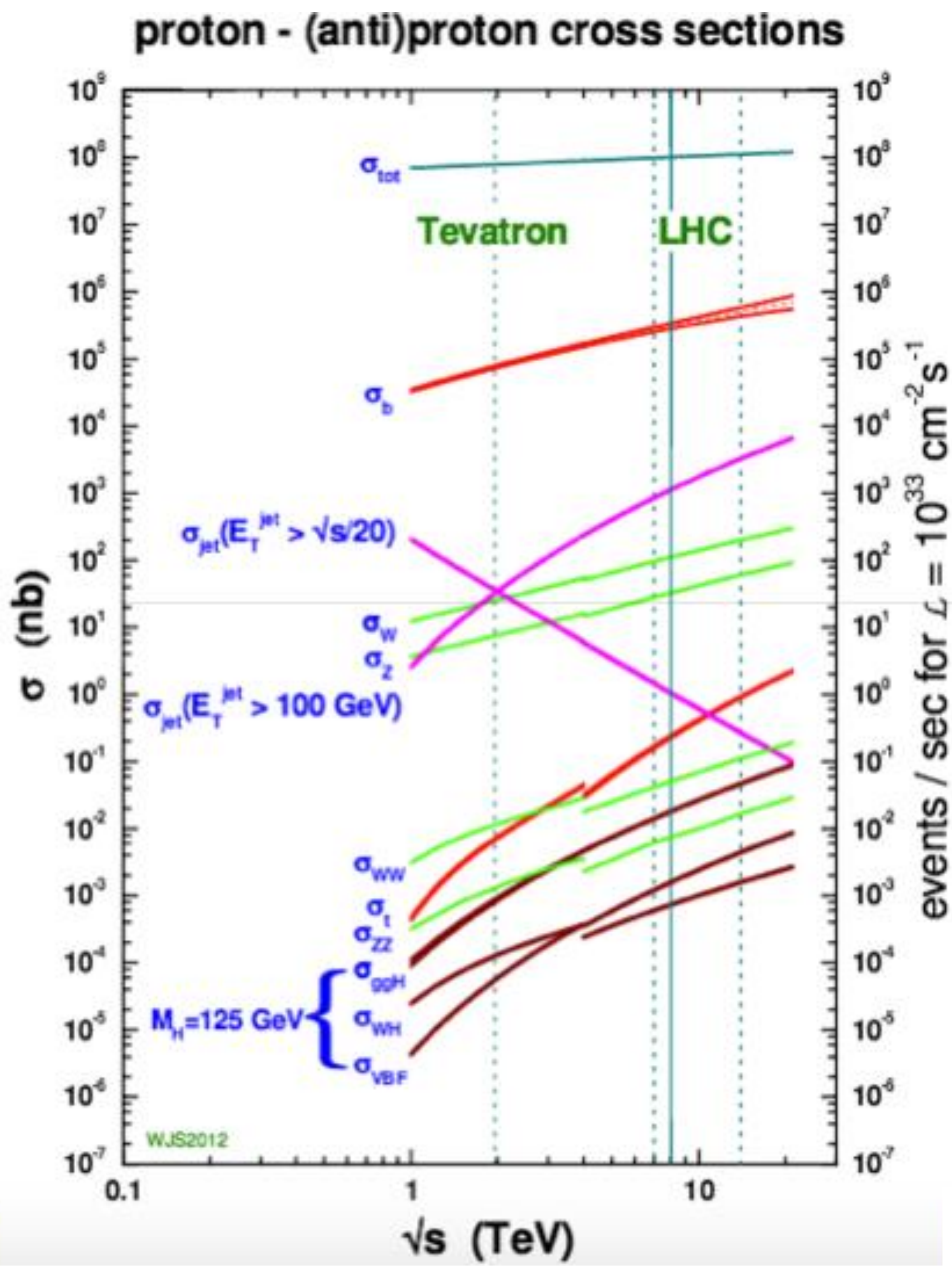

10^8 / s

10 / s

1 / day

15 nb x 10^{34} cm^{-2}s^{-1}
=
150 Hz

Reminder
1 pb = 10^{-36} cm^2

Why do we trigger?

- **Data rates at hadron colliders are too high**
  - most events are expected not to be interesting anyway
  - save to tape only relevant physics
  - need a trigger = online selection system which reduces rates by a factor of ~10^5

Collider	Crossing rate (kHz)	Event size (MB)	Trigger rate	Raw data rate (PB/year)	Data rate after trigger (PB/year)
LEP	45	0.1	5 Hz	10^2	~0.01
Tevatron	2.5	0.25	50-100 Hz	10^4	0.1
HERA	10	0.1	5 Hz	10^4	0.01
LHC	**40**	**1**	**100-200 Hz**	**10^5**	**1**

How do we trigger?

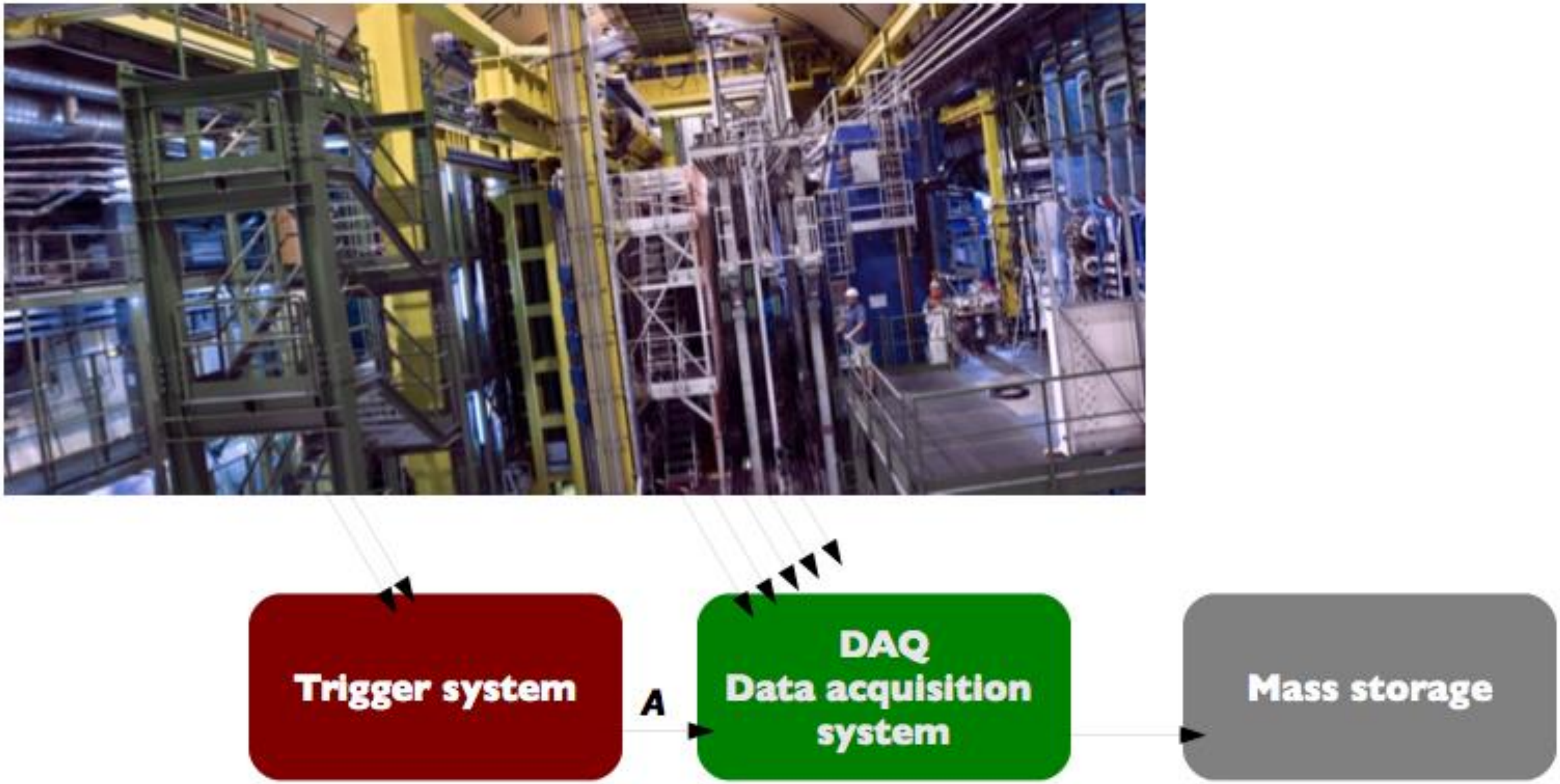

Performs real-time selection based on a subset of the data to record

Collects the data from all the sub-detectors and trigger systems and sends them to mass storage for offline analysis

Readout+decisions=dead-time

- **Signals are random but incoming at an approximate fixed rate**
- Need a busy logic
  - Active while trigger decides whether the event should be kept or not
  - Induces a deadtime in the system
  - <u>System will only accept a fraction of the triggers</u> $\nu = f(1-\nu\tau) \Rightarrow \nu = \frac{f}{1+f\tau} < f$

input rate readout time

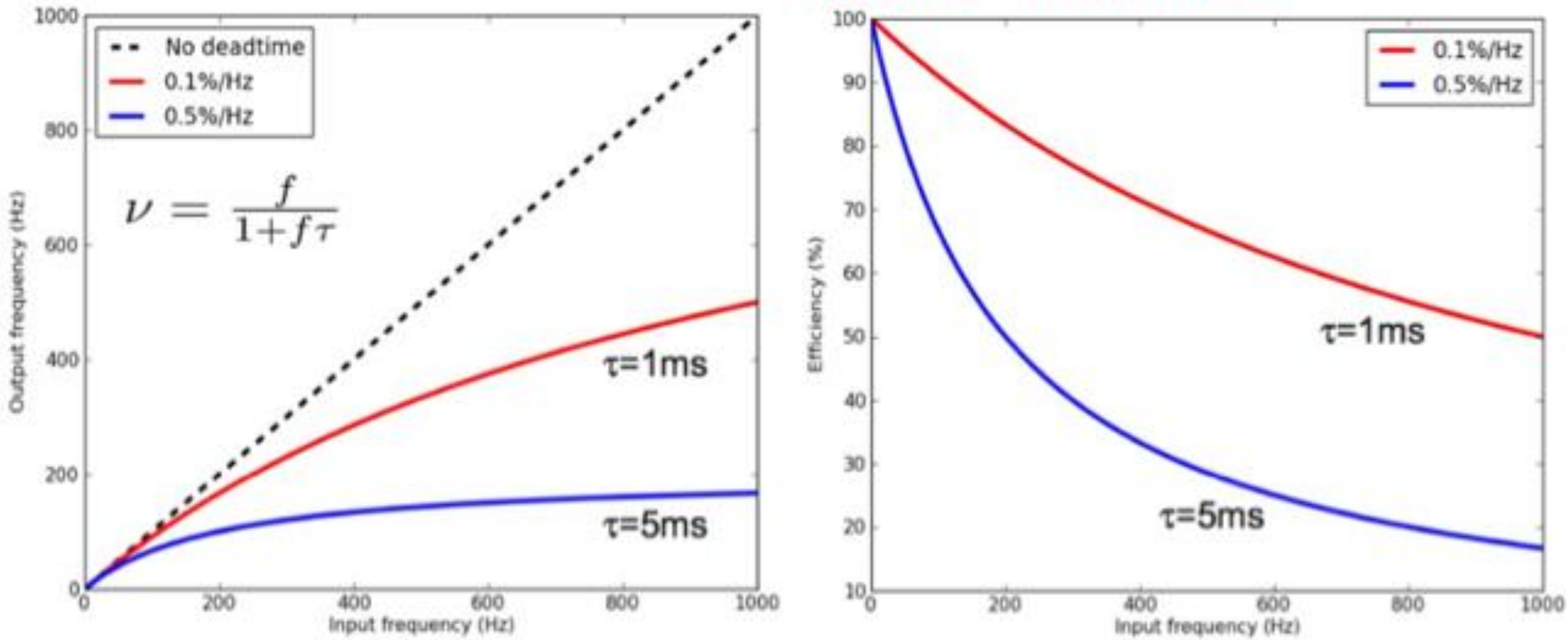

- **System tends to be inefficient for long readout times**

Solution: de-randomize with a buffer

- **A fast, intermediate buffer can be introduced**
  - Works as a FIFO queue

    (First In First Out)

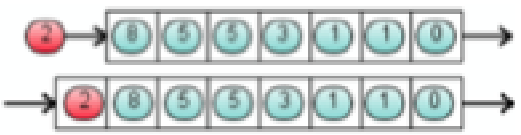

  - Smooths fluctuations = derandomizes
  - Decouples the slow readout from the fast front-end

- **A moderate size buffer is able to retain good efficiency**

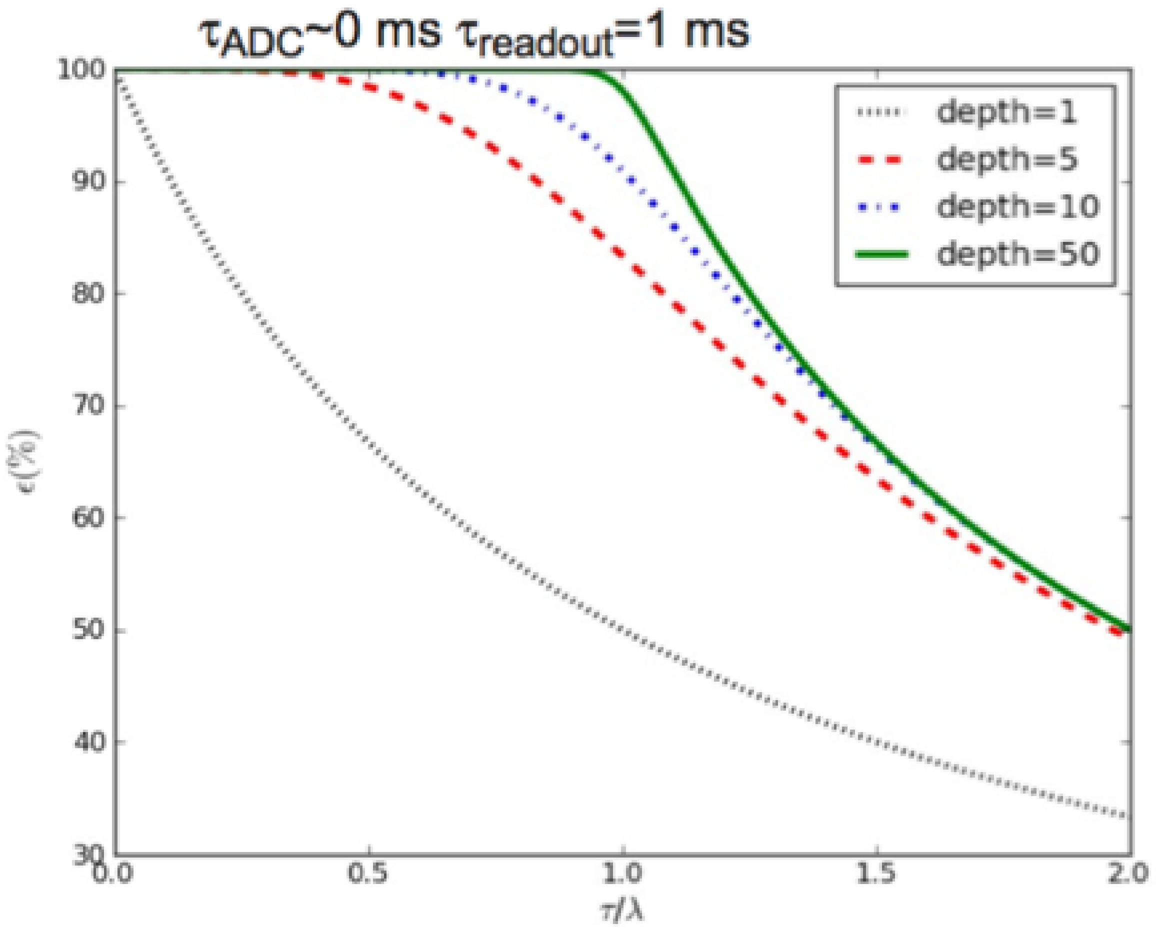

Trigger system architecture for bunched collisions

- The ADC are synchronous with beam crossings
- Trigger output is stochastic
  - FIFO is needed to derandomize
- **ATLAS LHC Run I architecture**
  - May need to accommodate several levels with increased complexity
  - If first layer latency is smaller than bunch crossing than the combined latency is $v_{L1} \times t_{L2}$

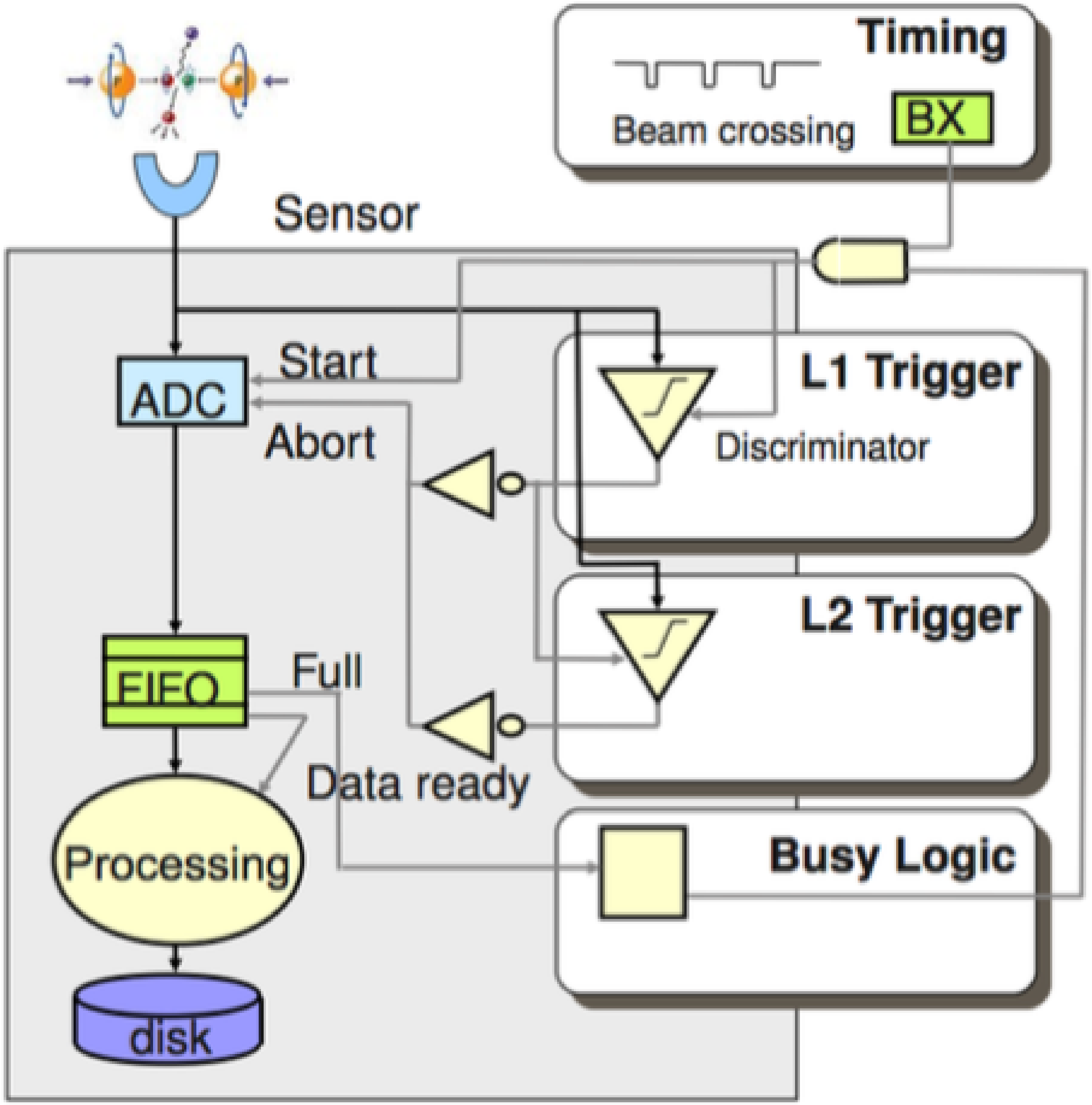

Trigger system architecture for bunched collisions

- The ADC are synchronous with beam crossings
- Trigger output is stochastic
  - FIFO is needed to derandomize
- **ATLAS LHC Run I architecture**
  - May need to accommodate several levels with increased complexity
  - If first layer latency is smaller than bunch crossing than the combined latency is $v_{L1} \times t_{L2}$
- **CMS architecture**
  - Add trigger level between readout and storage
  - CPU Farm used for high level trigger
  - Can access some/all processed data
  - Perform partial/full reconstruction

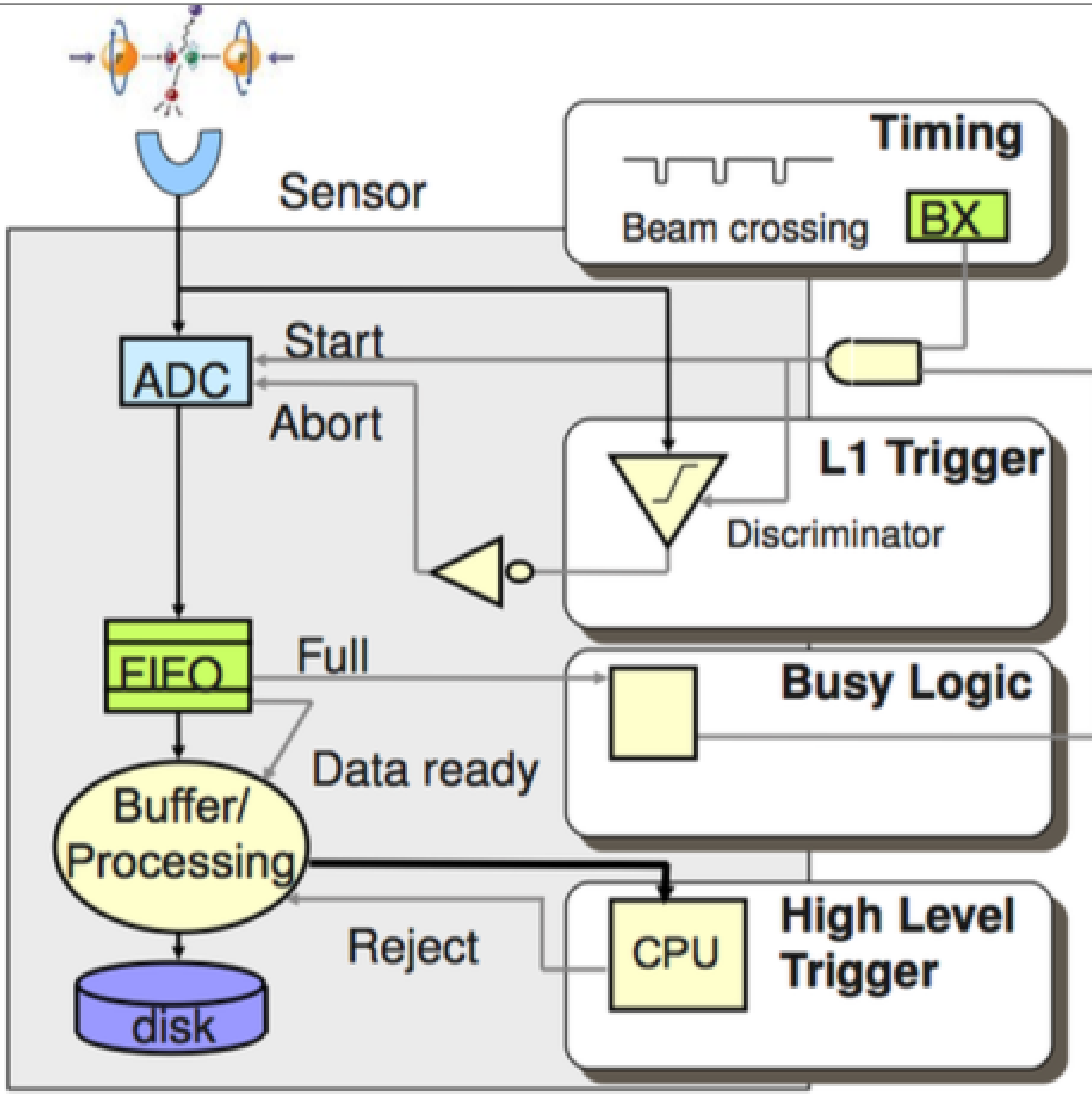

Be fast = keep it to the point, details come later

- **Can only use a sub-set of information**
  - Typically energy sums, threshold flags, coarser detector, tracklets
  - Resolutions (energy and position) are coarser by definition

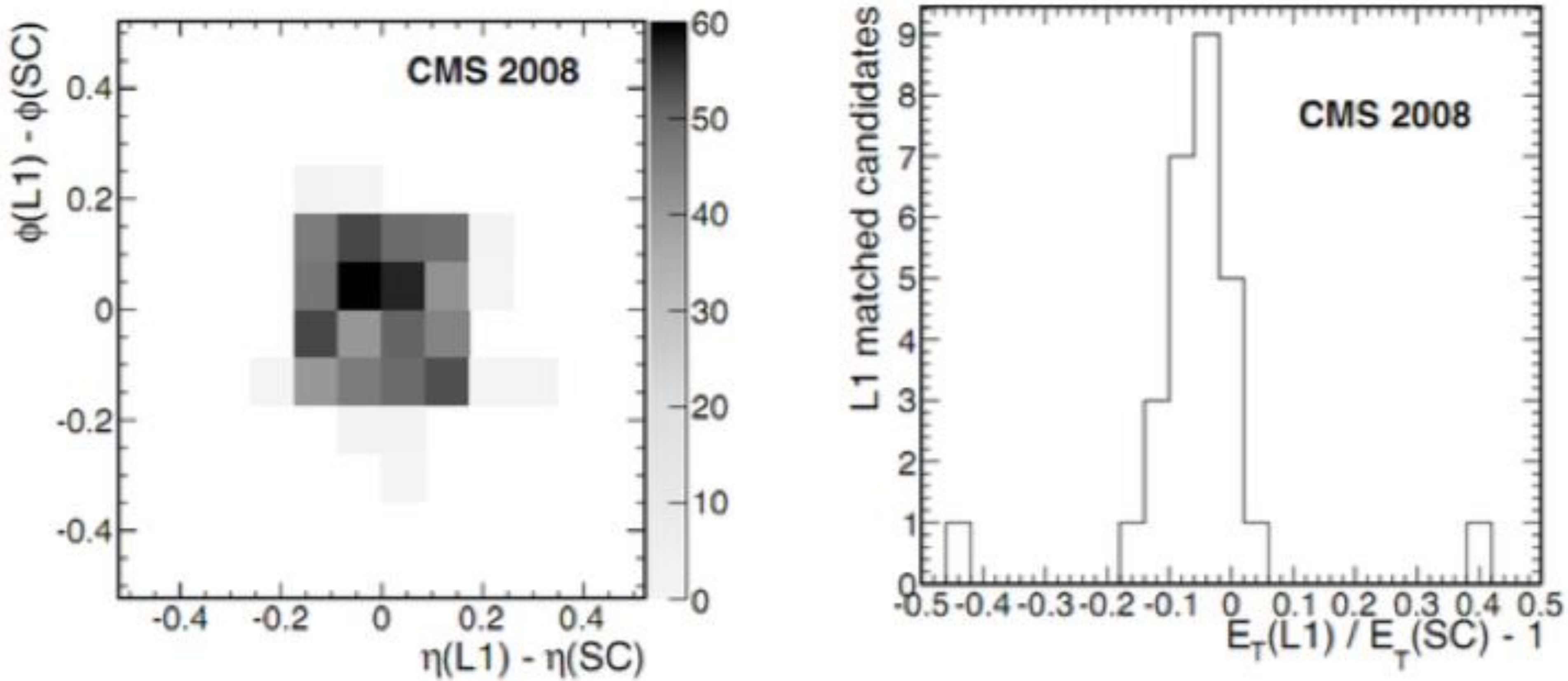

Tracking at L1 (muon case)

Reconstruct segments in each muon chamber
Combine segments to form track
and measure p_T (rough)

Example: CMS Muon L1

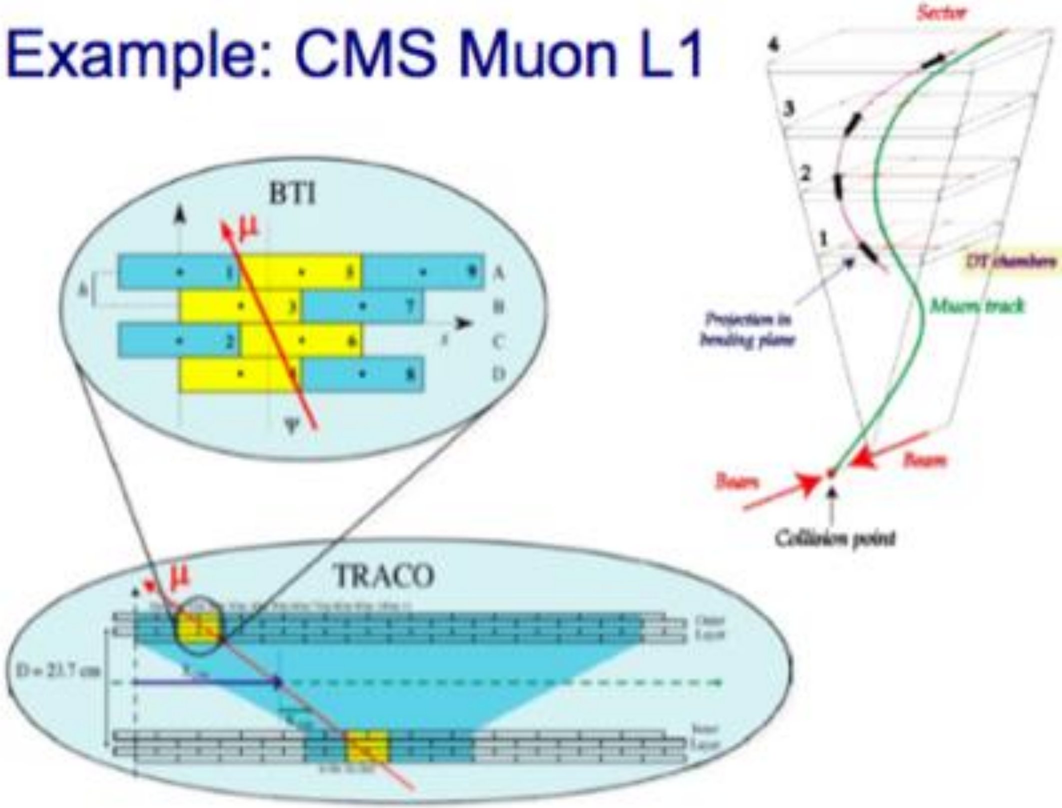

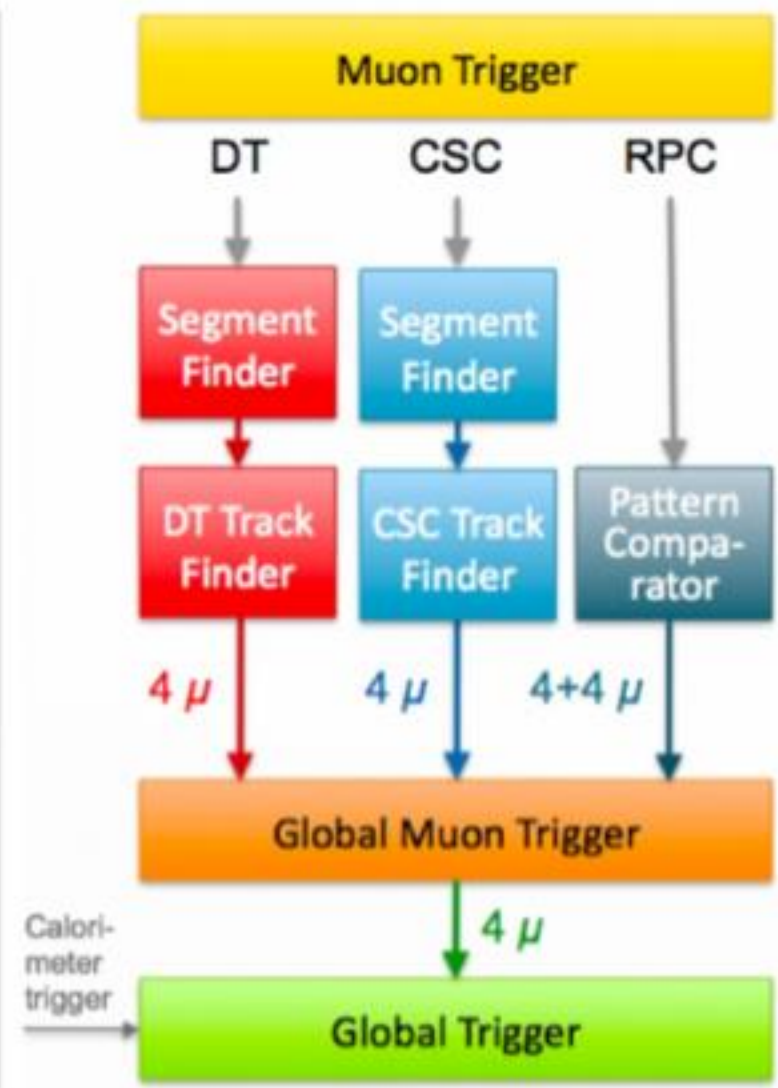

Combining information from different sub-detectors

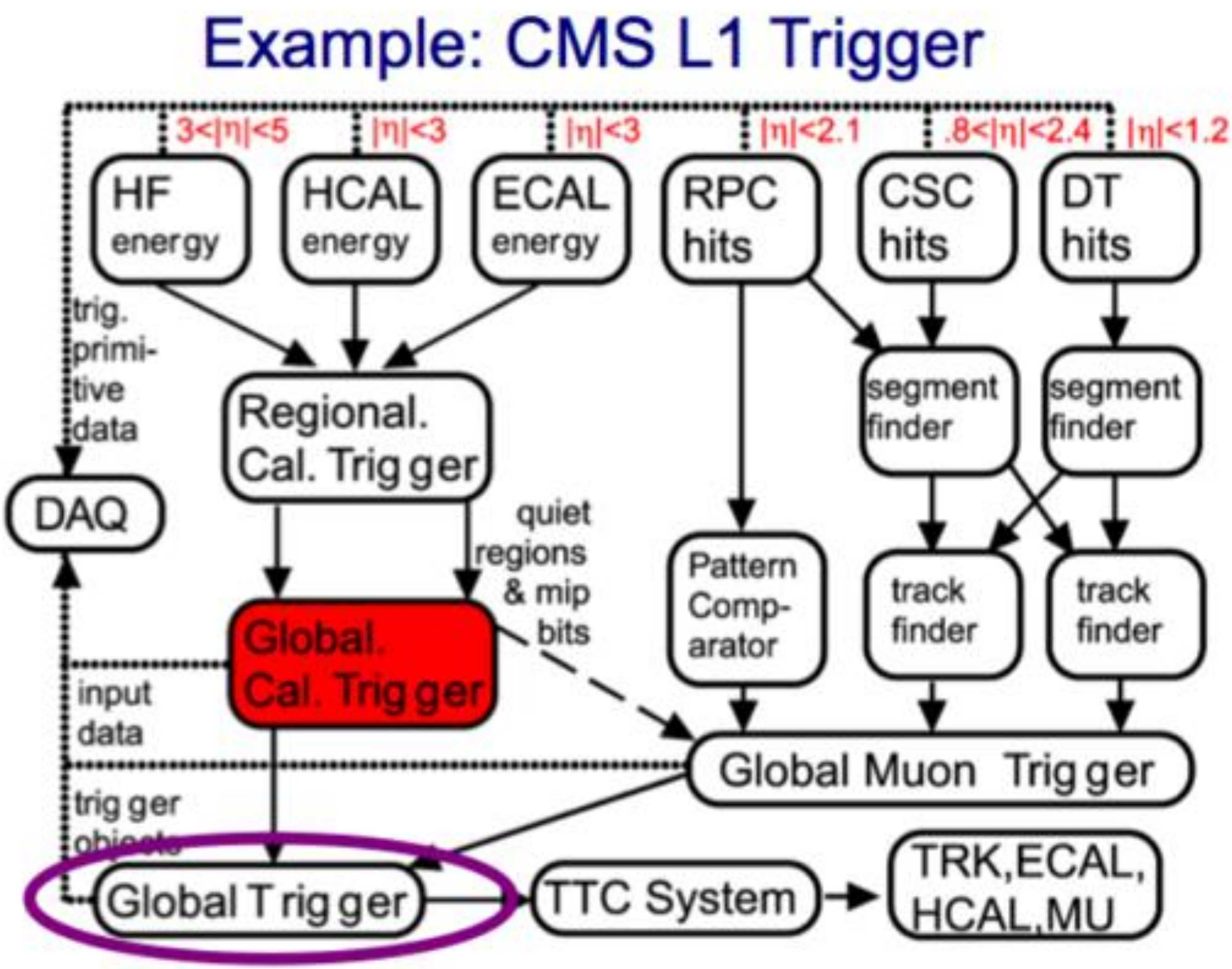

- **Accommodate several sources**
  - Busy logic needs to be included
  - Can perform a global OR
  - Or combine certain trigger objects and apply simple topological cuts
  - High level quantities (masses, square roots are expensive! Avoid if possible

Overall L1 trigger latency

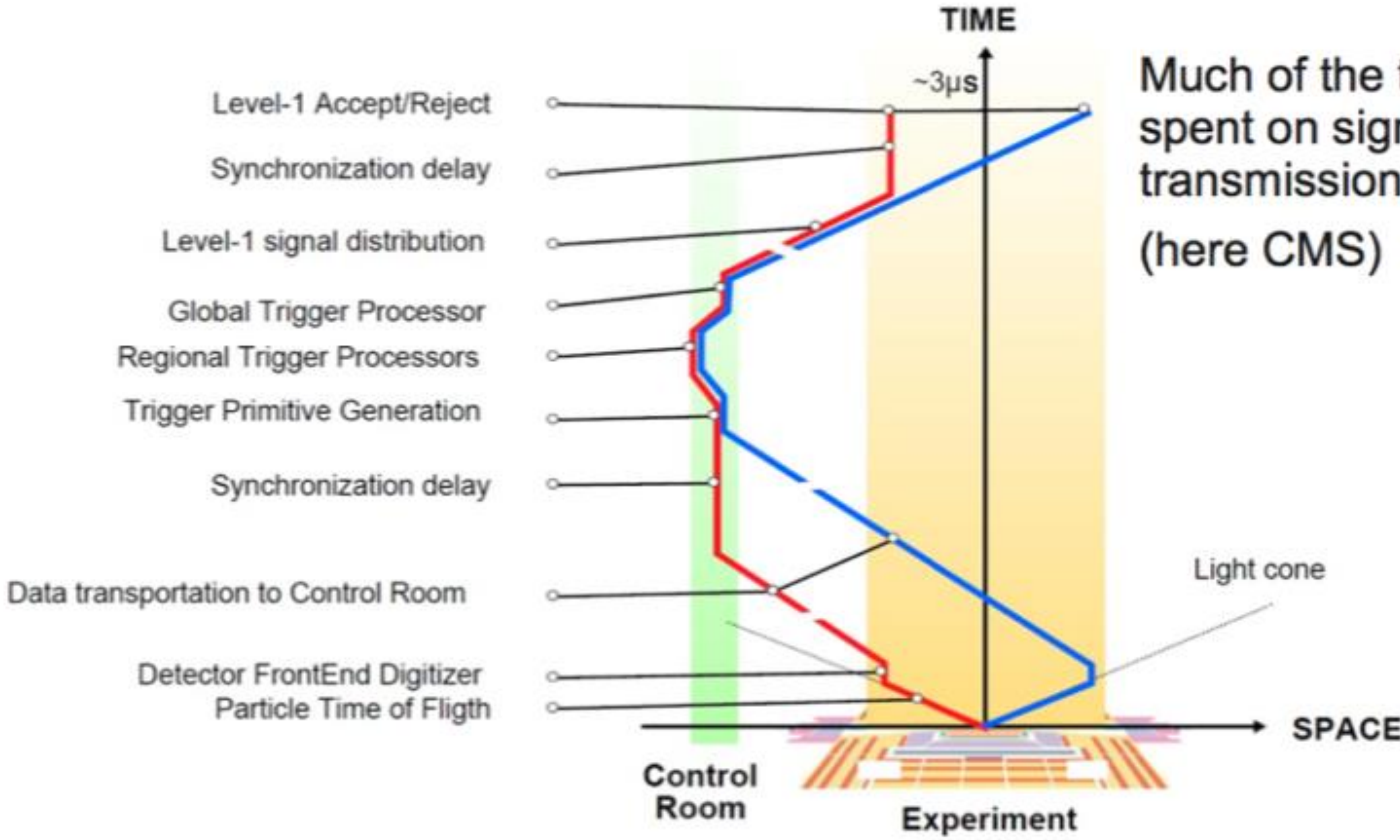

Much of the time spent on signal transmission

(here CMS)

Event building

- Parallelize the sum of the parts of the event to build = slicing
- At CMS 8 independent "slices" are used in order to achieve a 100 kHz rate

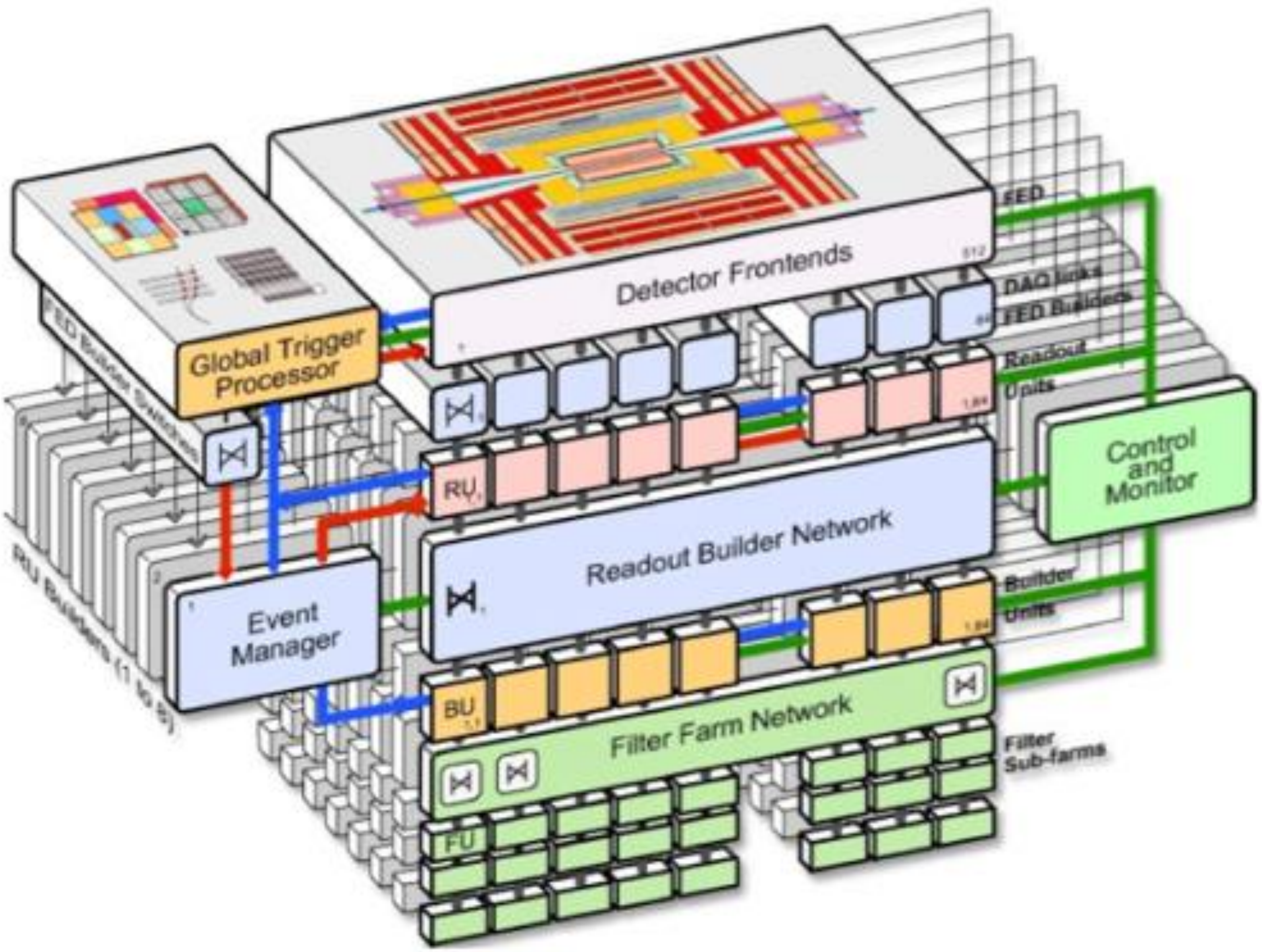

High level trigger

- After event is built can be shipped to a farm for processing before storage
- Events are independent : easy to parallelize
- Keep out rate at ~300Hz / latency at ~40-50 ms, can afford to use
    - high granularity of the detectors
    - offline reconstruction-like algorithms

ATLAS HLT farm:

LHCb readout switch:

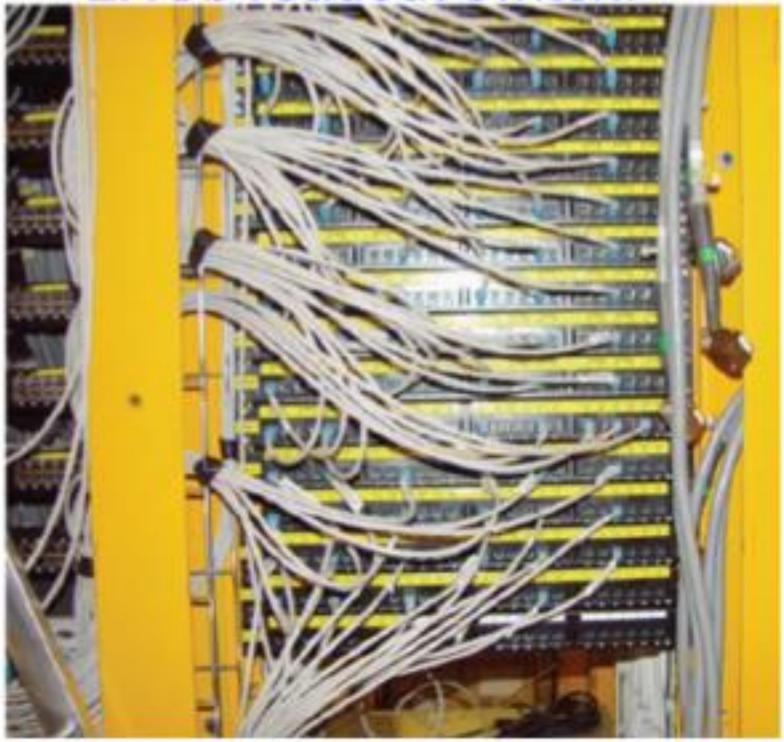

Trigger/DAQ performance in LHC experiments

- Typical values for LHC run I
  - May depend on luminosity
- Notice that the final bandwidth has to be kept
  - total trigger rate must not exceed allocated bandwidth
  - prescale triggers if needed

Collider	ATLAS	CMS	LHCb	ALICE
L1 latency [μs]	2.5	3.2	4	1.2/6/88
L1 output rate [kHz]	75	100	1000	2
FE readout bandwidth [GB/s]	120	100	40	25
Max. average latency at HLT [ms]	40 (EF 1000)	50	20	
Event building bandwidth [ms]	4	100	40	25
Trigger output rate [Hz]	200	300	2000	50
Output bandwidth [MB/s]	300	300	100	1200
Event size [MB]	1.5	1	0.035	Up to 20

Wrap-up

Summary I

- Hunting for new physics: wide variety of final states vs underlying event/pileup
  - general purpose detectors attempt to cover all possible signatures, rejecting background
  - choice of technology: trade-off between particle identification, resolution and budget
- Particle flow as a paradigm
  - use the best out of the detectors for optimal performance
  - yields a close 1:1 physics reconstruction of the hard process final state
- Magnetic field and tracking play a crucial role and set the base
  - B field is at the heart of the experiment
  - tracking detectors are at the base of the reconstruction

Summary II

- Calorimeters make the particles collapse to measure its energy, direction time
  - electromagnetic interactions have scaling properties, easy to reconstruct
  - hadronic interactions depend on energy, particle, have distinct properties
  - best performance conjugates careful/clever detector design and reconstruction
  - calorimeters provide most input to the trigger: coarse, fast information
- Trigger systems take decisions based on a preview of (parts of) the event
  - layered structure to allow to store ~1-1.5MB events at a rate of 300-200 Hz
  - first layers usually implemented in hardware, last layer in CPU farms

References

- W. R. Leo, "Techniques for Nuclear and Particle Physics Experiments", Springer
- H. Spieler, "Semiconductor Detector Systems", Oxford Science Publications
- R. Wigmans, "Calorimetry", Oxford University Press
- Fabjan and Gianotti, "Calorimetry for particle physics", Rev. Mod. Phys. 75, 1243
- Particle Data Group, "Experimental Methods and Colliders", Chin. Phys. C, 40, 100001 (2016)

Backup

The magnet is the heart of an experiment I

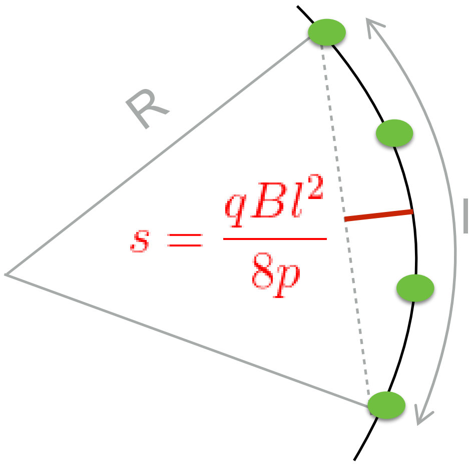

- Goal: measure 1 TeV muons with $\delta p_T/p_T$=10% without charge error
  - $$\frac{\sigma_{p_T}}{p_T} = \frac{8p_T}{0.3Bl^2}\sigma_s$$ this implies ~50μm uncertainty in measuring *s*
  - either use “continuous tracking” or “extreme field”

- From Ampere’s theorem: $\oint \vec{B} \cdot d\vec{s} = \mu_0 I \Rightarrow B = \mu_0 n I$

  ⇒ n= 2168 (120) turns per coil in CMS (ATLAS)

  - special design needed for superconducting cable in CMS
  - size limited by magnetic pressure (P≈6.4 MPa)

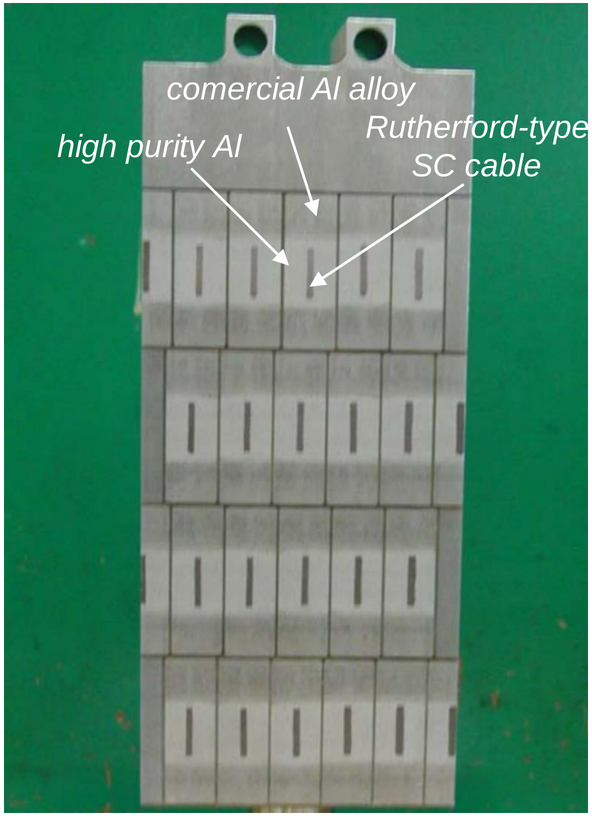

JINST 3 (2008) S08004

The magnet is the heart of an experiment II

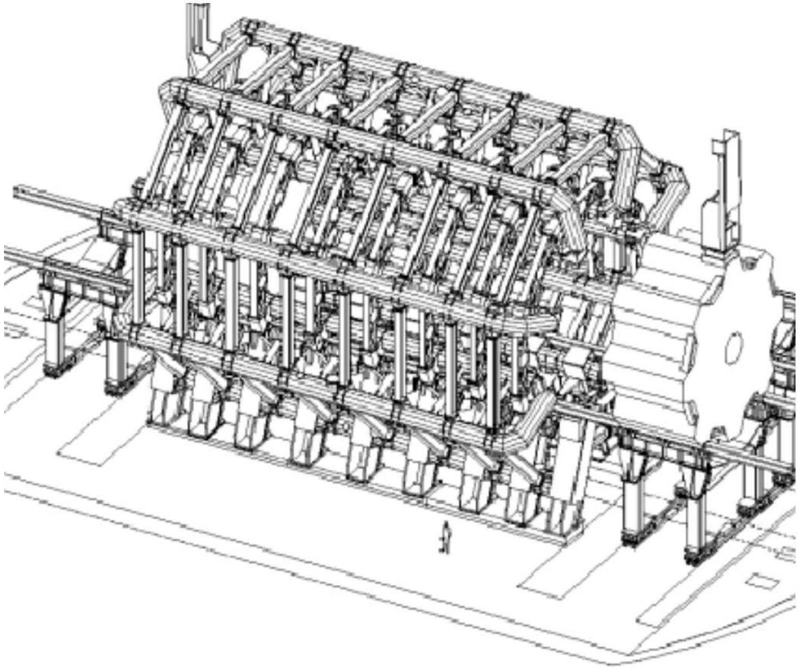

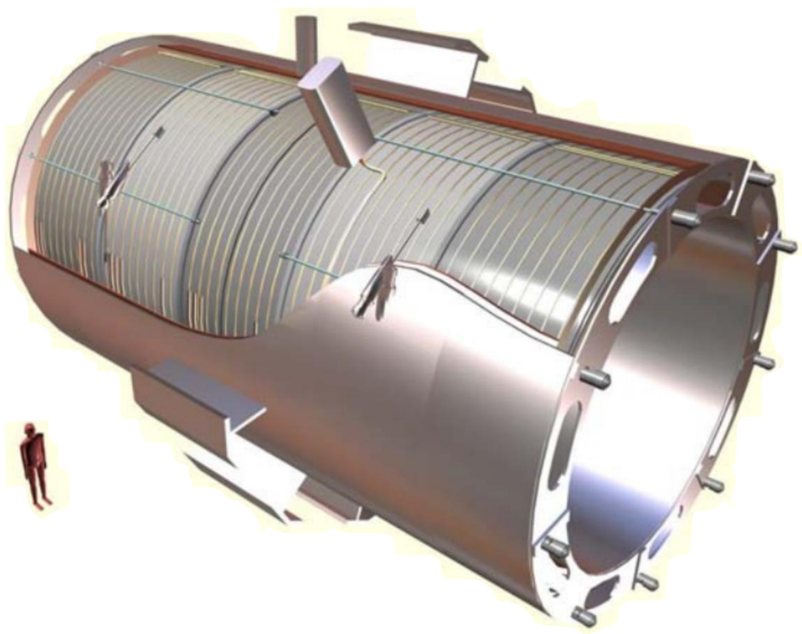

	ATLAS	CMS
B	0.6T (8 coils, 2x2x30 turns)	4T (1 coil, 2168 turns/m)
Challenges	• spatial/alignment precision over large surface • 1.5GJ energy stored	• design and winding of the cable • 2.7GJ energy stored
Drawbacks	• limited pointing capabilities • non-trivial B • additional solenoid (2T) needed for tracking • space needed	• limits space available for calorimetry • no photomultipliers for calorimeters • multiple scattering in iron core • poor bending at large angles

Radiation levels: a challenge for detectors and electronics

- Activation of materials, impurities, loss of transparency/response, spurious hits …
  - additional shielding/moderators needed to limit radiation impact in the detectors

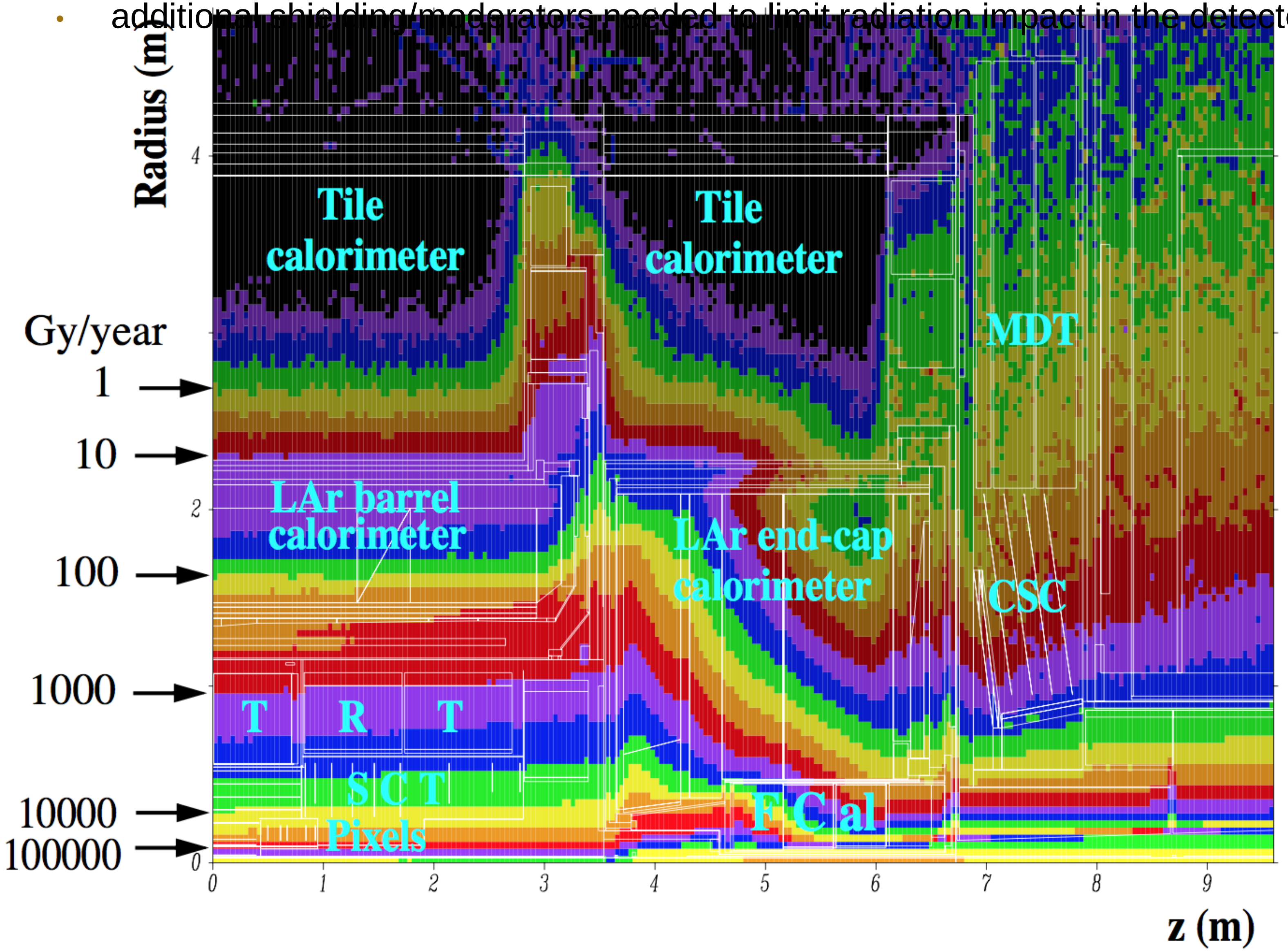

Reminder: 1Gy = 1 J/kg = 100 rad

JINST 3 S08003

Position resolution

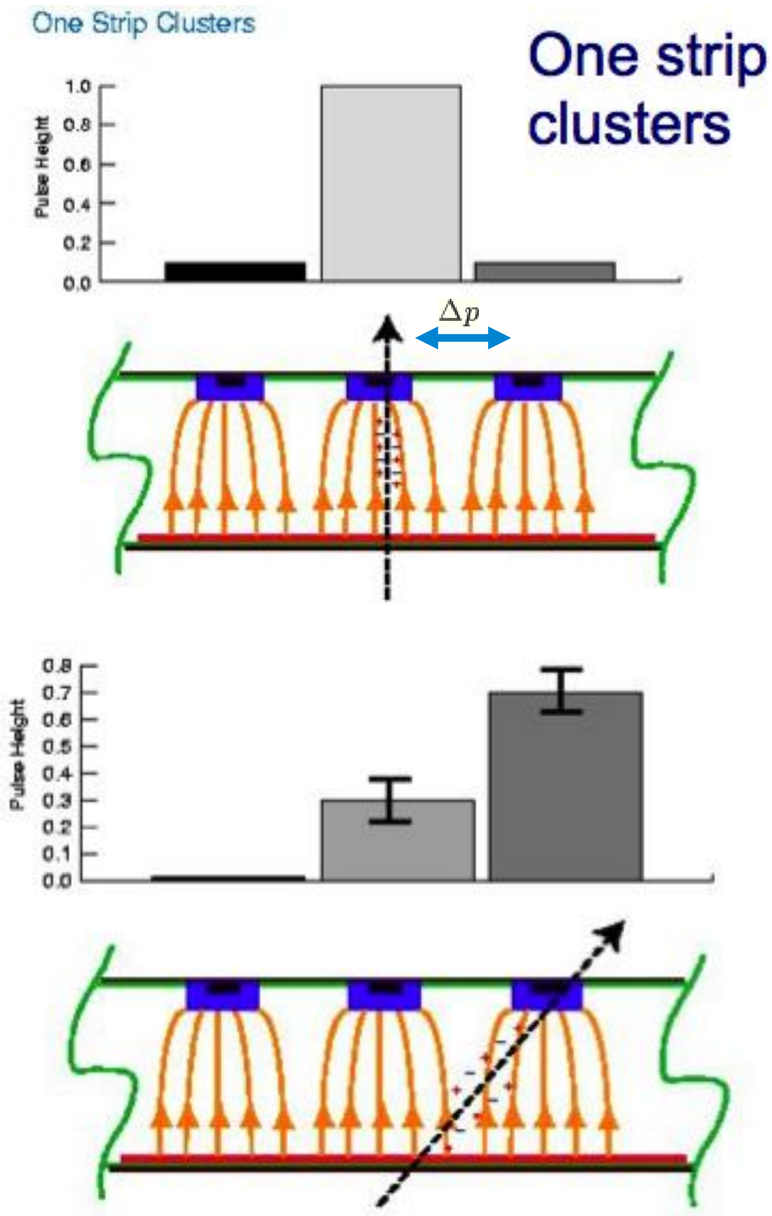

- Affected by different factors
  - transverse drift of electrons to track
  - strip pitch to diffusion width relationship
  - statistical fluctuations on energy deposition

$$\sigma_x \propto \frac{\Delta p}{S/N}$$

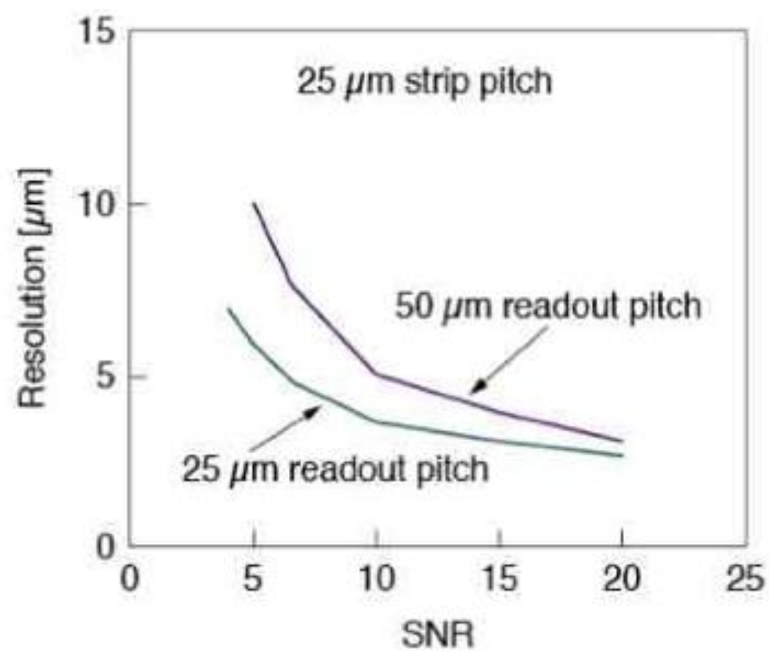

A. Peisert, *Silicon Microstrip Detectors*, DELPHI 92-143 MVX 2, CERN, 1992